Distribution Agreement

In presenting this thesis or dissertation as a partial fulfillment of the requirements for an advanced degree from Emory University, I hereby grant to Emory University and its agents the non-exclusive license to archive, make accessible, and display my thesis or dissertation in whole or in part in all forms of media, now or hereafter known, including display on the world wide web. I understand that I may select some access restrictions as part of the online submission of this thesis or dissertation. I retain all ownership rights to the copyright of the thesis or dissertation. I also retain the right to use in future works (such as articles or books) all or part of this thesis or dissertation.

Signature:

_____ _____

Alexander Bally Date

Genetic and Epigenetic Regulation of PD-1

By

Alexander P. R. Bally
Doctor of Philosophy

Graduate Division of Biological and Biomedical Science
Immunology and Molecular Pathogenesis

_____
Jeremy M. Boss
Advisor

_____
John Altman
Committee Member

_____
Rama Amara
Committee Member

_____
Joshy Jacob
Committee Member

_____
Jacob Kohlmeier
Committee Member

Accepted:

_____
Lisa A. Tedesco, Ph.D.
Dean of the James T. Laney School of Graduate Studies

_____
Date

Genetic and Epigenetic Regulation of PD-1

By

Alexander P. R. Bally
B.A., University of Colorado, 2010

Advisor: Jeremy Boss

An abstract of
A dissertation submitted to the Faculty of the
James T. Laney School of Graduate Studies of Emory University
in partial fulfillment of the requirements for the degree of
Doctor of Philosophy

in Graduate Division of Biological and Biomedical Science,
Immunology and Molecular Pathogenesis

2017

Abstract

Genetic and Epigenetic Regulation of PD-1
By Alexander P. R. Bally

The receptor PD-1 drives immune cell inhibition and exhaustion upon up-regulation. Blockade of this receptor has been shown to be an effective way to restore the function of cells during chronic inflammation, and has been employed therapeutically to that end in cancer patients. Here, systems and regulomes that drive PD-1 expression were studied across multiple cell types and in response to various immune stimuli. A novel driver of PD-1 expression (NF-κB) was identified as the primary driver of PD-1 expression in macrophages. This transcription factor, similarly to the previously identified NFATc1 and STAT3 activators and the repressor FoxO1, binds to the CR-C region of the *Pdcd1* locus. The function of this cis-element was found to be involved in driving early changes to PD-1 expression, but not necessary for the prolonged expression of PD-1 during chronic inflammation. Abrogating early PD-1 expression through deletion of CR-C, without altering later modalities of expression, resulted in a shift away from effector cell formation towards a stronger memory cell formation. Furthermore, the histone modifier LSD1 was shown to bind to and regulate the PD-1 locus on an epigenetic level, enforcing a silenced profile following the transient expression seen in the late stages of an acute infection. This partially accounts for the differential expression of PD-1 seen in acute compared to chronic inflammatory settings. In further analysis of the epigenetics of immune responses, distinct chromatin accessibility profiles were identified for naïve, effector, exhausted, and memory T cells during viral infection, and correlated with changes in mRNA expression. Specifically, a set of loci that remains accessible during the effector to memory transition identifies drivers of improved memory functionality compared to naïve cells. In addition to providing an understanding of which active immune environments may induce and be affected by PD-1's function, knowledge of both the molecular mechanisms regulating PD-1, as well as the dynamic epigenetics of the immune response, may help tailor future immunotherapies for fighting cancer, chronic HIV and HCV infections, or prevention of allergic responses, transplant rejection, and autoimmunity as well as improving durable responses to vaccines.

Genetic and Epigenetic Regulation of PD-1

By

Alexander P. R. Bally
B.A., University of Colorado, 2010

Advisor: Jeremy Boss

A dissertation submitted to the Faculty of the
James T. Laney School of Graduate Studies of Emory University
in partial fulfillment of the requirements for the degree of
Doctor of Philosophy

in Graduate Division of Biological and Biomedical Science,
Immunology and Molecular Pathogenesis

2017

Acknowledgements

Thank you to my parents Kim and John for encouragement and nourishment

Thank you to Ben for keeping me grounded and unconfounded

Thank you to my advisor Jerry for revising and advising

and financial backing

Thank you to the Boss lab for training and sustaining

And not sending me packing

And thank you to Kendra

Who laughed and suffered with me

And endured grad school's duress

Who found me in the hardest years

But loved me nonetheless

Table of Contents

List of Figures and Tables

Chapter 1

Chapter 2

Chapter 3

Chapter 4

Chapter 5

Chapter 6

Chapter 1: the PD-1 Regulome

*Contains content originally published as a brief review in the *Journal of Immunology*. Bally AP, Austin JW, Boss JM. Genetic and Epigenetic Regulation of PD-1 Expression. J Immunol. 2016. 196(6):2431-7. It has been modified in part for this dissertation.

Programmed Death 1

The inhibitory receptor Programmed cell death-1 (PD-1) is a mediator of central and peripheral immune tolerance and immune exhaustion during chronic exposure to antigen (Boussiotis et al., 2014; Day et al., 2006; Francisco et al., 2010; Nishimura et al., 2000; Nishimura et al., 2001; Trautmann et al., 2006). The immune inhibitory function of PD-1 was demonstrated in PD-1 and PD-L1 knock-out mice, which presented hyperactive immune phenotypes (Nishimura et al., 1999; Nishimura et al., 2001; Rui et al., 2013), and mutations in PD-1 have been associated with disease progression in multiple human autoimmune disorders (Kroner et al., 2005; Nielsen et al., 2003; Prokunina et al., 2002). Subsequently, high expression of PD-1 has been identified as a causative agent of CD8 T cell exhaustion during chronic viral infections (Barber et al., 2006; Day et al., 2006; Fuller et al., 2013; Golden-Mason et al., 2007; Grakoui et al., 2006; Peng et al., 2008; Petrovas et al., 2006; Trautmann et al., 2006; Urbani et al., 2006). PD-1^{hi} exhausted CD8 T cells are unable to secrete normal amounts of cytokines, proliferate, or perform immune functions such as initiating cellular cytotoxicity in response to antigen recognition (Barber et al., 2006; Chen, 2004; Gallimore et al., 1998; Wherry et al., 2007; Zajac et al., 1998). Elevated PD-1 expression has also been found on poorly functional tumor infiltrating cells or cancer-specific cells during an anti-cancer immune response (Blank et al., 2004; Curiel et al., 2003; Sierro et al., 2011; Taube et al., 2014; Winograd et al., 2015), suggesting that PD-1-mediated cell exhaustion may contribute to the failure to respond to such a challenge. Thus, the expression of PD-1 is critical to the development and maintenance of a healthy and normal immune response.

Expression of PD-1 is tightly and dynamically regulated during an immune response. On resting naïve T cells, as well as in certain populations of developing thymocytes, PD-1 is expressed at low basal levels (Agata et al., 1996; Hiroyuki

Nishimura, 1996). This expression in the absence of pathogen recognition has been linked to immune tolerance (Agata et al., 1996; Hiroyuki Nishimura, 1996; Nishimura et al., 2000). Following an initial immune stimulus, PD-1 is transiently expressed on multiple immune cells types, including CD4 and CD8 T cells, B cells, macrophages, and dendritic cells (Agata et al., 1996; Costa et al., 2015; Haynes et al., 2007; Honda et al., 2014; Okazaki et al., 2001; Yao et al., 2009; Zhang et al., 2011). If the antigenic challenge is cleared, as during an acute infection, PD-1 is down regulated concurrently with antigen clearance. However, if the challenge persists, PD-1 remains highly expressed and results in functional exhaustion, which can be partially reversed by blocking PD-1/PD-L interactions with antibodies (Barber et al., 2006; Day et al., 2006; Fuller et al., 2013; Golden-Mason et al., 2007; Grakoui et al., 2006; Peng et al., 2008; Petrovas et al., 2006; Trautmann et al., 2006; Urbani et al., 2006). These antibody-based immune checkpoint blockade therapies [nivolumab (under the trade name Opdivo) or pembrolizumab (Keytruda)] have been shown to be highly efficacious in reinvigorating the anti-tumor immune response in patients with advanced cancers (Brahmer et al., 2012; Duraiswamy et al., 2013b; Goding et al., 2013; Hamid et al., 2013; Jin et al., 2010; Topalian et al., 2012; Topalian et al., 2014). It is important to note, however, that these checkpoint blockades can also be associated with potent and dangerous immune-associated adverse events, likely do to autoimmune cells also being inhibited through the PD-1 pathway.

Models for Studying PD-1 Regulation

The expression and regulation of PD-1 has been studied in a variety of model systems. In culture, PD-1 has been studied using both the EL4 mouse T cell line and isolated mouse and human primary immune cells. A variety of stimuli can activate these cells, including the small molecule drugs phorbol 12-myristate 13-acetate (PMA) and

ionomycin (Io), concanavalin A, or anti-CD3/CD28 antibodies, which acutely activate immune cells and transiently induce PD-1 expression (Agata et al., 1996; Chemnitz et al., 2004; Lu et al., 2014; Oestreich et al., 2008; Vibhakar et al., 1997). In vivo, PD-1 expression is probably most studied and best understood during infection with lymphocytic choriomeningitis virus (LCMV) (Barber et al., 2006; Blackburn et al., 2009; Gallimore et al., 1998; Mueller et al., 2010; West et al., 2013; Youngblood et al., 2011; Zajac et al., 1998). The LCMV infection model includes two strains that differ by 2 amino acids (Wherry et al., 2007). Infection with the Armstrong strain (Arm) results in an acute infection, correlating with transient up-regulation and subsequent loss of PD-1 that coincides with viral clearance. In contrast, establishing a chronic infection with the Clone-13 strain (Cl-13) results in durable PD-1 expression and concurrent immune cell dysfunction and exhaustion. Side-by-side analysis of these two infections has provided direct comparisons between the transient/acute vs. the chronic prolonged modalities of PD-1 expression in CD8 T cells. Additionally, prolonged PD-1 expression during an anti-tumor response in mice has been studied using the B16.f10 melanoma cell line or Lewis lung carcinoma (LLC) cell line, both of which are terminally tumorigenic but nonetheless immunogenic in C57Bl/6 mice (Blank et al., 2004; Overwijk and Restifo, 2001; Xiao et al., 2012). Although these different models have largely been used to study separate aspects of PD-1 regulation, in vivo inflammation models have recapitulated findings from in vitro activated cell lines. While most of the studies to date have been performed on murine cells and cell lines (Austin et al., 2014; Cho et al., 2008; Kao et al., 2011b; Lu et al., 2014; Mathieu et al., 2013; Oestreich et al., 2008; Staron et al., 2014; Xiao et al., 2012; Youngblood et al., 2011), those performed with human cells have yielded similar findings (Terawaki et al., 2011; Youngblood et al., 2013). As described below, this is likely due to conservation of important regulatory elements at the PD-1 locus. In addition

to being critical to the existing understanding of PD-1 regulation, many of these systems are employed herein to query novel elements of the PD-1 regulome.

Identifying cis regulatory elements of the Pdcd1 gene

PD-1 is encoded in the *Pdcd1* gene (Figure 1-1). At least 8 cis-elements regulate *Pdcd1* expression. Strong mammalian DNA sequence conservation coupled with DNAse I hypersensitivity assays in EL4 cells and CD8 T cells initially identified two conserved regions (*CR-B* and *CR-C*) associated with *Pdcd1* activation (Oestreich et al., 2008). These elements, which are located 100bp and 1.1kb upstream of the transcription start site (TSS), each contain multiple transcription factor binding sites. An activator protein (AP)-1 binding site is encoded within *CR-B* (Xiao et al., 2012). *CR-C* contains an interferon-stimulated response element (ISRE) (Cho et al., 2008), a nuclear factor of activated T cells (NFAT)c1 binding site (Oestreich et al., 2008), and a FoxO1 binding site (Staron et al., 2014). Reporter constructs that utilize the PD-1 promoter but do not contain the *CR-C* region failed to induce PD-1 expression in response to a variety of stimuli (Oestreich et al., 2008). Collectively, this suggests that *CR-C* is of critical importance to the observed expression patterns of the gene.

Two conserved, DNase I hypersensitive elements located -3.7 and +17.1 kb from the TSS enhanced transcriptional activity following TCR and IL-6 or IL-12 cytokine stimulation. These elements encode STAT binding sites and were found to interact directly with the *Pdcd1* promoter following ex vivo cell activation and cytokine treatment (Austin et al., 2014). Additional elements at -26.7 and +17.5 kb bind the mammalian transcriptional insulator CCCTC-binding factor (CTCF) and form constitutively interacting chromatin loops (Austin et al., 2014). Because transcriptional insulators prevent the actions of distant enhancers from controlling a downstream gene (Hou et al., 2008), these CTCF sites likely define the extreme ends of the *Pdcd1* regulatory locus.

Transcription factors inducing acute PD-1 expression

PD-1 expression on CD8 T cells correlates with the strength of TCR signaling (Barber et al., 2006; Wherry et al., 2003; Youngblood et al., 2011). TCR stimulation initiates a signaling cascade through the calcineurin pathway, resulting in activation and translocation of the transcription factor NFATc1 (Rao et al., 1997). NFATc1 binds to the *CR-C* region and is likely one of the first steps in activating *Pdcd1* gene expression (Lu et al., 2014; Oestreich et al., 2008). Blocking this pathway using the calcineurin inhibitor cyclosporine A or the NFATc1-specific inhibitor peptide VIVIT abrogated PD-1 expression (Oestreich et al., 2008), indicating that NFATc1 is necessary for initial activation-induced expression of PD-1 in CD4 and CD8 T cells. PMA/Io mediated NFATc1 binding and transcriptional activity was also found at the -3.7 and +17.1 sites, suggesting that multiple NFATc1 elements are required for driving *Pdcd1* expression or that there is genetic redundancy in the mechanism by which *Pdcd1* is induced (Austin et al., 2014). Intriguingly, NFATc1 expression is repressed at extended time points after induction and this is likely part of the mechanism for restricting PD-1 expression during acute antigen exposure (Lu et al., 2014). However, during chronic LCMV infection, NFATc1 translocation is also impaired (Agnellini et al., 2007), suggesting that other mechanisms are required to maintain or augment PD-1 expression during chronic antigen exposure.

AP-1 frequently couples with NFAT activity during T cell activation (Macian et al., 2001). TCR-mediated stimulation of the Protein kinase C/Raf pathway activates the MAP kinase cascade, ultimately leading to AP-1 activity (Macian et al., 2001). Notably, PMA/Io stimulation, originally used to identify NFATc1 binding and activity at *CR-C*, concurrently triggers this same pathway. In an LLC tumor model, over expression of the AP-1 subunit c-Fos was found to inhibit anti-tumor T cell responses by direct binding to

the AP-1 site in the *CR-B* region of *Pdcd1*. This resulted in induction of PD-1 expression in CD4 and CD8 T cells (Xiao et al., 2012). A mouse containing a mutation of this AP-1 site had less PD-1 expression on tumor-infiltrating T cells and demonstrated increased anti-tumor immunity (Xiao et al., 2012). Unlike other NFAT-coupled AP-1 sites, which are typically adjacent (Macian et al., 2001), the *Pdcd1* AP-1 site was located over 1 kb away from the NFATc1 binding site (Oestreich et al., 2008).

Additionally, the Notch pathway, which regulates T cell effector functions (Cho et al., 2009b; Maekawa et al., 2008), also regulates PD-1 expression in acute antigen settings (Mathieu et al., 2013). In an *in vitro* experiment, blockade of the Notch pathway showed a moderate, dose-dependent reduction of PD-1 expression, without affecting the overall activation of the T cell (Mathieu et al., 2013). Corroborating this, the Notch intracellular domain and the recombination signal binding protein for immunoglobulin kappa J (RBPJκ), two critical components of the Notch signaling pathway, were bound to the *Pdcd1* locus within six hours of in vitro peptide-mediated TCR stimulation. Similarly, in T cells of patients experiencing sepsis-induced immunosuppression, Notch pathway activation also correlated with PD-1 expression (Pan et al., 2015). In a model using IL-10 and LPS to cause sepsis-induced immunosuppression in CD4 T cells and macrophages, inhibition of Notch signaling again reduced PD-1 expression. Thus, the Notch pathway appears to directly augment PD-1 expression during T cell activation settings.

Inhibitors of PD-1 expression

T-box expressed in T cells (T-bet) was the first identified inhibitor of PD-1 (Kao et al., 2011b). T-bet expression influences CD8 T cell differentiation with high T-bet levels associated with short-lived effector cells and intermediate levels with memory precursor cells (Joshi et al., 2007). Following TCR stimulation or in PD-1^{lo} memory CD8 T cells from acutely infected mice, T-bet binds 500 bp upstream of the *Pdcd1* TSS (Kao et al.,

2011b). In a chronic LCMV infection, T-bet over-expression (normally only expressed at intermediate levels) was inversely correlated with PD-1 expression, resulting in a PD-1^{int} phenotype (Kao et al., 2011b). Furthermore, PD-1 expression was further increased in this infection model in a T-bet knockout mouse. In acute LCMV infections, CD8 T cells from T-bet knockout mice only showed moderately higher expression of PD-1 compared to controls, rather than the PD-1^{hi} phenotype seen during chronic or peak acute infection. Collectively, these data suggest that while T-bet does repress PD-1, T-bet alone is neither sufficient nor necessary to completely down regulate PD-1, and other factors may synergize with T-bet following an acute infection to silence gene expression.

In acute LCMV viral infection, expression of the inhibitory factor B lymphocyte induced maturation protein 1 (Blimp-1 encoded by *Prdm1*) is induced by day 8 after T cell activation, and like T-bet is necessary for terminal T cell differentiation and functional memory formation (Kallies et al., 2009; Rutishauser et al., 2009). At day 8, Blimp-1 was bound between *CR-C* and *CR-B* (Lu et al., 2014). In this system, Blimp-1 binding resulted in the direct loss of NFATc1 occupancy at *CR-C*. Blimp-1 also directly down regulated PD-1 expression in tissue culture cells. Blimp-1 mediated repression of PD-1 occurred irrespective of whether NFATc1 was overexpressed from an exogenous vector. Moreover, acute LCMV infection of a Blimp-1 KO mouse resulted in prolonged PD-1 expression on virus-specific CD8 T cells (Lu et al., 2014). These experiments indicate that Blimp-1 is necessary for normal loss of PD-1 expression following an acute infection. Furthermore, T_{FH} cells, which express high levels of PD-1, are also noted for their lack of Blimp-1 expression (Johnston et al., 2009). In germinal centers, retrovirus-mediated exogenous expression of Blimp-1 resulted in a failure to generate PD-1^{hi} T_{FH} subsets, again showing an inverse correlation between Blimp-1 and PD-1 (Johnston et al., 2009). Furthermore, BCL6, an antagonist of Blimp-1 (Shaffer et al., 2000), was

necessary for generation of a PD-1^{hi} T_{FH} population (Johnston et al., 2009). However, a direct role for BCL6 inducing PD-1 expression has not been reported.

Chronic regulators of PD-1 and factors in other cell types

The transcription factor FoxO1 promotes transcription of a number of genes necessary for homeostatic maintenance of naïve and memory T cells (Kerdiles et al., 2009). FoxO1 antagonizes the transcription factor T-bet (Rao et al., 2012), and as such is a candidate for preventing PD-1 down-regulation. In chronic LCMV infections, FoxO1 protein is highly expressed and retained within the nucleus (Staron et al., 2014). Despite FoxO1 promoting homeostatic division and relative viral control by supporting high T cell numbers, it was also necessary to generate PD-1^{hi} T cells in the chronic infection model as FoxO1 knockout mice have lower PD-1 expression. FoxO1 acted directly on the *Pdcd1* locus by binding to a region in *CR-C*, and therein induced promoter activity and PD-1 expression. Interestingly, the putative FoxO1 binding site overlaps with one of the NFATc1 binding sites in *CR-C*. This may indicate a molecular system in which FoxO1 replaces NFATc1 and can override Blimp-1's repressive activity.

To partially replicate *in vitro* some of the immune microenvironments seen in chronic infection, CD8 T cells were activated with anti-CD3/CD28 beads and treated with IL-6 or IL-12, resulting in the activation of STAT3 and STAT4 (Austin et al., 2014). Under these conditions, STAT3 and STAT4 bound the -3.7 and +17.1 regulatory regions and were able to increase PD-1 expression in conjunction with TCR signaling. The STAT proteins alone were not sufficient, as cytokine stimulation of naïve T cells without concurrent TCR stimulation did not induce PD-1 expression (Austin et al., 2014). However, this could be due in part to the low levels of IL-12 receptor on naïve CD8 T cells (Rogge et al., 1997). Intriguingly, preconditioning CD8 T cells with IL-12 and/or IFN-α (which induces STAT1 / STAT2 / IRF9 activity) resulted in higher expression of the

repressor T-bet and subsequently led to lower expression of PD-1 upon later antigen encounter (Schurich et al., 2013). Thus, cytokine exposure prior to antigen-mediated TCR signaling may have profound effects on the level of PD-1 expressed.

PD-1 regulation in macrophages in response to cytokine stimuli has also been examined. Interferon-α stimulation of macrophages resulted in interferon-stimulated gene factor (ISGF)3 complex binding to the ISRE in the *CR-C* region and induction of PD-1 expression (Cho et al., 2008). ISGF3 is a complex composed of STAT1, STAT2, and interferon regulatory factor 9 (IRF9) (Horvath et al., 1996), again implicating the STAT family of transcription factors as key members of PD-1 regulation in addition to IRF9. Type I interferon activity was subsequently examined for its effects on cultured T cells (Terawaki et al., 2011). In T cells, IFN-α alone had no effect on PD-1 expression. However, although it could not autonomously induce expression, IFN-α administered concurrently with TCR stimulation induced IRF9 binding to the ISRE and enhanced TCR-mediated PD-1 expression (Terawaki et al., 2011). Much like the cytokine-induced STAT3 and STAT4 activity, interferon-stimulated STAT1, STAT2, and IRF9 seem to have supplementary roles in increasing PD-1 expression that require additional TCR-mediated signals.

Thus, collectively, to date ten transcription factor/complexes are known to modulate PD-1, including eight activators (NFATc1, c-fos/AP-1, Notch, FoxO1, STAT3, STAT4, ISGF3, and NF-κB) and two inhibitory molecules (Blimp-1 and T-bet), which all interact with the locus in response to different stimuli. The complexity and variability of the *Pdcd1* regulome, the entire set of transcription factors and genetic elements that affect this one gene, may contribute not only to a differential expression in response to different inflammatory stimuli, including the difference between acute and chronic infection, but may also account for differential patterns seen across multiple cell types in response to the same infection.

Epigenetic regulation of Pdcd1

Epigenetics refers to a stable, heritable mechanism by which cells may maintain transcriptional profiles and corresponding states of differentiation across cell generations without modifying the underlying genetic code. Such epigenetic mechanisms include DNA methylation, histone protein modifications, and overall chromatin looping and organization, which individually or together alter the chromatin state/accessibility and control transcriptional activity of a gene (Li, 2002). These processes are widely used by the immune system to control immune cell differentiation, fate and gene expression (Araki et al., 2009; Lee et al., 2001; Scharer et al., 2013; Shih et al., 2014).

Exhausted T cells, even upon total removal of antigen, stably maintain their exhausted phenotype during subsequent divisions (Utzschneider et al., 2013). This has been demonstrated in exhausted CD8 T cells adoptively transferred from chronic LCMV-infected mice into naïve mice, in which the cells proliferated yet remained functionally exhausted and PD-1^{hi} upon re-challenge with an acute virus (LCMV Armstrong), which otherwise would not induce exhaustion (Utzschneider et al., 2013). Similarly, PD-1 levels remain high on the CD8 T cells of human patients infected with HIV but undergoing anti-retroviral therapy, which drastically decreases viral loads (Youngblood et al., 2013). These data indicate that a heritable epigenetic mechanism establishes and maintains both the exhausted phenotype and expression of PD-1 itself after the exhaustion-inducing stimulus has been removed.

DNA methylation of Pdcd1

The DNA modification 5-methylcytosine (5mC) at CpG sites in transcriptional enhancers or at gene promoters is associated with silencing gene expression (Xu et al., 2007). In mice, two CpG-rich regions upstream of the *Pdcd1* TSS (*CR-C* itself and a regulatory

region starting approximately 300 bp upstream of the promoter and labeled as *CR-B*) were dynamically methylated in CD8 T cells responding to an acute LCMV infection (Youngblood et al., 2011). Both of these regions were fully methylated in resting, naïve CD8 T cells that do not express PD-1. At day 4 following acute LCMV infection, both regions showed a profound loss of methylation that was restored at day 8. DNA methylation was inversely correlated to both PD-1 expression and viral load. By contrast, during chronic LCMV infection, the regions remained unmethylated at day 8 and later time points. Similarly, in a model of antigen tolerance induced by peptide immunotherapy, it was found that de-methylation of the *Pdcd1* locus and corresponding induction of PD-1 was necessary for tolerizing T cells (McPherson et al., 2015). This inverse correlation between DNA methylation and PD-1 expression strongly indicates a role for DNA methylation in regulating *Pdcd1* gene expression.

In patients with chronic HIV, the PD-1 regulatory region was similarly demethylated in PD-1^{hi} virus-specific cells, and unmethylated in naïve, non-exhausted PD-1^{lo} cells from the same donors (Youngblood et al., 2013). Intriguingly, patients who were on anti-retroviral therapy at the time showed no re-methylation of DNA at the PD-1 locus, despite significantly lower viral loads. This indicates that there is no mechanism to reverse DNA methylation changes at the *Pdcd1* locus in exhausted cells, regardless of changes in viral burden.

There are two general models for how a gene loses DNA methylation. In the passive model, following DNA replication a locus fails to remethylate hemimethylated CpG-containing DNA, resulting in dilution of the methylation mark over successive divisions. In an active model, CpG loci are targeted by members of the ten-eleven translocase (TET) family, resulting in an initial catalytic oxidation of the 5mC to 5-hydroxymethyl cytosine (5hmC) as an intermediate (Hashimoto et al., 2012; Tahiliani et al., 2009). Continued oxidation and base removal results in replacement of the cytosine

with a non-methylated cytosine. It should be noted that the data discussed above (Youngblood et al., 2013; Youngblood et al., 2011) used bisulfite sequencing, which does not distinguish between 5mC and the 5hmC modification. Intriguingly, 5hmC was enriched at the *Pdcd1* locus (albeit at low levels compared to 5mC) in naïve mouse CD4 T cells (McPherson et al., 2015). Both 5hmC and 5mC were lost upon CD4 T cell activation and induction of PD-1 (McPherson et al., 2015). This result would argue that demethylation of the *Pdcd1* locus upon gene induction occurs through an active and targeted mechanism. The occurrence of this transitional mark in naïve cells may indicate that the *Pdcd1* locus rests in a state capable of rapid demethylation.

The histone landscape of PD-1

Modifications to histone proteins within a chromatin region can change chromatin accessibility and affect promoter and enhancer activity, leading to changes in gene transcription. On a genomic level, enhancers are marked by histones enriched for histone H3 lysine 4 monomethylation (H3K4^{me1}) and when considered "active", also contain H3K27 acetylation (^{ac}) (Creyghton et al., 2010). When PD-1 expression was induced on CD8 T cells in vitro, H3K9^{ac} (another activation specific mark) and H3K27^{ac} were present at *CR-C* and the promoter (Lu et al., 2014; McPherson et al., 2015). The other cis elements -3.7 and +17.1 did not contain active histone marks following TCR stimulation alone even though *Pdcd1* expression was induced (Austin et al., 2014), suggesting that these elements do not play a role unless cytokine stimulation occurs. In agreement, treatment of CD8 T cells ex vivo with the cytokines IL-6 or IL-12 alone resulted in the enrichment of the histone mark H3K4^{me1} at both the -3.7 and +17.1 regulatory sites (Austin et al., 2014). Cytokine stimulation did not result in the appearance of H3K27^{ac} at these sites nor induction of *Pdcd1* expression, suggesting that cytokine treatment was in effect "licensing" the elements for activity. When cytokine

treatment and TCR stimulation were combined, both H3K4^{me1} and H3K27^{ac} were enriched at these elements, indicating the formation of an active chromatin state at these elements that contributed to increased PD-1 expression (Austin et al., 2014). Thus, distinct cytokine profiles elicited during infections are capable of manipulating the epigenetic program governing *Pdcd1* gene expression.

Following resolution of an acute CD8 T cell activation, the *CR-C* region of *Pdcd1* was enriched for the repressive histone modifications H3K9^{me3}, H3K27^{me3}, and H4K20^{me3} (Lu et al., 2014). However, H3K9^{me3} and H3K27^{me3} were absent from the locus at the same time point in chronic infection or in tolerized cells expressing high levels of PD-1, showing a correlation between appearance of these inhibitory histone profiles and loss of PD-1 expression (McPherson et al., 2015; Youngblood et al., 2011). Exogenous expression of Blimp-1 in acutely activated T cells was capable of inducing these repressive modifications, and driving down PD-1 expression (Lu et al., 2014). Although Blimp-1 itself is not known to directly modify histone proteins, it does recruit other repressive histone modifying enzymes, including the histone deacetylases HDAC1 and HDAC2, the histone methyltransferase G9a, and the H3K4$^{me2/me1}$ lysine specific demethylase LSD1 (Gyory et al., 2004; Su et al., 2009; Yu et al., 2000). It is important to note that both repressive and activating marks are absent from the locus in naïve cells (Lu et al., 2014; Youngblood et al., 2011), indicating that active repression is employed only after PD-1 induction, and that the low PD-1 expression in naïve cells may be maintained exclusively by the absence of transcriptional activators and DNA methylation.

Lysine-specific Demethylase 1 and its effects on the immune system

As already noted, the transcriptional repressor Blimp-1 is involved in silencing PD-1 expression after an acute infection (Lu et al., 2014). Surprisingly, during a chronic infection, where PD-1 levels are at their highest, Blimp-1 is also expressed in exhausted

CD8 T cells yet fails to repress PD-1 (Shin et al., 2009). In CD8 T cells from chronically infected Blimp-1 KO mice, the high levels of PD-1 expression were slightly reduced (Shin et al., 2009), suggesting a novel role for Blimp-1 in activating *Pdcd1* in these cells. The molecular mechanism for how Blimp-1 could function differentially as a repressor or activator of gene expression is unclear.

As a repressor, Blimp-1 is known to recruit additional transcriptional repressors that result in silencing the local chromatin environment (Shin et al., 2013; Su et al., 2009; Yu et al., 2000). These transcription factors include LSD1, G9a, HDAC1, and HDAC2. HDAC1 and 2 serve as histone deacetylases, while G9a is a histone methyltransferase that is complemented by the histone demethylase LSD1. (Su et al., 2009). LSD1 predominantly targets for removal the marks H3K4 mono/demethylation associated with transcriptional activation (Jenuwein and Allis, 2001; Shi et al., 2004), thereby facilitating gene silencing. Furthermore, LSD1 has been shown to directly repress immune genes (Janzer et al., 2012; Su et al., 2009). Given the ability of Blimp-1 to repress genes through recruitment of histone modifiers such as LSD1, these cofactors are likely mediators of the PD-1 phenotypes seen in Blimp-1 knockout mice following an acute stimulation, and differential recruitment by Blimp-1 of factors such as LSD1 during chronic infection could account for the failure to down-regulate PD-1 in the continued presence of high Blimp-1.

PD-1, immune memory, and programming T cell fate

Following an acute immune response, the highly expanded polyclonal population of short-lived effector T cells generated in response to the challenge contracts, leaving behind a sub-population of long-lived memory cells (Whitmire and Ahmed, 2000). This memory population persists in the absence of antigen (Kaech et al., 2002b). However unlike naïve T cells, which are constantly regenerated from thymocyte progenitors,

memory cells are able to homeostatically proliferate in order to maintain a population of constant specificity (Goldrath et al., 2002). Upon a secondary encounter with antigen, memory cells respond with a greater antigenic affinity (Busch and Pamer, 1999; Kim et al., 1999; van Faassen et al., 2005), enhanced proliferative capacity (Pihlgren et al., 1999; Veiga-Fernandes et al., 2000), and an induction of effector molecules greater in both speed and quantity (Kersh et al., 2006; Pihlgren et al., 1999; Zimmermann et al., 1999) compared to naïve cells. This enables the immune system to more rapidly clear re-infection by a conserved pathogen. Intriguingly, interrupting PD-1 signaling either by genetic deletion or antibody blockade skews CD8 T cell populations away from effector cells towards a memory phenotype (Allie et al., 2011; Ribas et al., 2016; Rutishauser et al., 2009). Thus, modulating PD-1 expression to shape immunological memory may be a valuable consideration during vaccine design. Whether the observed changes in memory are due to altered PD-1 signaling during the secondary response, or differential programming following the primary response have not yet been elucidated.

Novel technologies for studying T cells

Recent technologies have made more accessible the profiling of immune cell populations. The Assay for Transposase Accessible Chromatin (ATAC)-seq provides a genome-wide overview of chromatin structure, based on genomic accessibility to Tn5 transposase (Buenrostro et al., 2013). This assay cannot discern the underlying molecular modifications that define a region as active or silenced, such as DNA methylation, histone methylation and acetylation, and chromatin looping. However, it can differentiate accessible, and therefore presumably active, chromatin from silenced regions on a genome-wide basis using comparatively small populations of cells, making it a useful tool for analyzing programming changes in rare populations such as memory

cells, early virus-specific cells, and even cells that have undergone a specific number of divisions.

With the advent of cheaper sequencing, and single cell sequencing assays that have also become more accessible to more researchers in recent years, the systems biology approach to analyze global changes in cell populations has enabled new discoveries in T cell development, differentiation and function. In particular, single cell RNA sequencing (scRNA-seq) has allowed the identification of unique sub-populations of cells from within a bulk-sorted population. This has made it possible to identify the dynamics of the T cell response to antigens when combined with trackers of cell division (Kakaradov et al., 2017). By identifying and characterizing unique transcriptional profiles of individual cells after a single round of division, such assays suggest that T cell differentiation is coupled with asymmetric division upon initial antigen encounter.

Herein, the mechanisms that govern PD-1 expression in multiple inflammatory environments and across different cell types are explored. The mechanisms that drive PD-1 induction in B cells, CD4 T cells, and macrophages are examined. Furthermore, the role of the cis-regulatory element *CR-C* in regulating PD-1 expression is studied. I will further explore how loss of PD-1 expression due to a *CR-C* knockout affects T cell memory formation. Finally, I illustrate how the histone modifying enzyme LSD-1 modifies the epigenetic landscape around PD-1 in different inflammatory environments, and drives differential expression in acute vs chronic infections. In addition to providing an understanding of which active immune environments may induce and be affected by PD-1's function, knowledge of the molecular mechanisms regulating PD-1 may help tailor future immunotherapies for fighting cancer, chronic HIV and HCV infections, or prevention of allergic responses, transplant rejection, and autoimmunity (McPherson et al., 2015), as well as boosting long-lived memory responses to vaccines (Allie et al., 2011).

Figure 1

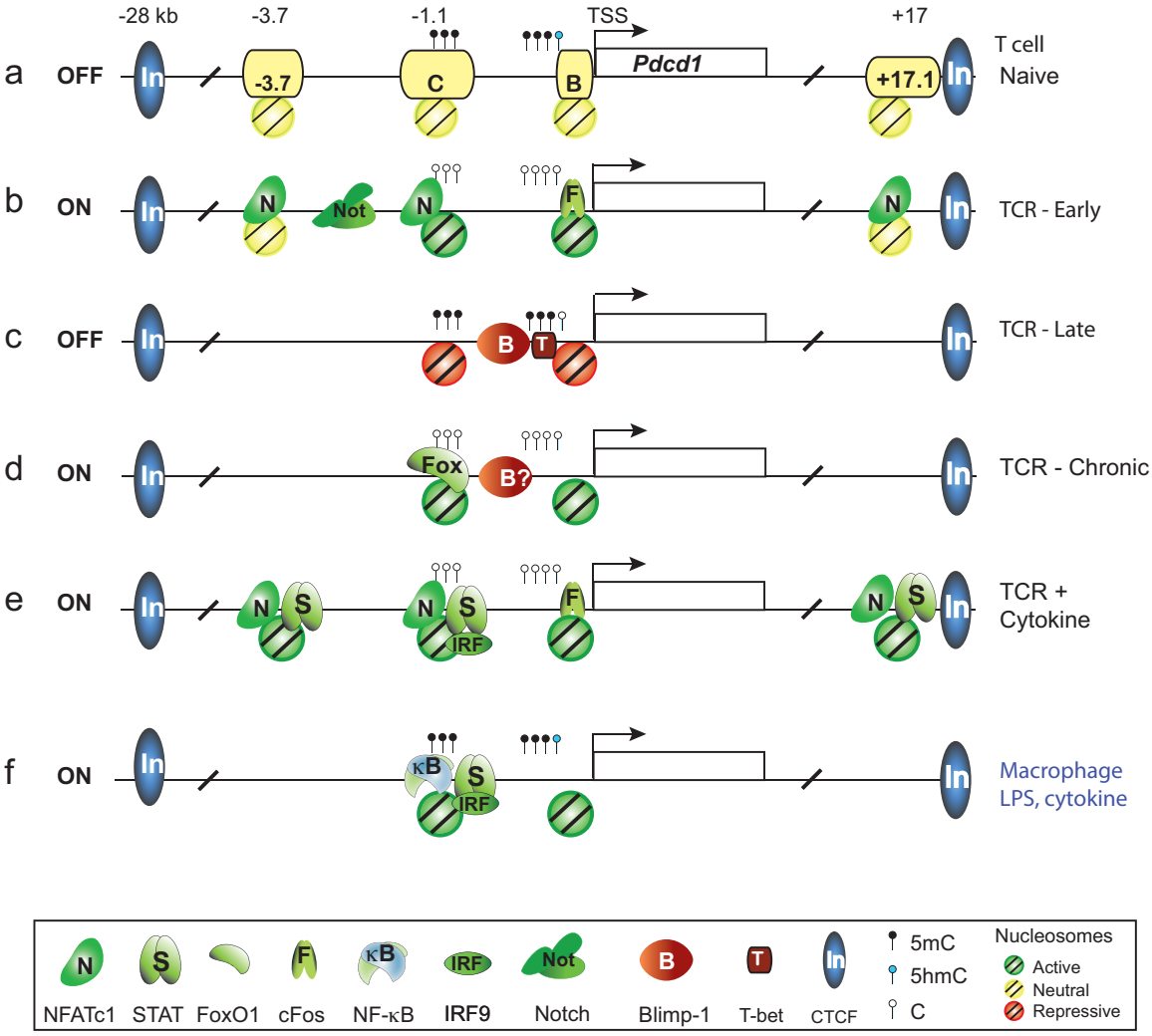

Figure 1- 1: Summary of the *Pdcd1* regulome

Chapter 2: Regulation of PD-1 in B cells, CD4 T cells, and Macrophages

Alexander P.R. Bally[†], Peiyuan Lu[†], Yan Tang[†‡], James W. Austin[⇑], Christopher D. Scharer[†], Rafi Ahmed[†], and Jeremy M. Boss[†]

[†]Department of Microbiology & Immunology and Emory Vaccine Center, Emory University School of Medicine, Atlanta, GA 30322;

[‡]Xiangya School of Medicine, Central South University, Changsha, Hunan, China 410008;

[⇑] Current Address: Laboratory of Immunology, National Institute of Allergy and Infectious Diseases, National Institutes of Health, 9000 Rockville Pike, Bethesda, MD 20892, USA.

*Originally published in the *Journal of Immunology*. Bally AP, Lu P, Tang Y, Austin JW, Scharer CD, Ahmed R, Boss JM. NF-κB regulates PD-1 expression in macrophages. J Immunol. 2015 May 1;194(9):4545-54.

Introduction

During immune activation and chronic inflammation, elevated levels of the co-inhibitory receptor Programmed Cell Death-1 (PD-1) appear on a variety of immune cells, including CD4 and CD8 T cells, NKT cells, B cells, dendritic cells, and macrophages (Agata et al., 1996; Moll et al., 2009; Yao et al., 2009; Zhang et al., 2011). PD-1, also known as CD279, is a member of the B7/CD28 group of immunoglobulin superfamily receptors (Ishida et al., 1992) and is encoded by the *Pdcd1* gene. When PD-1 is engaged by its ligands PD-L1 and -L2, it mediates immune cell suppression via an immunoreceptor tyrosine-based inhibitory motif and an immunoreceptor tyrosine-based switch motif located in its cytoplasmic tail (Chemnitz et al., 2004; Parry et al., 2005). In CD8 T cells, PD-1/PD-L interactions are responsible for the characteristic exhausted phenotype observed during chronic viral infections, which is defined by poor cell division, cytokine secretion, and cellular cytotoxicity in response to stimuli (Day et al., 2006; Wherry et al., 2003). Causality of PD-1 inducing exhaustion has been demonstrated through antibody blockade against either PD-1 or its ligands, which reverses this exhaustion (Barber et al., 2006; Butler et al., 2012; Dirks et al., 2013; Golden-Mason et al., 2007; Trautmann et al., 2006; West et al., 2013). More recently, PD-1/PD-L1 blockade produced durable, objective responses in some patients with advanced stage melanomas, non-small-cell lung cancers, and renal-cell cancers (Brahmer et al., 2012; Hamid et al., 2013; Topalian et al., 2012).

While PD-1 is expressed on a variety of immune cell types and at a number of different stages of immune development and inflammation, mechanisms governing its expression are best defined in CD8 T cells. In CD8 T cells, activation of NFATc1 drives transient expression of PD-1 following TCR-stimulation during the initial phases of antigen recognition (Oestreich et al., 2008). This process may be augmented by various

cytokines signaling through STAT transcription factors (Austin et al., 2014; Terawaki et al., 2011), as well as cell activation-driven c-Fos (Cho et al., 2008; Xiao et al., 2012). During the late stages of an acute CD8 T cell effector response, the transcriptional repressor Blimp-1 is expressed and directly silences PD-1 expression through a process of chromatin reconfiguration, ultimately resulting in the loss of NFATc1 binding (Lu et al., 2014). Various cis-regulatory elements play roles in these processes, including regions conserved in mammalian genomes, termed Conserved Regions (CR) -B and -C (Oestreich et al., 2008). To activate PD-1 transcription, NFATc1 binds to CR-C (Oestreich et al., 2008) and c-Fos binds to a site located in CR-B (Cho et al., 2008). A sequence between CR-B and CR-C contains the binding site for Blimp-1 (Lu et al., 2014). Additional DNase I-hypersensitive regions located -3.7 kb upstream or +17.1 kb downstream of the transcriptional start site (TSS) bind NFATc1 in response to TCR stimulation, as well as STAT proteins following signals from IL-6 or IL-12 (Austin et al., 2014; Oestreich et al., 2008). Additionally, the regulatory regions around CR-B and CR-C upstream of the promoter are subject to dynamic DNA methylation that correlates directly with the expression of the PD-1 gene in both acute and chronic T cell activation (Youngblood et al., 2011).

In addition to CD8 T cells, PD-1 expression in other cell types impacts immune function. High PD-1 expression is necessary for regulatory T cell (Treg) development, and follicular helper T (T_{FH}) cells also constitutively express high PD-1 (Boussiotis et al., 2014; Crotty, 2011; Francisco et al., 2010; Johnston et al., 2009), although PD-1 regulation has not been studied in this population. Furthermore PD-1 induction on circulating CD4 T cells slows the immune response during initial acute antigen recognition by reducing tissue residency and cytokine production, as well as by decreasing formation of helper cells during the early immune response (Honda et al., 2014; Rui et al., 2013), presumably acting to reduce inflammation-induced tissue

damage. Reduced PD-1 expression on T_{FH} cells is linked to decreased antibody responses, suggesting a vital role for PD-1 in T cell help (Haynes et al., 2007). Viremic, HIV-infected patients express substantially more PD-1 on the surface of blood monocytes compared to both aviremic HIV-infected individuals and healthy donors (Said et al., 2010). When expressed on macrophages and monocytes, PD-1 expression correlates with increased IL-10 and decreased IL-12 levels in the blood of HIV-infected patients, which in turn limits T cell responses against the infection (Cho et al., 2009a; Said et al., 2010). A variety of bacterial-derived Toll-like Receptor (TLR) ligands, including lipopolysaccharide (LPS) and CpG DNA, induce PD-1 expression on human macrophages (Said et al., 2010), suggesting a role for TLR signaling pathways in regulating PD-1. Additionally, PD-1 expression in macrophages can be induced by multiple cytokines. IFN-α signaling through STAT1/2 heterodimers and an interferon-sensitive response element leads to increased PD-1 expression, as does treatment with TNF-α, IL-1β, or IL-6 (Cho et al., 2008; Terawaki et al., 2011). However, cytokine-stimulated regulation of PD-1, particularly when signaling through STAT proteins or interferon response factors, does not correlate with the observed increases in PD-1 expression levels induced directly by TLR ligands in these cells nor does it adequately address modulation of PD-1 levels seen in vivo. Although no “exhausted”-like phenotype has been observed in macrophages expressing PD-1, the induced anti-inflammatory cytokine profile in PD-1- expressing macrophages has ramifications for the proper functioning of the immune system during infection.

TLR signaling is of vital importance in the early immune response prior to the engagement of the adaptive immune system and the corresponding cytokines secreted at that time. In response to its ligands, transcriptional signaling through TLRs is mediated by NF-kB (Piras and Selvarajoo, 2014). While NF-κB activation can occur through multiple distinct pathways, this transcription factor has not been shown

previously to be involved in PD-1 regulation. Here we have investigated the fundamental mechanisms that initiate PD-1 expression following cellular activation of B cells, CD4 T cells, and macrophages. Although each produced varied levels of induction, IgM crosslinking of B cells, TCR-mediated activation of CD4 T cells, or treatment PMA and ionomycin (Io) resulted in PD-1 expression through pathways that were inhibited by cyclosporine A (CsA), implicating NFAT as the critical inducer/activator of PD-1 expression in these cell types. In contrast, following stimulation of macrophages with TLR ligands, PD-1 expression was induced by NF-κB. Furthermore, PD-1 expression in macrophages was unaffected by either engagement or disruption of the calcineurin pathway, making macrophages the first cell type found to regulate PD-1 independent of NFATc1. Following LPS stimulation, the NF-κB subunit p65 bound CR-C at a consensus site. p65 binding to CR-C was coupled with histone modifications associated with gene activation and increased accessibility of the region. Intriguingly, the CR-B region, which loses DNA methylation in a manner that follows PD-1 expression in effector CD8 T cells (Youngblood et al., 2011), remained fully methylated following LPS stimulation and increased PD-1 expression. Thus, these results demonstrate that the pathways that mediate PD-1 expression in macrophages are distinct from those used in lymphoid cells.

Methods

Cell Lines and Mouse Strains

The murine macrophage line RAW264.7 and fibroblast cell line L-929 were obtained from American Type Culture Collection and cultured in DMEM supplemented with 10% FBS and 100 U/ml penicillin/streptomycin. Primary CD4 T cells and primary B cells were isolated from wild-type C57BL/6 mouse spleens using negative selection magnetic bead separation columns (Miltenyi Biotech Inc., San Diego, CA) according to the

manufacturer's instructions. Primary bone-marrow derived macrophages (BMDMs) were prepared from femur bone marrow of C57BL/6 or MyD88^{tm1Aki} mice as previously described (Zhang et al., 2008). Briefly, bone marrow cells were isolated from mouse femurs and cultured for 7 days in DMEM with 10% FBS, 100 U/mL penicillin/streptomycin, and 20% L-929 cell line-conditioned media, which contains cell line-produced M-CSF. Purity of BMDMs was determined by flow cytometry for CD11b+, CD11c-, and MHC-II+ and was >90%. Where indicated, cells were treated with anti-CD3/CD28 activation beads (Life Technologies Co, Grand Island, NY) according to manufacturer's protocol, 50 ng/ml PMA (Sigma-Aldrich Co. LLC, St. Louis, MO) and 2 μM Io (Sigma-Aldrich Co. LLC, St. Louis, MO), 2.5μg/ml F(ab)$_2$ anti-IgM (Jackson Immuno Research Inc., West Grove, PA), 10μg/ml lipopolysaccharide (Sigma-Aldrich Co. LLC, St. Louis, MO), 10μg/ml zymosan (InvivoGen, San Diego, CA), 5μg/ml Poly(I:C)-LMW (InvivoGen, San Diego, CA), 1 μg/ml CsA (Sigma-Aldrich Co. LLC, St. Louis, MO), 8μM helenalin (Santa Cruz Biotechnology Inc., Santa Cruz, CA), or 3μM BMS 345541 (Sigma-Aldrich Co. LLC, St. Louis, MO) for the times indicated. All animal experiments were conducted in accordance with protocols approved by the Emory University Institutional Animal Care and Use Committee.

Flow cytometry and antibodies

Cells were stained for flow cytometry at 4° C for 30 minutes in FACS buffer (PBS, 1% BSA, and 1mM EDTA) plus appropriate antibodies and fixed in 0.1% paraformaldehyde for at least 1 hour. Magnetically sorted B cells were gated on CD19+ B220+ CD11b- and CD11c- events. Magnetically sorted CD4 T cells were gated on CD3+ CD8- CD4+ CD11b- and CD11c- events. Primary BMDMs were gated on CD11b+ CD11c- MHCII+ cells. RAW 264.7 macrophages, primary BMDMs, T cells, and B cells were also stained

with anti-PD-1 antibody for analysis. Antibodies used were CD4 PerCP-Cy5.5 (clone RM45, Tonbo Biosciences Corp., San Diego, CA), CD8 FITC (clone 53-6.7, Tonbo Biosciences Corp., San Diego, CA), CD19 FITC (clone 1D3, BD Pharmingen, San Diego, CA), B220 APC (clone RA3-6B2, BD Pharmingen, San Diego, CA), CD11b FITC (clone M1/70 BD Pharmingen, San Diego, CA), CD11C APC (clone HL3, BD Pharmingen, San Diego, CA), PD-1 PE (clone RMP1-30, Biolegend Inc., San Diego, CA). Flow cytometry was performed on a BD LSR-II and analyzed using FlowJo 9.6.4 software.

mRNA quantification by RT-qPCR

Total RNA was isolated from cells using the RNeasy kit (Qiagen Sciences Inc., Germantown, MD). cDNA was prepared from 1µg RNA using the SuperScript II reverse transcriptase (Life Technologies Co, Grand Island, NY). PD-1 mRNA levels were quantified in technical duplicates by real-time PCR. Primers used for real-time PCR are listed in Table 2-1. qRT-PCR experiments were performed from three independent RNA preparations. The data presented were normalized to 18s ribosomal RNA levels using a $\Delta\Delta$CT analysis as described previously (Yoon et al., 2012)

Bisulfite Sequencing

The protocol for bisulfite sequencing was adapted from Youngblood et al. (Youngblood et al., 2011). Briefly, genomic DNA from BMDMs cultured in the presence or absence of LPS for 24 hours was isolated and bisulfite converted using the EpiTect Bisulfite Kit (Qiagen Sciences Inc., Germantown, MD). Bisulfite converted DNA was amplified via PCR and cloned using the TOPO TA cloning kit (Life Technologies Co., Grand Island, NY). Primers used for cloning are listed in Table 2-1. Three independent DNA preparations were used and approximately 8 colonies were selected for Sanger

sequencing (Beckman Coulter Genomics, Danvers, MA) from each preparation. Data were aligned to the *in silico* bisulfite converted genome using the R / Bioconductor Biostrings package and custom scripts as previously describe (Scharer et al., 2013). Following compilation of the data, a Fisher's exact test was used to determine the statistical significance between samples.

Cloning and Luciferase Gene Reporter Assays

DNA sequences containing the *Pdcd1* promoter, CR-B, and CR-C regions with mutated potential NF-κB binding sites were generated by PCR from existing plasmids (Austin et al., 2014; Oestreich et al., 2008) using primers listed in Table 2-1. These sequences were cloned into a pGL3-Basic luciferase reporter vector (Promega Co, Madison, WI) using *Xho*I (New England Biolabs Inc., Ipswitch, MA). All clones were verified by DNA sequencing. Cell transfections were performed using an Amaxa Nucleofector® II instrument. 2 x 10^6 RAW264.7 cells were transfected in 100 µl of a solution of 120mM $NaPO_4$ buffer pH 7.2, 5mM KCl, and 15mM $MgCl_2$ with 200 ng of pRL-TK *Renilla* luciferase gene plasmid and 1,000 ng of indicated firefly luciferase reporter plasmid. Transfected cell populations were split into multiple cultures for different treatments and allowed to rest in culture for 16 h. Cells were subsequently stimulated with LPS or helenalin for the times indicated. Luciferase activities of the reporter plasmids were quantified using the Dual-Glo Luciferase Assay System (Promega Co, Madison, WI), and the Firefly luciferase activity was normalized to luminescence of the constitutively active *Renilla* gene. All transfections were performed at least three times. Data were plotted as mean plus standard deviation and statistical significance was determined by ANOVA.

Chromatin Immunoprecipitation.

Chromatin immunoprecipitation (ChIP) assays were performed as previously described (Beresford and Boss, 2001; Lu et al., 2014). Chromatin was prepared from RAW 264.7 cells treated with LPS for 4 hours and crosslinked in 1% formaldehyde for 10 minutes. Chromatin was sonicated to an average length of 400-600bp. 5 µg of chromatin was immunoprecipitated with Protein A beads using 0.5µg of antibodies for control IgG (rabbit polyclonal antibody, EMD Millipore, Billerica, MA), NF-κB p65 (clone sc-372, Santa Cruz Biotechnology Inc., Santa Cruz, CA), H3K4me1 (rabbit polyclonal antibody, EMD Millipore, Billerica, MA), H3K4me3 (rabbit polyclonal antibody, EMD Millipore, Billerica, MA), or H3K27ac (rabbit polyclonal antibody, EMD Millipore, Billerica, MA). Immunoprecipitates were then quantitated by quantitative real-time PCR and calculated as a percent of input. Primer sets used in these assays are provided in Table 2-1. All ChIP assays were performed at least three times from independent experiments. The data were averaged and plotted as percent of input chromatin.

Statistical analyses

Statistical significance was calculated using Student's t-test in Microsoft Excel, Fisher's Exact test, or a 2-Way ANOVA with repeated measures using a Bonferroni post-test calculated by GraphPad Prism 4.0 software, where appropriate. * indicates $p<.05$; ** indicates $p<.01$; and *** indicates $P<.001$.

Results

NFATc1 regulates PD-1 on B and T cells, but not Macrophages

Although the basic mechanisms of *Pdcd1* gene induction in CD8 T cells has been explored, little is known about its regulation in CD4 T cells, B cells, or macrophages. A variety of CD4 T cells express PD-1, including effector cells upon initial activation and T_{FH} cells, which constitutively express PD-1 within germinal center reactions (Haynes et

al., 2007). Like T cells, B cells and macrophages also display a transient increase in PD-1 expression upon initial activation (Zhang et al., 2011). To explore the general activation of PD-1 ex vivo, mouse splenic CD4 T cells and B cells were isolated and stimulated with PMA and Io, a process that directly activates cells through their antigen receptor pathways (Davis and Lipsky, 1986). Following a 48 h stimulation with PMA/Io or anti-CD3/CD28 beads, CD4 T cells showed a durable response with greater than 50% of cells expressing PD-1 (**Figure 2-1A**). B cells stimulated with PMA/Io for 24 h displayed a high level of PD-1 expression with over 90% expressing PD-1 (**Figure 2-1B**). Likewise, upon activation of the B cell antigen receptor by crosslinking with anti-IgM, ~40% of the cells became PD-1 positive, but this level was not as high as with PMA/Io (**Figure 2-1B**). Thus, PD-1 expression can be induced ex vivo on both CD4 T and B cells through engagement of their antigen receptors or through processes that mimic receptor signaling and activation of the calcineurin pathway.

To determine if the induction of PD-1 in CD4 T cells and B cells was mediated by processes similar to that of CD8 T cells, which utilize NFATc1 as the primary activator of PD-1 expression following T cell receptor stimulation (Oestreich et al., 2008), the calcineurin pathway inhibitor Cyclosporine A (CsA) was used (**Figure 2-1**). Prior to activation, NFATc1 is phosphorylated and resides in the cytoplasm. Upon activation, the phosphatase calcineurin dephosphorylates NFAT proteins, facilitating their translocation to the nucleus. CsA blocks the activity of calcineurin in this process and ultimately prevents the activation of NFAT (Bernardi et al., 1993; Liu, 1993). PD-1 surface expression induced in primary murine CD4 T cells activated with anti-CD3/CD28 beads or PMA/Io was completely blocked by pre-treatment of cells with CsA **(Figure 2-1A**). Similarly, PD-1 surface expression in B cells was inhibited fully by treatment with CsA irrespective of whether stimulation was through PMA/Io or anti-IgM crosslinking (**Figure 2-1B**). Collectively, these data implicate the same NFAT pathway that modulates PD-1

expression in CD8 T cells is the primary driver of expression in both CD4 T cells and B cells in response to stimuli targeting their respective antigen receptors. In contrast, treatment of RAW267.4 cells (a murine macrophage cell line) with PMA/Io failed to induce PD-1 (**Figure 2-1C**), indicating that the NFAT-mediated pathway is non-functional in inducing PD-1 in this macrophage cell line. This result was recapitulated in primary bone marrow derived macrophages (BMDMs) (**Figure 2-1D**), again showing that macrophages do not induce PD-1 through the PMA/Io-induced NFAT pathway.

TLR agonists are common activators of macrophages (Cohen and Mosser, 2013), and have previously been correlated with increased PD-1 surface expression in peripheral blood monocytes (Said et al., 2010). Treatment of primary CD4 T cells using LPS, a potent stimulator of TLR4, yielded no changes in expression of PD-1 (**Figure 2-2A**), indicating that this pathway was not involved in PD-1 regulation in CD4 T cells. However, treatment of either B cells, RAW264.7 macrophage cells, or primary macrophages with the TLR4 ligand LPS resulted in a robust induction of PD-1 with nearly 90% of B cells and RAW264.7 cells (**Figure 2-2B and 2-2C**) or 55% of primary BMDM cells (**Figure 2-2D**) responding. Pretreatment of either B cells, RAW267.4 cells, or primary macrophages with CsA prior to stimulation with LPS showed no effect in reducing PD-1 expression on the above cells (**Figures 2-2B, 2C,** and **2D**), suggesting that PD-1 induction through this TLR pathway was independent of calcineurin signaling. Thus, distinct pathways may be utilized by different cell types in response to different classes of stimuli; TCR/BCR mediated through the NFATc1 pathway and TLR mediated through an independent mechanism.

To correlate surface protein levels of PD-1 with *Pdcd1* gene transcription, *Pdcd1* mRNA levels in B cells, CD4 T cells, and RAW264.7 cells following activation were compared with and without inhibition of the calcineurin/NFATc1 pathway with CsA. B cells induced by anti-IgM antibody or PMA/Io exhibited a 10 and 30 fold induction of

Pdcd1 mRNA expression, which was inhibited by treatment with CsA (**Figure 2-3A, left**). Similarly, CD4 T cells also failed to upregulate *Pdcd1* mRNA in response to CD3/CD28 beads or PMA/Io stimulation following inhibition with CsA (**Figure 2-3A, middle**), again indicating that both of these cell types require NFAT activation to induce *Pdcd1* expression. As seen in surface protein expression, PMA/Io failed to induce *Pdcd1* mRNA in RAW 264.7 cells (**Figure 2-3A, right**). As above, and correlating with protein expression, LPS induced *Pdcd1* mRNA in B cells and RAW264.7 cells, but not in CD4 T cells (**Figure 2-3B**). As above, CsA had no effect on LPS-activated *Pdcd1* mRNA in RAW264.7 cells (**Figure 2-3B**). These data demonstrate that LPS-mediated induction of *Pdcd1* in macrophages occurs through a pathway that is independent of the NFAT/calcineurin pathway used by antigen receptors in lymphocytes. Given that macrophages modulate PD-1 mRNA and surface expression independently of the previously described NFAT-dependent mechanism, *Pdcd1* gene regulation in macrophages was further examined.

NF-κB governs PD-1 induced by TLR ligands

TLR signaling in macrophages can result in the activation of multiple transcription factor pathways, including members of NF-κB family of transcription factors such as p65/p50 heterodimers (Piras and Selvarajoo, 2014). To determine if NF-κB plays a role in PD-1 regulation in macrophages, helenalin, a selective NF-κB inhibitor that works by alkylation of the DNA binding site of p65 (Buchele et al., 2010; Lyss et al., 1998), was used to examine the dependence on p65 for induction of PD-1 expression in macrophages. Treatment of RAW264.7 cells with helenalin resulted in complete ablation of *Pdcd1* induction by LPS (**Figure 2-4A**, left). To verify these results, and rule out possibilities of off-target effects of treatment with helenalin, TLR stimulated RAW264.7 cells were treated with BMS-345541, an alternative inhibitor that blocks p65 activity by neutralizing

the function of the IκB kinase complex (Burke et al., 2003). Macrophages treated with this small molecule inhibitor also exhibited a complete loss of *Pdcd1* mRNA induction triggered by LPS (**Figure 2-4A**, right), confirming the findings with helenalin.

TLR2 and TLR3 signal through distinct pathways that are each shared with TLR4. TLR2 utilizes the MyD88 pathway (Kawai et al., 1999); whereas TLR3 uses the TRIF pathway (Piras and Selvarajoo, 2014; Yamamoto et al., 2003). To identify relevant signaling pathways and to determine if other toll-like receptors could similarly induce *Pdcd1* expression, RAW264.7 cells were activated with zymosan and Poly(I:C) to stimulate TLRs 2 and 3, respectively. While zymosan robustly induced PD-1 expression, Poly(I:C) failed to modulate PD-1 mRNA levels. Moreover both p65 inhibitors, helenalin and BMS-345541, fully blocked the zymosan-induced PD-1 expression (**Figure 2-4B**).

To verify that experiments performed in a macrophage cell line reflect similar events in primary cells, bone marrow-derived macrophages (BMDMs) were treated with the TLR ligands zymosan, Poly(I:C), and LPS. The effects of NF-κB inhibition by helenalin was also examined in these cells at 4 h post treatment. As observed in RAW264.7 cells, primary BMDMs showed an increase in PD-1 mRNA in response to zymosan and LPS that was fully blocked by helenalin-mediated inhibition of p65 (**Figure 2-4C,** top). Surface expression of PD-1 following LPS stimulation was also examined on BMDMs. In this experiment, a 24 h time point was used. Because helenalin shows cytotoxicity at 24 hrs (but not at 4 h), BMS-345541, which is not toxic at 24 h (data not shown) was used to inhibit NF-κB activity. As observed in RAW264.7 cells, induction of surface PD-1 in primary macrophages by LPS was fully blocked upon NF-κB inhibition (**Figure 2-4D**).

Together, these data indicate that *Pdcd1* expression triggered by TLR-2 or TLR-4 stimuli in macrophages, but not in the TRIF-dependent TLR-3 activation pathway, acts through the p65 subunit of NF-κB and thus may be mediated through the MyD88 pathway. To test the involvement of MyD88 in activating the NF-κB pathway to induce *Pdcd1*, the

same experiment was repeated in BMDMs derived from MyD88$^{-/-}$ knockout mice. In cells from these mice, zymosan-driven expression of PD-1 was not observed (**Figure 2-4C,** bottom), consistent with a MyD88-dependent pathway for PD-1 induction. When treated with LPS, however, MyD88$^{-/-}$ BMDMs still induced PD-1 mRNA to approximately two-thirds of that observed in wild-type BMDMs (**Figure 2-4C**). The decrease in PD-1 expression is consistent with the MyD88-dependent hypothesis. However, the residual expression that is seen may be due to MyD88/TRIF independent activation of cells by LPS, as was recently reported in TLR4$^{-/-}$ mice in which LPS was still able to induce inflammatory responses through non-canonical pathways (Hagar et al., 2013; Kayagaki et al., 2013).

Cis-elements in CR-C regulate LPS-triggered PD-1 expression

A recent ChIP-seq study performed in macrophages activated with the TLR4 agonist KLA examined the binding of the NF-κB subunit p65 across the macrophage genome (Kaikkonen et al., 2013). Peaks of p65 occupancy appeared at multiple sites within the *Pdcd1* gene following macrophage activation. The strongest peak in this region appeared within CR-C, with notable peaks located -3.7 and +17.1 kb from the TSS (Kaikkonen et al., 2013). CR-C, the -3.7, and the +17.1 regions were previously shown to be responsible for NFATc1- and STAT3-mediated activation of *Pdcd1* (Austin et al., 2014). To determine if these regions continue to function in gene regulation in response to LPS signaling, luciferase reporter constructs containing the *Pdcd1* promoter driving a firefly luciferase reporter gene in the pGL3 basic plasmid vector were utilized as described previously (Austin et al., 2014). In these plasmids, the *Pdcd1* promoter was contiguous with CR-B (pPD-1 B), CR-B and CR-C (pPD-1 B/C), or with CR-B spliced together with the -3.7 (pPD-1 B/3.7) or +17.1 (pPD-1 B/17.1) regions, as illustrated in **Figure 2-5A**. These reporter plasmids were cotransfected into RAW264.7 cells along

with a Renilla control luciferase gene reporter, and cells were activated with LPS with or without helenalin to assess the contribution of NF-κB p65 (**Figure 2-5B**). The pPD-1 B/C plasmid responded to LPS treatment with increased activity, while the pPD-1 B, pPD-1 B/3.7 and pPD-1 B/17.1 plasmids failed to respond to LPS in these cells (**Figure 2-5B**). However, the untreated, background levels of pPD-1 B/3.7 and pPD-1B/17.1 showed significant expression of the reporter gene compared to the inactive pPD-1 B plasmid, suggesting that additional factors or mechanisms in these cells could contribute to a basal level of PD-1 expression through these elements in an LPS-independent manner. When cells were simultaneously cultured with LPS and helenalin to block NF-κB activity, the LPS-mediated induction of the reporter construct observed with the pPD-1 B/C plasmid was abrogated (**Figure 2-5B**), indicating not only that the LPS-responsive DNA element resides solely within CR-C, but also that activity of this cis-element requires NF-κB. It should be noted that the level of luciferase induction in Figure 2-5B is lower than that observed in earlier experiments due to the short 4 h LPS stimulation that was required due to toxicity associated with helenalin in transfected RAW 264.7 cells at 24 h time points.

A 10 bp Site within CR-C is required for PD-1 induction by LPS

To locate the specific sequence and cis-acting DNA element where NF-κB is acting on PD-1, the LPS-responsive CR-C sequence, located in the pPD-1 B/C plasmid, was analyzed using the online JASPAR database (located at jaspar.genereg.net) to find predicted NF-κB p65/RELA binding sites based on established transcription factor binding site motifs. Two potential binding sites were highly predicted within the pPD-1 B/C plasmid, and corresponded with sequences excluded from the unresponsive pPD-1 B plasmid. The highest predicted sequence 5'GGGGATCCCC is located near the

middle of the CR-C conserved region. A slightly lower predicted sequence, 5'AGAATGCCCC resides at the proximal end of CR-C and correlates with the center of the p65 ChIP-seq peak (Kaikkonen et al., 2013). These two potential binding sites were scrambled to 5'TGTAGCAATT or 5'TCTAACCTCT, respectively, sequences that were predicted to have no NF-κB p65 or other transcription factor binding potential. The scrambled sequences were then cloned into the pPD-1 B/C plasmid, subsequently termed pPD-1 B/C κB1 or pPD-1 B/C κB2, for the higher and lower predicted binding sites, respectively (**Figure 2-5A**). Mutant plasmids, the wild-type pPD-1 B/C plasmid, or empty pGL3 basic vector were nucleofected into RAW264.7 cells and activated with and without LPS for 24 hours. In this system, the mutant pPD-1 B/C κB2 vector showed a near complete loss of induction following LPS treatment (**Figure 2-5C**). In contrast, both the wild-type and pPD-1 B/C κB1 constructs showed greatly increased reporter activity in response to LPS activation at a comparable level to each other (**Figure 2-5C**). These data demonstrated that the κB2 site but not κB1 was the functional NF-κB site required for LPS-initiated *Pdcd1* gene activation through CR-C. Additionally, the fact that κB1 reporter vector did not change its expression level provided a mutated control for these experiments.

NF-κB p65 binds to the CR-C region

To prove that the LPS responsive element in CR-C is in fact the site to which p65 binds and from which it can directly promote PD-1 expression in this system and to validate the previous ChIP-seq data, a chromatin immunoprecipitation paired with qPCR (ChIP-qPCR) assay was performed. In addition to CR-C, the -3.7 and +17.1 regions associated with the two other major NF-κB peaks from the ChIP-seq dataset (Kaikkonen et al., 2013) in *Pdcd1* were also examined even though these regions did not

demonstrate LPS responsiveness on their own in the above luciferase assays. Using a p65 specific antibody, a nearly 10-fold increase in p65 binding was observed for CR-C but not -3.7 or +17.1 following LPS treatment of the macrophage cell line (**Figure 2-6A**). A previously described site in the *Sod2* gene with very high levels of p65 binding served as a positive control (Guo et al., 2003; Kaikkonen et al., 2013; Xu et al., 1999), displaying significant p65 occupancy only after LPS treatment (**Figure 2-6A**). A negative control region located 8.5 kb upstream of the *Pdcd1* promoter showed minimal levels of p65 binding both before and after LPS treatment (**Figure 2-6A**). ChIP using a control IgG antibody showed no binding at any of these sites (**Figure 2-6A**).

Despite the CR-C, -3.7, and +17.1 sites all showing enhancer activity in CD8 T cells (Austin et al., 2014), as well as being predicted as potential p65 binding sites by ChIP-seq, the luciferase assays and p65 ChIP showed no activity at the -3.7 and +17.1 sites. To determine if these sites displayed histone modifications that are associated with regulatory or enhancer activity, a ChIP for histone 3 lysine 4 (H3K4) mono-methylation and H3K27 acetylation was performed at CR-B, CR-C, -3.7 and +17.1. The results showed that only H3K27ac was found at CR-B and CR-C (**Figure 2-6B, left**). This is consistent with the modification patterns observed in CD8 T cells, in which H3K27ac, but not H3K4me1, is seen at CR-B and CR-C (Austin et al., 2014). The -3.7 and +17.1 sites did not show any histone marks associated with enhancer or regulatory activity before or after LPS treatment. H3K4 trimethylation, a mark associated with active promoter regions, was only found in macrophages stimulated with LPS at the CR-B region, which is adjacent to the *Pdcd1* promoter (**Figure 2-6B, top right**). Again, a control IgG antibody showed no binding across the locus (**Figure 2-6B, bottom right**), and a control site located near PD-1 did not bind to any of our antibodies. These data suggest that the conserved regions located at -3.7 and +17.1 kb are not utilized in macrophages as enhancers, and instead only the CR-B and CR-C regions are sufficient to enable *Pdcd1*

expression in response to LPS.

CR-B does not de-methylate to induce PD-1 expression

The above data indicate that the regulatory elements for *Pdcd1* operate under a novel paradigm in macrophages. Epigenetic modifications, such as the methylation of cytosines in promoter and regulatory regions, correlate with the silencing of a locus and may contribute to the regulation in macrophages. In naïve CD8 T cells, sequences surrounding CR-B and CR-C are extensively methylated. Following activation of CD8 T cells, these sequences lose their DNA methylation and then regain it as the cells transition to late effector and memory phases of an immune response, in correlation with the transient gain and subsequent loss of PD-1 expression (Youngblood et al., 2011). To determine if the same epigenetic dynamics exist in macrophages, the DNA methylation states of CpG sites in surrounding CR-B and CR-C were analyzed using bisulfite sequencing before and after LPS induction of primary BMDMs. In the uninduced state, BMDMs showed nearly complete methylation of the CpGs within CR-B that were queried. Contrary to the patterns observed in CD8 T cells, following LPS stimulation for 24 hours the CR-B sequences exhibited no loss of methylation (**Figure 2-7A**) despite highly elevated expression of PD-1 on the cell surface (data not shown). Intriguingly, in resting BMDMs, the CpGs associated with CR-C were largely unmethylated and did not change after stimulation (**Figure 2-7B**). These data suggest that the basic epigenetic states of the PD-1 regulatory regions are distinct among cell types and that the locus in macrophages does not undergo dynamic changes in DNA methylation following induction.

Discussion

PD-1 expression is critical to both chronic conditions of antigen persistence, as well as in

the acute settings of primary antigen stimulation. In the latter settings PD-1 expression and signaling may ultimately slow down immune responses, allowing time for the appropriate differentiation signals to be processed by the cell in addition to preventing pathology caused by an overactive response. For macrophages, the increased production of anti-inflammatory cytokines in PD-1 expressing cells, such as IL-10, would support a role for PD-1 signaling as a mechanism to slow down or redirect systemic immune responses. With multiple cell types inducing PD-1 upon activation, this report set out to determine if the fundamental mechanisms that control PD-1 induction were similar across a variety of cells. The results suggest that there are at least two major pathways that induce PD-1. These pathways share common features. First, PD-1 expression is initiated by recognition of a cell-activating ligand, either antigen signaling to lymphoid cells using antigen specific receptors or using pattern recognition receptors on macrophages. Second, both pathways utilize two major transcription factors of immune cells that respond to extracellular challenges: NFAT and NF-κB. Intriguingly, the pathways were distinct to the cell types in that CD8 T cells did not respond to LPS signaling or TNF treatment (data not shown) to induce PD-1 through NF-κB, and macrophages did not respond to NFAT activation by PMA/Io. This may ensure that only antigen-specific signals induce PD-1 on T cells. Intriguingly, B cells, which may act as antigen presenting cells and/or differentiate into functional plasma cells, were able to engage both the BCR-induced NFAT pathway, as well as the TLR-induced NF-κB pathway. In this respect, B cells demonstrate that some cells may engage multiple distinct PD-1 inducing pathways either discretely or simultaneously upon recognition of certain pathogens.

Although statistically less than wild-type BMDMs, MyD88-deficient BMDM cells still induced PD-1 following LPS stimulation. As LPS induction of NF-κB can occur through both a MyD88 dependent and TRIF-dependent pathway (Hagar et al., 2013;

Kayagaki et al., 2013; Piras and Selvarajoo, 2014), this observation suggests that both signaling pathways could be involved in PD-1 expression or that one can substitute for the other. The MyD88 independent pathway, utilizing TIR domain-containing adapter inducing IFNb (TRIF) as the signaling adapter, is not sufficient or the main pathway for PD-1 expression as stimulation of TLR3, a receptor which signals exclusively through TRIF, did not lead to PD-1 induction. Conversely, PD-1 induction following stimulation of TLR2, which is exclusively dependent on MyD88, was fully blocked in the MyD88 knockout BMDMs. Thus, it is most likely that while TLR3-based TRIF activation does not induce PD-1, both pathways may be nonetheless operational in regulating PD-1 expression in these cells through stimulation of TLR4, and that there is the potential for other TLR ligands to stimulate PD-1 expression.

ChIP-seq data sets suggested that NF-κB was bound to several regions across the PD-1 gene. Among those regions were CR-C, -3.7, and +17.1, three key regions for induction of *Pdcd1* expression in CD8 T cells following TCR and STAT signaling. When tested by conventional ChIP, only CR-C, which was the strongest of the peaks in the ChIP-seq datasets, was found to bind NF-κB following LPS stimulation. One reason for the discrepancy is likely to be that the ChIP-seq study used disuccinimidyl glutarate (DSG) as a second crosslinking agent. DSG fixes interactions occurring at a much greater distance than formaldehyde (Sutherland et al., 2008). As the -3.7 and +17.1 regions interact with the *Pdcd1* promoter during cell activation and PD-1 expression (Austin et al., 2014), the additional crosslinking may be revealing these chromatin structures rather than direct p65 binding.

The finding that NF-κB binds to CR-C continues to denote this region as the critical cis-element for the induction of *Pdcd1* expression as it is the focal point of binding for at least two major transcriptional control pathways: the NFAT pathway in CD8 T cells and NF-κB in macrophages. This is recapitulated by the luciferase data. Similarly to

what was seen in T cells, the CR-C region alone is sufficient to induce a reporter gene construct following stimulation of macrophages. In contrast, the -3.7 and +17.1 regions were insufficient without CR-C to induce significant expression, although the ability of these other two regions to augment CR-C activity was not tested.

The DNA methylation experiments provided a surprising addition to our understanding of the regulation of PD-1. In murine CD8 T cells, the CpG rich regions designated as CR-C and CR-B are highly methylated in naïve cells. As mentioned above, following activation, both regions lose methylation and this is coincident with PD-1 expression. At the late effector cell stage for CD8 T cells, PD-1 expression is lost and DNA methylation returns, with memory CD8 T cells showing similar patterns to the naïve state. Because of this, it was assumed that CpG methylation at CR-B and CR-C must be lost in order for PD-1 expression to occur in T cells. In stark contrast, BMDMs showed complete methylation of CR-B and nearly no initial methylation at CR-C. Following LPS stimulation and *Pdcd1* expression, no changes in DNA methylation were observed at either CR-B or CR-C. These data suggest that unlike CD8 T cells(Oestreich et al., 2008), in macrophages, CR-B is not utilized for *Pdcd1* expression and/or that DNA methylation serves to restrict the binding of factors that could modulate *Pdcd1* expression in macrophages prior to activation. The lack of DNA methylation at CR-C in macrophages implies that the region is constitutively accessible for the binding of NF-κB and rapid activation of *Pdcd1* transcription. The finding of histone H3K27 acetylation at 3-4 times background levels at the CR-C supports an accessible chromatin configuration. LPS stimulation of BMDMs and induction of *Pdcd1* was maximal at 4 hrs. By contrast, stimulation of CD8 T cells ex vivo through the TCR is not immediate with expression peaking at 24 hrs. The difference in chromatin accessibility and DNA methylation may account for the difference in the timing of *Pdcd1* induction as both NFAT and NF-kB are induced immediately upon stimulation of their pathways. While the

mechanism that specifically methylates CR-B and CR-C in naïve CD8 T cells or causes demethylation of these regions upon T cell activation is unknown, its failure to fully engage in macrophages reinforces the concept that these cells regulate inhibitory receptors through unique pathways. Thus, these data show that demethylation of CR-B is not an absolute requirement for cellular expression of PD-1 in all cell types, although it may aid in or be necessary for durable expression, as is seen on exhausted T cells.

Chronic-phase immune system failure remains an important problem in medicine. It is now understood that PD-1 plays a critical role in inducing and maintaining CD8 T cell exhaustion. This function of PD-1 may be necessary on an evolutionary scale in order to help prevent or reduce autoimmunity (Nishimura et al., 1999; Nishimura et al., 2001). However, despite numerous observations of PD-1 expression on other cell types, an “exhausted” phenotype has never been described in macrophages or dendritic cells, although in all of these cell types the function of PD-1 has been shown to be the same: slowing of effector functions and cell replication (Cho et al., 2009a; Honda et al., 2014; Rui et al., 2013; Said et al., 2010). The importance of PD-1 expression on cells other than CD8 T cells is coming into light. As PD-1 is a critical mechanism for controlling both the early and chronic stages of immune responses, understanding regulation of this gene has important implications for many immunological processes, including those associated with chronic infections, transplantation, and cancers. The data presented herein demonstrate that two major transcription factor activation pathways of immune cells (NFAT and NF-kB) are both critical components of the PD-1 system across multiple inflammatory cell types. The finding here of TLR-mediated induction of PD-1 opens up the intriguing possibility that bacteria or other microbes may take advantage of this pathway with the ultimate goal of inducing an immune inhibitory responses. Thus, understanding the molecular mechanisms that control PD-1 expression is critical to being able to target this molecule for therapeutic interventions or enhancements in a

wide variety of inflammatory conditions.

Figure 1

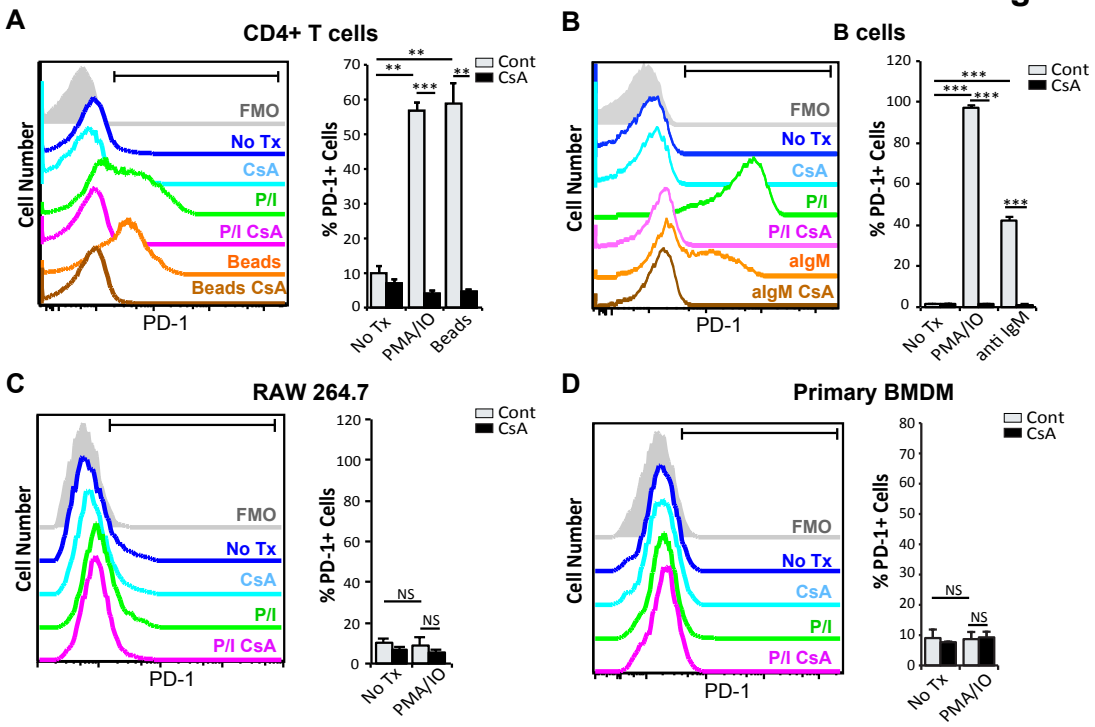

Figure 2- 1: NFAT regulates surface PD-1 in CD4 T cells and B cells, but not macrophages.

(A) Splenic CD4 T, (B) B cells (C) RAW264.7 macrophages, or (D) primary bone marrow-derived macrophages (BMDM) were treated for 48 (T cells) or 24 (B cells and macrophages) hours with PMA/Io (P/I), anti-CD3/CD28 beads (Beads), or anti-IgM $F(ab)_2$ (anti IgM) in the presence or absence of CsA as indicated and analyzed by flow cytometry. Representative histogram plots for PD-1 surface expression are shown with FMO (fluorescence minus one) controls. Primary cell cultures (CD4 T cells, B cells, and macrophages) were performed from two independent cohorts of three mice each and the experiments from RAW264.7 cells represent at least 6 independent experiments. Quantitation of the percent of PD-1 positive cells from these samples is shown with

standard deviation. Statistical significance was determined by student's T test. * p<.05, ** p<.01, *** p<.001, NS, not significant

Figure 2

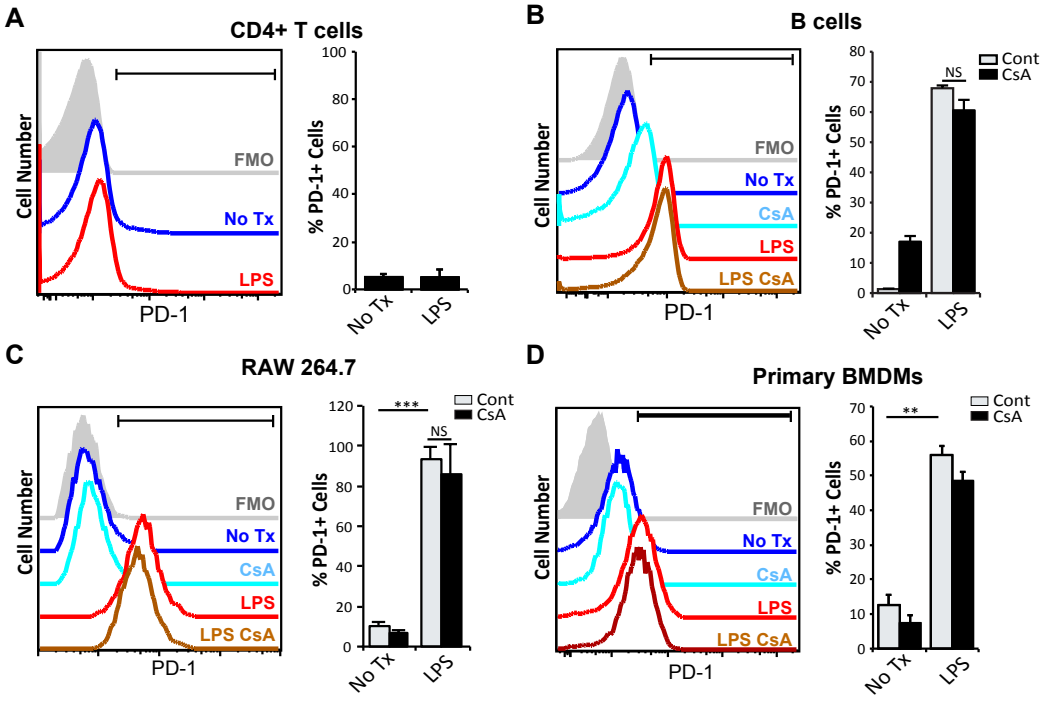

Figure 2- 2: LPS induces PD-1 in an NFAT-independent manner in B cells and macrophages

(A) Primary splenic CD4 T cells, (B) B cells, (C) RAW264.7 macrophages, or (D) BMDMs were treated for 24 hours with LPS with/without CsA as indicated. At 24 hours, cells were analyzed by flow cytometry. Representative histogram plots are shown (left) with FMO controls, and average frequency of PD-1 positive cells across all samples is graphed with standard deviation (right). Primary cell cultures of CD4 T cells, B cells, and BMDMs were prepared from independent preparations from three separate mice, and the data in RAW264.7 cells were collected from at least 6 independent splits of cell culture. Experiments in RAW264.7 cells were performed concurrently with those in Figure 1C; and therefore untreated (No Tx Cont), CsA-only (No Tx CsA), and FMO

controls are the same as that figure. Statistical significance was determined by student's T test. * p<.05, ** p<.01, *** p<.001, NS, not significant.

Figure 3

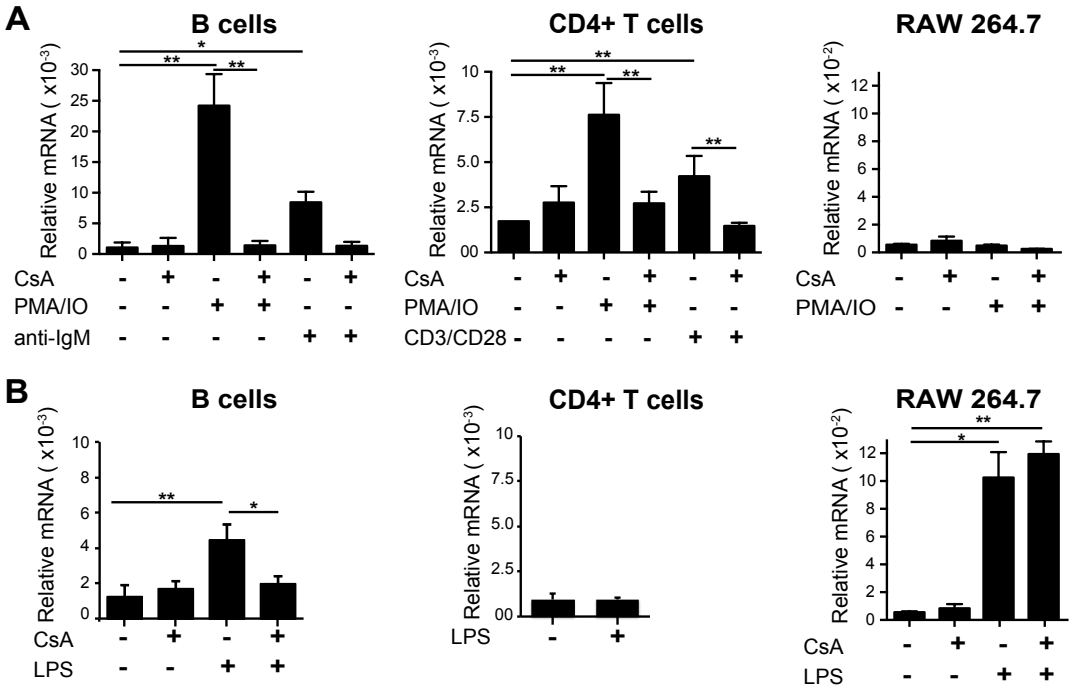

Figure 2- 3: PD-1 mRNA is regulated by NFAT in B cells and CD4 T cells, but not in macrophages

Primary B cells or CD4 T cells from spleens of two cohorts of three C57BL/6 mice were stimulated with Anti-IgM $F(ab)_2$, CD3/CD28 beads, or PMA/Ionomycin (A) or LPS (B) in the presence or absence of CsA for 24 hours. Three separate populations of RAW264.7 cells were stimulated for 4 hours with PMA/Io (A) or LPS (B) with and without CsA. In all cases, RNA was prepared from cell lysates, and the relative *Pdcd1* mRNA levels were quantitated using real-time RT-PCR. All RAW264.7 cell experiments were performed at the same time; and thus, the controls shown in panel B are the same as shown in A. *Pdcd1* mRNA levels are shown as percentage of 18s rRNA. Statistical significance was determined by student's T test. * p<.05, ** p<.01, *** p<.001

Figure 4

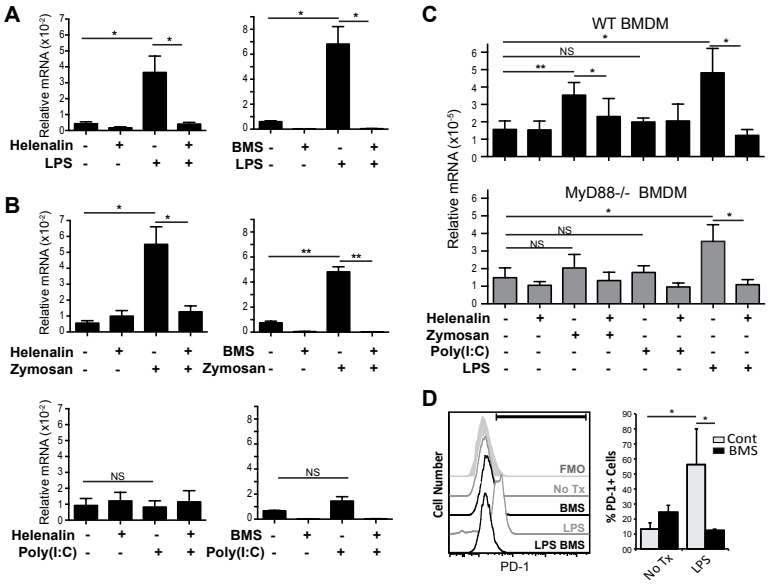

Figure 2- 4: NF-κB is necessary for PD-1 up-regulation in macrophages.

(A) Three independent populations of RAW264.7 cells were activated with LPS for 4 hours, and NF-κB activation was blocked with helenalin or BMS-345541 (BMS). (B) RAW264.7 cells were activated with TLR2 and TLR3 agonists Zymosan (top) or Poly(I:C) (bottom), respectively, for 4 hours. As indicated samples were co-treated with helenalin or BMS 345541. For all panels in (A) and (B), independent populations of cell lines were activated in triplicate, and *Pdcd1* mRNA was analyzed by RT-PCR, with results graphed as a percentage of 18s rRNA. (C) BMDMs from wild-type or MyD88$^{-/-}$ mice were activated for 3 h with TLR ligands Zymosan, Poly(I:C), or LPS, and co-treated with helenalin as indicated. *Pdcd1 mRNA* levels are shown as percentage of 18s rRNA. (D) BMDMs were stimulated with LPS and/or BMS-345541 for 24 h. PD-1 surface expression was analyzed by flow cytometry, and characteristic histograms are shown on the left, graphed with FMO. Frequency of PD-1 positive cells is graphed on the right.

Significance was determined by student's T test. * p<.05; ** p<.01; NS, not significant.

Figure 5

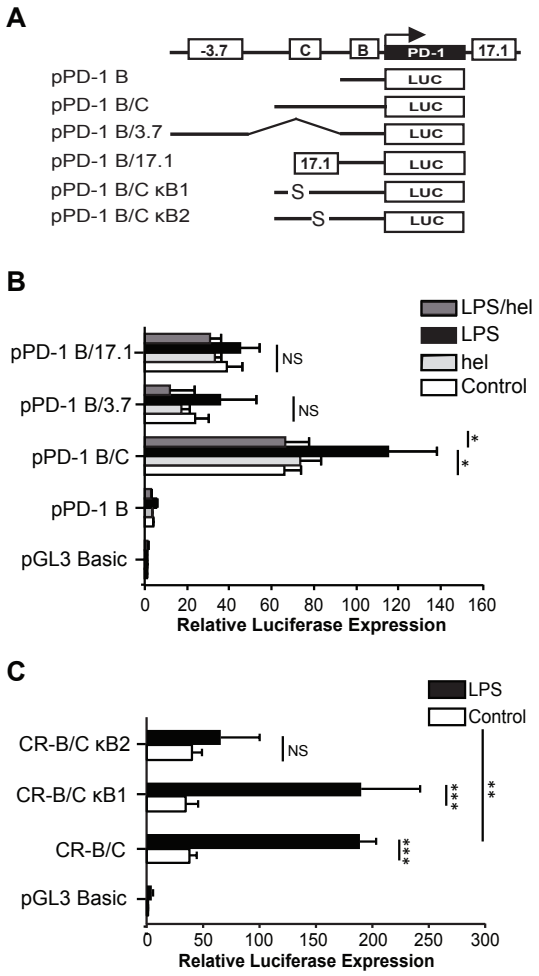

Figure 2- 5: NF-κB binding sequence located in CR-C is necessary for PD-1 induction in macrophages

(A) Schematic of luciferase constructs based in the pGL3 basic luciferase reporter vector compared to the native murine gene locus. Constructs contain the PD-1 promoter and CR-B with either CR-C, -3.7, or +17.1 regulatory regions. An "S" signifies the location of the scrambled NF-κB consensus element in plasmids pPD-1 B/C κB1 and κB2. (B) RAW264.7 cells were nucleofected twice in triplicate with plasmids containing different regulatory regions, allowed to rest for 16 hours, and stimulated for 4 hours with LPS with and without helenalin (hel), after which firefly luciferase expression was quantitated. (C) RAW264.7 cells were nucleofected in two triplicates with wild-type and NF-κB plasmids. Cells were allowed to rest for 16 hours and then stimulated for 24 hours with LPS. Significance was determined by 2-way ANOVA. * p<.05, ** p<.01, *** p<.001, NS, not significant.

Figure 6

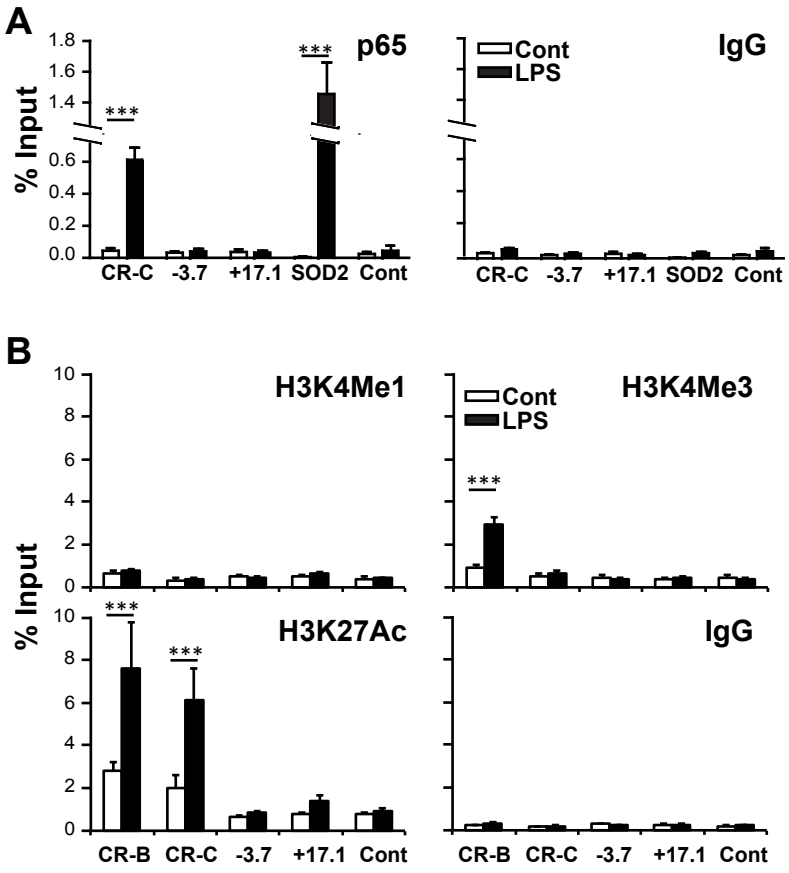

Figure 2- 6: p65 binds to CR-C

Chromatin immunoprecipitations were performed using (A) anti-p65 antibody or (B) anti-histone modification antibodies H3K4me1, H3K4me3, and H3K27ac. Chromatin was prepared from two sets of three independently stimulated populations of RAW264.7 cells, treated with or without LPS for 3 hours. A non-specific, control IgG was used with each set of chromatin IPs to determine background levels of detection. The intronic enhancer from the *Sod2* gene was used as a positive control for NF-κB binding (Jones et al., 1997), and cont represents a non-specific sequence located ~8kb from the *Pdcd1* gene (Lu et al., 2014). Significance was determined by 2-way ANOVA. * p<.05, ** p<.01, *** p<.001

Figure 7

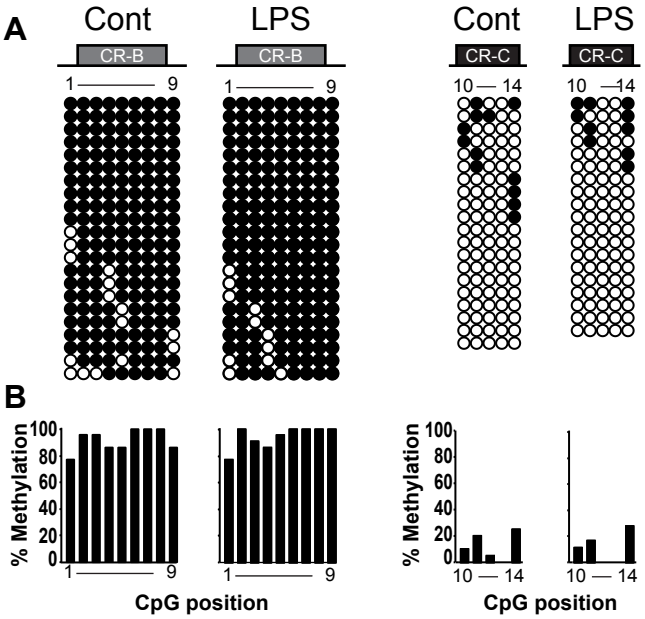

Figure 2- 7: CR-B is not demethylated following activation while CR-C is initially unmethylated in macrophages

BMDMs from three C57BL/6 mice were grown and treated +/- LPS for 24 hours. DNA from cells was bisulfite converted, PCR amplified and cloned. Eight clones from each mouse were sequenced. Incomplete sequences were discarded. Clonal CpG DNA methylation is shown for sequences at CR-B (A) and CR-C (B) before and after LPS. Black circles represent methylated CpG sites; open circle represent un-methylated sites. Percentage of total clones methylated at each site is represented below. Differences in untreated and LPS-treated cells were not significant at both regions as determined by Fischer's Exact Test

Chapter 3: the role of CR-C on PD-1 expression and memory

Alexander P. R. Bally[1,2], Yan Tang[1,3], Joshua T. Lee[2], Benjamin G. Barwick[2], Ryan Martinez[2], Brian D. Evavold[2], and Jeremy M. Boss[2]

[1]These authors contributed equally to this work

[2]Department of Microbiology & Immunology and [3]Emory Vaccine Center; Emory University School of Medicine; Atlanta, GA 30322

[3] Department of Dermatology; Xiangya Hospital, Central South University; Changsha, Hunan 410008, China.

*Originally published in the *Journal of Immunology*. Bally AP, Tang Y, Lee JT, Barwick BG, Martinez R, Evavold BD, and Boss JM. NF-κB regulates PD-1 expression in macrophages. J Immunol. 2017 Jan 1;198(1):205-217.

Introduction

The immune-inhibitory receptor Programmed Death 1 (PD-1) is expressed on CD8 T cells upon activation (Jaikumar Duraiswamy, 2007; Kloverpris et al., 2014; Wherry et al., 2007). In chronic viral infections and in anti-cancer immune responses, PD-1 is highly expressed on antigen-specific T cells for the duration of the immune challenge (Breton et al., 2013; Chauvin et al., 2015; Day et al., 2006; Severson et al., 2015; Zhang et al., 2015). This high expression, combined with PD-1 binding to its ligands PD-L1 and PD-L2 (Chemnitz et al., 2004; Laura L. Carter, 2002), results in CD8 T cell functional exhaustion, a cellular state characterized by reduced proliferation, cellular toxicity, and cytokine secretion (Barber et al., 2006; Wherry et al., 2003). Antibody blockade of the PD-1/PD-L interaction mediates reinvigoration of CD8 T cell function (Barber et al., 2006; Day et al., 2006). As such, this PD-1 immune checkpoint antibody blockade therapy is now used to treat patients with melanoma or non-small cell lung cancers (Blank et al., 2004; Brahmer et al., 2012; Topalian et al., 2012). Understanding the molecular mechanisms that govern initial PD-1 induction may aid in the development of future therapies, as well as give an understanding of the context in which these therapies are applied.

A variety of factors tightly regulate *Pdcd1*, the gene that encodes PD-1, across multiple cell types and in response to different stimuli (reviewed in (Bally et al., 2016)). In T cells, TCR signaling induces Nuclear Factor of Activated T cells (NFAT)c1 (Oestreich et al., 2008) and Activator Protein-1 (Xiao et al., 2012) binding to the *Pdcd1* locus. TCR-mediated NFAT signaling is both necessary and sufficient to induce PD-1 expression in T cells. Other regulatory factors, including the transcription factors STAT3, STAT4 and IRF9, require TCR signaling in addition to their individual stimuli in order to

augment expression of *Pdcd1* (Austin et al., 2014; Cho et al., 2008; Terawaki et al., 2011).

In the mouse genome, conserved region C (*CR-C*) is located between 1009 bp and 1,301 bp upstream of the *Pdcd1* transcriptional start site. This region is conserved across mammalian species and highly DNAse I hypersensitive (Oestreich et al., 2008). *CR-C* is a complex element that can respond to a variety of stimuli in a cell type specific manner. When bound by NFATc1 in response to TCR stimulation in CD8 T cells, *CR-C* is able to induce expression of a luciferase reporter in vitro (Austin et al., 2014; Bally et al., 2015; Oestreich et al., 2008). FoxO1, another transcriptional activator, also binds to *CR-C* and perpetuates PD-1 expression in CD8 T cells of mice that are chronically infected with lymphocytic choriomeningitis virus (LCMV) (Staron et al., 2014). In both T cells and macrophages exposed to acute activating factors, IRF9 binds to an interferon-sensitive response element in *CR-C* and promotes PD-1 expression (Cho et al., 2008; Terawaki et al., 2011). Lastly, in murine macrophages activated through TLRs 2 or 4, *CR-C* binds NF-κB in a manner necessary for the transient induction of PD-1 in these cells (Bally et al., 2015).

CR-C also undergoes dynamic epigenetic modifications that are concordant with PD-1 expression. CpG dinucleotides within *CR-C* are highly methylated in naïve CD8 T cells. DNA methylation is associated with gene silencing (Smith and Meissner, 2013). During the initial stages of an acute infection with LCMV, the *CR-C* region in antigen-specific CD8 T cells becomes demethylated as PD-1 is expressed, suggesting an increase in accessibility at the locus (Youngblood et al., 2013; Youngblood et al., 2011). Additionally, *CR-C* chromatin gains the histone mark histone 3 lysine 27 acetylation (H3K27Ac) following T cell stimulation (Lu et al., 2014), a modification associated with active enhancers (Creyghton et al., 2010). Following resolution of an acute infection and loss of PD-1 expression, *CR-C* loses its active chromatin modifications and gains

epigenetic marks associated with repressive chromatin structures, including $H3K9^{me3}$, $H3K27^{me3}$, and $H4K20^{me3}$ (Lu et al., 2014). *CR-C* CpG loci also become remethylated at this stage. Thus, *CR-C* is a highly active and dynamic regulatory region, implicating it as a major control element of PD-1 expression.

PD-1 knockout mice exhibit altered immune cell development and function. Such mice displayed a higher frequency of thymocytes and early thymic emigrants (Blank et al., 2003; Nishimura et al., 2000) and were more susceptible to autoimmune diseases (Nishimura et al., 1999; Okazaki et al., 2001). Moreover, loss of PD-1 resulted in a much stronger memory response to an acute infection, in both number and effector function of cells produced (Allie et al., 2011). In chronic infections, PD-1 knockout CD8 T cells were more functionally active and induced fatal circulatory failure due to an over-active immune response (Frebel et al., 2012). While these studies examined the complete loss of PD-1 on T cell responses, it is not known how *Pdcd1* cis-regulatory elements alter PD-1 expression in vivo and influence T cell development or immune responses.

To derive a functional role for one critical element in vivo, mice carrying a genetic deletion of *CR-C* were generated (termed CRC^{-} mice herein). T cells in CRC^{-} mice appear to develop normally and there is no increase in susceptibility to autoimmunity. In cell culture, and in acute and chronic LCMV viral infection, *CR-C* deletion resulted in significant loss of PD-1 expression on both virus-specific CD8 T cells and CD4 T cells following activation. In CRC^{-} mice bearing melanoma tumors, PD-1 expression was decreased on tumor-infiltrating T cells, as well as antigen-specific T-cells in the tumor draining lymph nodes. This resulted in a greater anti-tumor response and slower tumor growth. Although CRC^{-} mice produced fewer antigen-specific CD8 T cells during primary infection, they displayed more effective memory responses in both quantity and quality of memory cells. Collectively, these data demonstrate that *CR-C* is critical to the

expression of PD-1 in vivo and that alterations in PD-1 expression can mediate changes in the immune effector:memory axis.

Methods

Generation of CRC knockout mice

Homology targeting fragments (5' and 3', respectively) surrounding *CR-C* (chr1:95950331-95953209 and chr1:95949964-95950330) were inserted into the pM30 targeting plasmid (Meyers et al., 1998) using *Sac*II and *Mlu*I sites (upstream region) or *Nhe*1 and *Kpn*1 sites (downstream region). The pM30 plasmid was previously modified to contain an *Mlu*I site and a second *Lox*P site. A 400 bp fragment containing *CR-C* (chr1:95949964-95950330) was inserted between the *Lox*P sites using *Sal*I. This yielded a plasmid-targeting construct that contained the *CR-C* fragment flanked by two *LoxP* sites, within the homology arms of the *Pdcd1* locus. All insertion fragments were generated by PCR, and inserted using In-Fusion Dry-Down PCR Cloning Kit (Clontech). The Brigham and Women's Hospital Transgenic Core Facility directed by Dr. Arlene Sharpe used the resulting pM30_PD-1_CRC plasmid to generate homologously recombined JM8.N4 ES cells (trans-NIH Knock-Out Mouse Project (KOMP) repository-www.komp.org), which are derived from the C57Bl/6 strain (Pettitt et al., 2009). These recombined cells were used to produce $CRC^{fl/fl}$ mice used in this study. $CRC^{fl/fl}$ founder mice were bred to B6-Tg (CAG-FLPe) mice to remove the neo cassette (Kanki et al., 2006), and subsequently maintained on a C57Bl/6 background. To delete *CR-C*, mice were crossed with C57BL/6-Tg(Zp3-cre)93Knw/J mice to generate CRC^{-} mice. Mice were genotyped using the following CR-C primers: 5'-CCTGAGCATGCCAGAAAGACA and 5'-CTAACACCAGGCTGGGGTAGACTC. Wild-type C57Bl/6 mice (Jackson laboratories) were used as controls for CRC^{-} experiments, where indicated. Mice that were 6-8 weeks old were used for experiments unless otherwise noted. For

establishing bone marrow chimeras, 10^7 bone marrow cells from CRC^- or B6.SJL-$Ptprc^a$ $Pepc^b$/BoyJ (WT mice carrying the CD45.1 allele) were adoptively transferred into B6129S7-$Rag1^{tm1Mom}$/J hosts (Jackson laboratories) that had been irradiated with a dose of 500 rads. All mice were cared for in accordance with approved Emory University Institutional Animal Care and Use Committee protocols.

Experimental Autoimmune Encephalitis (EAE)

The EAE inducing peptide $MOG_{35–55}$ (MEVGWYRSPFSRVVHLYRNGK) was synthesized in house on a Prelude Peptide Synthesizer as previously described (Kersh et al., 2014). For EAE induction, 200 μg of the MOG_{35-55} peptide was emulsified in Complete Freund's Adjuvant (CFA, desiccated M.Tb concentration at 5 mg/ml) and 150 μl of the emulsion was injected subcutaneously on days 0 and 7. On days 0 and 2, 300ng of pertussis toxin was injected intraperitoneally. EAE scoring was performed on the 5-point scale: 0=not sick, 0.5= distal limp tail, 1= proximal weak tail, 2= hind limb weakness, 3= complete hind limb paralysis, 4= inability to flip over, 5=death or moribund. Mice in EAE experiments were sacrificed if there was >25% body weight reduction for 72 hours.

Melanoma model

The B16-F10.gp33 melanoma cell line was kindly supplied by Dr. R. Ahmed with permission from Dr. H. Pircher (Universitätsklinikum Freiburg) (Prevost-Blondel et al., 1998). These cells were cultured with Dulbecco's modified Eagles's medium (DMEM) containing 10% fetal bovine serum (FBS), 1% glucose and 100 U/ml Penicillin/Streptomycin at 37 °C. Low passage number B16-F10.gp33 melanoma cells were harvested and then resuspended at 10^7 cells per ml in serum free DMEM media. $1x10^6$ cells were injected into the study animals subcutaneously on the right flank. Tumor

growth was measured daily using calipers. Tumor infiltrating lymphocytes were isolated from whole tumors and analyzed following purification by a Ficoll gradient.

Virus Infections and Plaque Assays

Viral stocks of LCMV strains Armstrong and Clone-13 were produced as described previously (Matloubian et al., 1990). Mice were injected with $2x10^5$ pfu Armstrong intraperitoneally or with $2x10^6$ pfu LCMV-Cl13 intravenously in the lateral tail vein. For day 28 chronic experiments, mice were injected intraperitoneally with 200 µg anti-CD4 antibody (clone GK1.5, BioXcell, West Lebanon, NH) at the day before and the day after viral infection to deplete CD4 T cells as described (Zajac et al., 1998).

Vero cells (ATCC CCL-81) were cultured in DMEM containing 10% FBS and 100 U/ml Penicillin/Streptomycin at 37 °C and used for viral plaque assays as previously described (Ahmed et al., 1984). Briefly, $5x10^5$ cells were plated in each well of a 6 well plate and allowed to rest for one day. Mice were bled by lancet from the submandibular vein. Serum samples were extracted from whole blood by centrifugation and serially diluted in 10-fold increments into DMEM +10%FBS. Diluted serum was adsorbed onto cells for one hour at 37°C. Samples were subsequently overlaid with 199 media containing 0.5% agarose and then incubated at 37°C. On Day 4, 199 media/agarose containing 0.002% Neutral Red were added to each well to stain infected/dead cells. Plaques were counted on day 5 and viral titers calculated.

Ex vivo T cell activation

Naïve CD8 T cells were isolated from spleens of healthy mice by magnetic activated cell sorting (MACS), using the CD8a+ T Cell Isolation Kit according to manufacturer's instructions (Miltenyi Biotec, Auburn, CA). Anti-CD3 antibody (clone 145-2C11, Fisher Scientific) was adhered to a 24 well plate at 5 µg/ml in sterile PBS. The plate was sealed

with parafilm and incubated at 37 °C for 2 hours to adhere antibodies. The plate was then placed at 4° C overnight. On the next day, the plate was washed twice with 500µl sterile PBS, and $0.5x10^6$ primary CD8 T cells were incubated in each well with 10 µg/ml soluble anti-CD28 antibody (clone 37.51, Fisher Scientific) at 37 °C for the time points indicated. Cell samples were harvested and stained for flow or stored as a pellet at -80°C for RT-PCR.

Flow cytometry and Antibodies

Cells were stained for flow cytometry in FACS buffer (PBS, 1% BSA, and 1 mM EDTA) and antibodies at 4°C for 30 minutes, and then fixed in 1% paraformaldehyde for 30 minutes. Antigen-specific CD8 T cells were gated by CD8+CD44+CD62L-Tetramer+ (including gp33, gp276 and np396 tetramers). Activated CD4 T cells were gated on CD4+CD44+CD62L- markers. Antibodies used included CD4 PerCP-Cy5.5 (clone RM4.5, Tonbo Biosciences, San Diego, CA), CD8 FITC (clone 53-6.7, Tonbo Biosciences), CD44 APC-Cy7 (clone IM7, BioLegend, San Diego, CA), CD62L Alexa Fluor 700 (clone MEL-14, BioLegend, San Diego, CA), CD69 PE-Cy7 (Clone H1.2F3, BioLegend, San Diego, CA) CD127 BV510 (Clone SB/199, BD Horizon), PD-1 PE (clone RMP1-30, BioLegend, San Diego, CA). gp33 var C41M (KAVYNFATM), gp276 (SGVENPGGYCL), and np396 (FQPQNGQFI) biotinylated monomers on H-$2D^b$ were obtained from the NIH Tetramer Core facility at Emory University and tetramerized to streptavidin-APC (Prozyme). Flow cytometry was performed on a BD LSR II and analyzed using FlowJo 9.6.4 software. Intracellular cytokine staining was performed using the Fixation and Permeabilization Solution Kit with BD GolgiPlug (Becton, Dickinson and company) according to the manufacturer's protocols.

Real-time PCR

Total RNA was isolated with the RNeasy Mini Prep kit (Qiagen, Germantown, MD). cDNA was prepared from 1 μg total RNA with SuperScript II reverse transcriptase (Invitrogen). mRNA levels were quantified in technical duplicates by real time PCR. mRNA levels were calculated relative to expression of 18s rRNA. Primers used for real-time PCR include the following: PD-1 forward 5'-GCTGAAGGCTCCTCCTTCTGACAT; PD-1 reverse, 5'-AGATATCCCAGCCCCTCGCCC; IL-2 forward, 5'-ACCCACTTCAAGCTCCACTTCA; IL-2 reverse, 5'-TGGCCTGCTTGGGCAAGTAAA; 18s forward, 5'-GTAACCCGTTGAACCCCATT; 18s reverse, 5'-CCATCCAATCGGTAGTAGCCG.

Bisulfite Sequencing

Genomic DNA was isolated from antigen specific CD8 T cells of mice infected with LCMV Armstrong 5 days post infection. DNA was bisulfite converted using the EpiTect bisulfite kit (Qiagen). Bisulfite-converted DNA was amplified through PCR and then cloned using the TOPO TA cloning kit (Life Technologies). Twelve colonies from each sample were analyzed by sequencing. Primers used for cloning and sequencing 5'-GGTGGGTTTTTATTTTTTAGGGATTGAGG and 5'-CTAAAACTAAAACCAAACTCTTATCCC.

Statistical Analyses

Student's T-tests were carried out to assess the significance of differences in results where indicated. Two-way ANOVA was used for comparisons in ex vivo stimulations and viral time-courses, as well as comparing tumor growth across time. Wilcoxon rank sum test was used to compare survival rates. Fisher's exact test was used to compare DNA methylation across different populations in bisulfite conversion experiments.

Statistical analyses were performed using data combined from independent groups of mice.

Results

Deletion of CR-C *does not alter thymocyte maturation*

To characterize the effects of the *CR-C* region on the expression of PD-1 and the development of immune responses, mice containing a floxed *CR-C* conditional allele (CRC^{fl}) were generated (Figure 3-1A). These mice were crossed to Cre-zp3 transgenic mice, resulting in germ-line deletion of the locus and generation of a mouse strain lacking *CR-C*. These mice were termed CRC^{-}. Using a PCR based assay, appropriate deletion of *CR-C* was observed in total splenic CD8 T cells from CRC^{-} but not in WT mice (Figure 3-1B**)**.

To begin the characterization of these mice and to determine if deletion of *CR-C* affected T cell development, thymocytes from naïve mice were analyzed by flow cytometry (Figure 3-1C). Frequencies of double negative (DN), double positive (DP), CD4+, and CD8+ thymocyte populations were unaffected by the deletion, indicating normal T cell development occurred. This differs significantly from the phenotype seen in $PD\text{-}1^{-/-}$ mice, which have increased frequency of both DN and DP thymocytes due to disrupted positive and negative selection processes mediated by PD-1 (Blank et al., 2003; Nishimura et al., 2000). However, changes in PD-1 expression on developing thymocytes were observed in CRC^{-} mice. PD-1 expression on DN cells (in which PD-1 is usually highly expressed on the DN4 population (Nishimura et al., 1996)), as well as on both CD4 and CD8 single positive immature thymocyte populations was significantly reduced in *CR-C* knockout cells (Figure 3-1D), indicating that *CR-C* was necessary for full and normal thymic PD-1 expression. The residual levels of PD-1 on these cell populations may be sufficient to facilitate the positive- and negative-selection associated

anergy that is mediated by PD-1 (Blank et al., 2003; Nishimura et al., 2000) and account for the differences in T cell development in these mice compared to PD-$1^{-/-}$ mice.

PD-1 expression on thymocytes is necessary for development of central and peripheral tolerance (Blank et al., 2003; Nishimura et al., 1999). To test if the observed differences in PD-1 expression in the CRC^{-} mice led to a breakdown of tolerance despite comparable numbers of developing thymocytes, mice were tested for susceptibility to developing immunity to the self-antigen MOG using experimental autoimmune encephalitis (EAE). The clinical scores of EAE in CRC^{-} mice were not significantly greater than in the WT (Figure 3-1E). This indicates that the CRC^{-} mice are not pre-disposed to autoimmunity or a breakdown of immune tolerance, despite lower thymic expression of PD-1. Thus, given the normal numbers of immature thymocyte populations and no increased susceptibility to a model of autoimmune disease, CRC^{-} mice appear to have normal immune systems.

CR-C *is required for ex vivo expression of PD-1*

In promoter reporter assays, *CR-C* was shown to be a critical regulator of *Pdcd1* expression (Austin et al., 2014; Oestreich et al., 2008), suggesting that it is necessary for activating expression in responses to TCR stimulation. To test if *CR-C* was necessary for ex vivo TCR-mediated expression of *Pdcd1*, magnetically enriched primary splenic CRC^{-} or WT CD8 T cells (Figure 3-2A) were stimulated with anti-CD3/CD28 beads in culture for 24 h. In WT mice, ex vivo induction of *Pdcd1* mRNA peaked at 24 hours after activation (Figure 3-2B). In contrast, CRC^{-} CD8 T cells failed to fully induce *Pdcd1*, increasing mRNA expression only 3 fold over baseline, compared to over 15 fold seen in the WT cells. Importantly, both wild-type and knockout populations induced very high and similar levels of IL-2 mRNA (Figure 3-2B, right), indicating that comparable activation of these cells occurred, and the lower PD-1 levels were not due to a failure to

integrate TCR signaling. To correlate surface expression with mRNA levels, CD8 T cells were also analyzed by flow cytometry on days 1, 2, and 4 after activation. Surface expression of PD-1 peaked on WT cells within 24 hours and subsequently declined over time to day 4 (Figure 3-2C). In CRC$^-$ cells, PD-1 levels were significantly lower than in WT cells at all times after Day 0. Using CD69 as a marker for T cell activation, both WT and knockout populations showed comparable levels of stimulation (Figure 3-2D), indicating that failure to express PD-1 was not due to failure to stimulate T cells in the CRC$^-$ cultures. These data indicate that *CR-C* is necessary in culture to induce PD-1 expression through TCR stimulation, and redundant mechanisms such as those mediated by *Pdcd1*'s distal enhancer regions, which also bind NFATc1 (Austin et al., 2014), are insufficient to induce PD-1 expression under these experimental conditions.

CR-C *is necessary for normal PD-1 expression in acute infection*

To assess the function of *CR-C* in vivo, CRC$^-$ mice were infected with LCMV Armstrong, which produces an acute infection that is typically cleared within eight days (Wherry et al., 2003). Viral load and the frequency of LCMV specific CD8 T cells were similar between CRC$^-$ and WT mice (Figures 3A and B). However, *Pdcd1* mRNA expression was reduced by 50% on CD8 T cells from acutely infected CRC$^-$ mice compared to WT mice (Figure 3-3C). Flow cytometry analysis of CD8 T cells, using the gating strategy shown in Figure 3-3D, showed a nearly 50% loss of PD-1 expression on virus-specific CD8 T cells at both day 4 (Figure 3-3E) and day 6 (Figure 3-3F). Differences in PD-1 expression were not due to changes in levels of T cells activation, as CD69 and KLRG1 expression profiles at these time points were similar between CRC$^-$ and WT mice (Figure 3-3E and F). These data argue that *CR-C* is necessary for maximal PD-1 expression following acute activation of T cells in vivo.

Loss of PD-1 expression has been shown to result in compensatory increased expression of other immune-inhibitory receptors (Odorizzi et al., 2015). To determine if *CR-C* deletion and its effects on PD-1 expression affected other inhibitory pathways, surface expression of other immune-inhibitory receptors (Tigit, 2B4, and Lag-3) was analyzed. While surface levels of 2B4 and Lag-3 showed no significant changes in WT compared to the CRC^- virus-specific T cells, expression of Tigit was increased in the CRC^- animals (Figure 3-3F). It is unlikely that deletion of a regulatory element in the *Pdcd1* locus would directly affect expression of Tigit. Instead, this change agrees with previous reports, suggesting that an intricate feedback network may regulate expression of some immune-inhibitory receptors (Odorizzi et al., 2015).

As PD-1 is also significantly induced on CD4 T cells during acute infection (Agata et al., 1996; Carter et al., 2002), changes in PD-1 expression were also examined on these cells on day 6 after acute LCMV infection. Similar to CD8 T cells, CRC^- CD4 T cells showed a greater than 50% loss of PD-1 expression compared to WT (Figure 3-3G). This indicates that *CR-C* is also necessary in CD4 T cells to induce maximal induction of PD-1 in an acute viral infection. As in CD8 T cells, CRC^- and WT CD4 T cells showed similar levels in CD69 expression (Figure 3-3G, right), indicating comparable activation. Thus, *CR-C* is important for induction of PD-1 in both CD4 and CD8 T cells.

CR-C-*induced PD-1 expression is necessary for maximal effector T cell formation*

To determine if there were functional consequences resulting from lower early PD-1 expression, the ability of cells from LCMV Armstrong infected CRC^- mice to secrete cytokines was measured by intracellular cytokine staining (ICCS). At day 6 post infection, a lower frequency of CD8 T cells from CRC^- mice secreted either IFNγ or TNFα in response to LCMV peptides gp33 or gp276 compared to WT (Figure 3-3H). Although,

the frequency of cells secreting IL-2 was comparable between strains, the frequency of cells secreting at least two cytokines or all three cytokines in response to gp33 or gp276 stimulation was decreased in cells from CRC^- animals (Figure 3-3H). Thus, concurrent with lower PD-1 expression, there were fewer poly-functional virus-specific effector CD8 T cells at day 6 in CRC^- mice than in WT. This suggests that optimal cytokine responses are governed in part by *CR-C* mediated PD-1 expression.

Changes to PD-1 expression in CRC mice are cell intrinsic

Changes in PD-1 expression in CRC^- mice were observed on CD4 and CD8 T cells during an immune response, and frequency of some effector cell populations was altered. However, because PD-1 was deleted in all cells, this raises the possibility that the loss of expression and these subsequent changes may be the result of variations in the cellular environment. To determine if the changes to PD-1 expression observed on CRC^- CD4 or CD8 T cells were cell intrinsic, mixed bone marrow chimeras using $CD45.1^+$ WT and $CD45.2^+$ CRC^- bone marrow were established in sublethally-irradiated $RAG1^{-/-}$ hosts. CD8 T cells carrying the WT allele (CD45.1+) or CRC^- CD8 T cells (CD45.2+) were analyzed from the spleens of established chimeric mice 6 days after infection with LCMV Armstrong (Figure 3-4A). Total WT and CRC^- CD4 and CD8 T cells were represented in equal numbers, indicating that there was no competitive advantage/disadvantage or survival to the mutant T cells (Figure 3-4A, left). Similar to findings from Figure 3-3G, fewer virus-specific CRC^- cells were found within each chimera compared to WT virus-specific cells (Figure 3-4A, right), indicating that these cells are less capable of proliferating or responding to virus than their WT counterparts within the same inflammatory environment. Furthermore, in agreement with Figure 3-3, surface expression of PD-1 on CRC^- virus-specific CD8 T cells was approximately 50% lower compared to WT cells within the same chimeric animals (Figure 3-4B). As both WT

and CRC$^-$ cells were derived from the same environment, cellular stimulation was identical, as indicated by similar up-regulation of the activation marker, KLRG1 (Figure 3-4B). Moreover, within the chimeras CRC$^-$ CD4 T cells expressed less PD-1 on their surface than WT CD4 T cells (Figure 3-4C). The activation marker CD69 showed a slight decrease in expression in CRC$^-$ cells (Figure 3-4B and 3-4C). However, because CD69 is expressed fully at much earlier time points (as shown in Figure 3-3D and 3-3E), the biological significance of this is not known. Cumulatively, these data demonstrate that *CR-C* is intrinsically necessary for full PD-1 expression in an acute inflammatory environment.

CR-C *coordinates downstream epigenetic changes*

CR-B is a promoter proximal element that binds AP-1 in response to T cell activation. The methylation of cytosines upstream of *CR-B* (-332 to -721 bp from the promoter) and those within *CR-C* itself are highly correlative with PD-1 expression (Youngblood et al., 2013; Youngblood et al., 2011). As *CR-C* is required for TCR-mediated induction, this raises the question as to whether *CR-C* is required for subsequent alterations in DNA methylation at other regions, such as the sequences upstream of *CR-B* or whether these epigenetic changes could occur in the absence of *CR-C*. To address this, a DNA methylation-sensitive restriction enzyme digest assay within the above region was performed. Using the relative frequency of uncut (methylated) to cut (unmethylated) DNA from T cells of naïve mice, 80-100% methylation was observed at the queried CpG site (3-5B). As expected, the antigen-specific CD8 T cells from WT mice lost over 50% methylation at this site by day 5 post infection with LCMV Armstrong. In contrast, cells from the CRC$^-$ mouse showed no significant loss of DNA methylation.

When multiple CpGs within the region were analyzed by clonal bisulfite sequencing, a large loss of overall methylation across the entire region was observed by

day 5 in cells from WT mice (Figure 3-5C). Although some demethylation occurred at the locus in the CRC$^-$ mouse, cells from these mice retained significantly more methylation after LCMV Armstrong challenge compared to the WT mouse. These data suggest that the loss of DNA methylation in this region is coordinated by the actions of *CR-C*.

CR-C *deletion decreases PD-1 expression in chronic infection*

The expression and function of PD-1 as an immune-inhibitory receptor is exemplified during chronic infections (Barber et al., 2006; Zajac et al., 1998). To determine if *CR-C* is involved in PD-1 regulation during chronic antigenic stimulation, WT or CRC$^-$ mice were infected with LCMV Clone-13 under conditions that lead to chronic infection. At day 8 post infection, virus-specific CD8 T cells from CRC$^-$ mice displayed a decrease of *Pdcd1* mRNA (Figure 3-6A). IL-2 mRNA expression was unchanged in CRC$^-$ mice (Figure 3-6A, bottom), indicating that cellular activation and effector function were not affected by the *CR-C* deletion.

PD-1 surface expression on virus-specific tetramer+ CD8 T cells during chronic infection was also analyzed using flow cytometry. As with mRNA levels, PD-1 surface levels were decreased in CRC$^-$ mice at day 8-post infection (Figure 3-6B, left). Similarly PD-1 expression was also decreased on CD4 T cells at this same time point (6B, right). The loss of PD-1 expression on CD8 T cells in chronically infected CRC$^-$ mice was less severe than that seen during acute infection. Again, as in acute infection, there was no overall change in cell activation to account for the differences in PD-1 expression as measured by up-regulation of CD69 or loss of the IL-7 receptor CD127 on CD8 T cells or induction of CD69 on CD4 T cells (Figure 3-6B).

PD-1 expression was also detected on CD8 and CD4 T cells of chronically infected animals at day 28 post infection with Clone-13 virus. Similarly to day 8, PD-1

mRNA was decreased at day 28, although to a lesser degree (Figure 3-6C). However, unlike at day 8, CRC$^-$ CD8 T cells at day 28 did not show a significant loss of PD-1 surface expression, although PD-1 expression did trend lower in correlation with changes in mRNA (p=.06) (Figure 3-6D, left). This may indicate that other regulatory elements, such as the -3.7 and +17.1 distal enhancer regions (Austin et al., 2014) are sufficient to induce or maintain PD-1 on CD8 T cells at late time points in chronic infection. Collectively, these data indicate that *CR-C* is necessary for early PD-1 expression during acute infection and early chronic infection prior to the establishment of T cell exhaustion, but is not necessary for high PD-1 expression seen on exhausted CD8 T cells during prolonged antigen exposure. In contrast, activated CD4 T cells showed a decrease in PD-1 expression at day 28 after chronic infection (Figure 3-6D, right), indicating that *CR-C* continues to play a role in PD-1 expression on certain cell types even during prolonged antigen exposure.

The frequency of cytokine secreting effector CD8 T cells was also measured at day 28 after chronic Clone-13 infection. In both genotypes, there were fewer CD8 T cells in the chronic infection capable of secreting cytokines in response to gp33 or gp276 than seen in the acute infection (Figure 3-3H compared with 3-6E). This is most evident in the populations of polyfunctional double-positive or triple-positive cells responding to each peptide, which were depleted (Figure 3-6E compared to 3-3H)). These results are indicative of CD8 T cell exhaustion in both mutant and WT mice. However, in this chronic infection model, the frequency of cytokine secreting cells was depressed even further in CRC$^-$ mice compared to wild-type (Figure 3-6E), suggesting that the defect in effector cell formation that is established early during initial antigen response in these mice may result in lower T cell numbers throughout the duration of infection.

CR-C *deletion results in a stronger anti-tumor response*

PD-1 has been shown to play an important role in modulating effector functions during anti-tumor immune responses (Blank et al., 2004; Ribas et al., 2016; Xiao et al., 2012). To determine if *CR-C*-induced PD-1 expression affects cellular function in this inflammatory setting, CRC^- mice or WT controls were inoculated with B16.f10-gp33 cells, a melanoma cell line that expresses the LCMV gp33 peptide, making it possible to track tumor-specific CD8 T cells using established LCMV peptide:MHC tetramers. Tumor growth was delayed in CRC^- compared to WT mice (Figure 3-7A). However, CRC^- mice ultimately succumbed to the tumor at a comparable rate as WT mice (Figure 3-7B). Tumor infiltrating lymphocytes (TILs) were isolated and analyzed at day 18. In the CRC^- mouse, PD-1 expression was significantly reduced on gp33-specific CD8 TILs (Figure 3-7C) and highly reduced on CD4 TILs compared to WT mice (Figure 3-7D). This indicates that *CR-C* is responsible for inducing maximal PD-1 expression on anti-tumor T cells. T cells in the tumor-draining lymph nodes of WT or CRC^- mice were also analyzed, and tumor-specific CD8 T cells identified using MHC tetramer staining for the gp33 epitope. Similar to the TILs, CRC^- T cells within the lymph node displayed decreased PD-1 expression in both CD8 (Figure 3-7E) and CD4 (Figure 3-7F) populations compared to WT.

CR-C deletion influences CD8 T cell memory and functionality

PD-1 expression during acute infection was shown to modulate memory formation (Allie et al., 2011). Because CD8 T cells from CRC^- mice expressed less PD-1 and showed fewer functional effector cells after an acute LCMV infection, it is possible that cell differentiation was skewed towards other populations, including memory. To determine if *CR-C* influences CD8 T cell memory formation and function, mice were infected with LCMV Armstrong and allowed to clear virus. At day 35 after acute infection, approximately 4 weeks after virus was cleared from the serum of these animals, the

frequency of LCMV gp33-specific CD8 T cells was assessed by MHC tetramer staining. CRC^- mice had double the frequency of LCMV peptide-specific CD8 memory T cells as WT mice (Figure 3-8A). To characterize the nature of memory cells formed, the frequencies of central memory (Tcm) and effector memory (Tem) T cells were determined as measured by expression of CD44 and CD62L (van Faassen et al., 2005). The frequency of Tcm cells ($CD44^{hi}CD62L^{hi}$) were slightly decreased in the CRC^- mice compared to WT (Figure 3-8B). Conversely, CRC^- mice had a slight increase in frequency of Tem cells ($CD44^{hi}CD62L^{lo}$) as a proportion of total virus-specific T cells (Figure 3-8B). This shift from Tcm to Tem may indicate a more effective memory response at this time point. To further characterize the nature of the memory response, and to ensure that the antigen-specific cells being analyzed at this time point were in fact memory CD8 T cells and not naïve or effector T cells (Jameson and Masopust, 2009; Kaech and Wherry, 2007), multiple additional phenotypic markers were analyzed. As expected (Youngblood et al., 2011), tetramer positive CD8 T cells from mice 35 days after Armstrong infection expressed only slightly more PD-1 compared to naïve cells (Figure 3-8C). There was no difference in PD-1 expression between memory cells from WT and CRC^- animals, indicating that the basal expression of PD-1 on this cell type is not governed by *CR-C*. Tetramer-specific CD8 T cells from both groups were $CD44^{hi}$ (compared to naïve, Figure 3-8C), indicating that they were not naïve T cells, and were also $CD127^{hi}$ (compared to FMO and naive) in both mouse strains, indicating that they were not effector T cells despite a predominant expression of CD44. Similarly, memory T cells from both WT and CRC^- mice showed a high expression of CCR7 and a large population of $KLRG1^+$ cells, again characterizing them as predominantly Tem cells (Figure 3-8C).

In addition to measuring the quantity of memory T cells generated following an acute infection, the ability of memory CD8 T cells generated in CRC^- mice to respond to

secondary exposure to antigen was also assayed using ICCS as a measure of overall functionality. Coinciding with the greater overall frequency of memory cells at day 35, CRC^- mice showed a greater proportion of cells secreting IFNγ (Figure 3-9A). In both WT and CRC^- mice the majority of cells responding to gp33 peptide expressed two or more cytokines (Figure 3-9A), as expected in a memory population. However, in CRC^- mice a greater proportion of responding cells were polyfunctional compared to WT (Figure 3-9A), suggesting an overall increase in the functionality of the memory CD8 T cell population.

To characterize the ability of memory T cells formed following acute infection to respond to a secondary challenge, equivalent numbers of CRC^- or WT, LCMV gp33-specific memory CD8 T cells were adoptively transferred into host WT mice bearing early stage (5 days post inoculation) B16.f10-gp33 melanoma tumors. The immune function of the memory cells was assayed by their ability to clear or prevent tumor growth. Mice that received WT memory cells showed no decrease in tumor growth compared to mice that received naïve T cells (Figure 3-9B), indicating that the number of WT memory cells adoptively transferred was insufficient to respond to and clear the established tumors growing in the host mice. In sharp contrast, mice that received the same number of memory T cells from CRC^- donors failed to develop any tumors (Figure 3-9B), indicating that the memory response from these CRC knockout T cells was significantly stronger on a per cell basis. Collectively, these data indicate that lower initial PD-1 expression during an acute infection, caused here by deletion of the *CR-C* region, resulted in greater quantity and quality of antigen-specific memory CD8 T cells.

Discussion

CR-C is a complex regulatory element controlling PD-1 expression. Previous work identified and showed that *CR-C* encoded functional binding sites for NFATc1 (Oestreich

et al., 2008), NF-κB (Bally et al., 2015), and FOX01 (Staron et al., 2014), which were active depending on stimulation conditions and cell type. Although the initial molecular analyses and manipulation of *CR-C* in in vitro systems showed that its function was likely important for PD-1 expression (Oestreich et al., 2008), its role in vivo could only be determined through genetic ablation of the element. Here, *CR-C* was found to be critical to optimal expression of PD-1 during both acute and chronic LCMV infections in both CD4 and CD8 T cells. Furthermore, the loss of *CR-C* prior to an acute infection and the corresponding decrease in PD-1 induction resulted in a larger pool of antigen-specific memory CD8 T cells that displayed more enhanced functionality, suggesting that alterations in the timing or full expression of PD-1 during initial T cell activation have a significant influence on T cell differentiation.

In the LCMV Armstrong system, *Pdcd1* expression was reduced by ~50% in CRC^{-} mice. This suggests that although *CR-C* is required for full expression of PD-1 in vivo, distal elements described previously (Figure 3-1: -3.7, +17.1) (Austin et al., 2014) or other redundant elements that have not been characterized are critical for its in vivo expression. There was a less severe PD-1 expression phenotype in the chronic model, indicating a greater employment of the other cis regulatory elements. Unlike *CR-C,* the -3.7 and +17.1 distal elements bind and respond to STAT3 or STAT4 in addition to NFATc1 and are therefore sensitive to the local or systemic environmental differences attributed to chronic LCMV infection that signal through receptors beyond the TCR (Austin et al., 2014). Intriguingly, a new element located at -20 kb, identified using a chromatin accessibility assay, is active during chronic LCMV infection (unpublished data) and may over ride the deletion of *CR-C*. Thus, the redundancy of NFAT responsive elements and the ability to respond to inflammatory cytokines are likely responsible for providing a distinct in vivo control of PD-1 gene expression during chronic versus acute stimulation of CD8 T cells. These diverse modalities of PD-1 regulation may be used to

direct the development of T cells into short-lived effector T cells (T_{SLEC}) or exhausted T cells in the context of different immune challenges.

The rapid loss of DNA methylation upstream of *CR-B* and at *CR-C* during the initial effector stage of *Pdcd1* expression and the regaining of DNA methylation at late effector and memory time points suggested that this epigenetic mechanism was critical to the overall regulation of *Pdcd1* (Youngblood et al., 2011). The failure of the *CR-B* upstream sequences to reach their wild-type levels of demethylation during acute CD8 T cell responses in CRC^- CD8 T cells suggests that DNA demethylation is mediated by the activity of the *CR-C* region, with the possibility that NFATc1 itself is responsible for initiating the epigenetic change. The findings also suggest that cytosine methylation of the promoter proximal sequences was not sufficient to completely block induction of *Pdcd1* expression. In agreement with this finding is the fact that in macrophages treated with LPS to induce PD-1, DNA methylation at *CR-C* is not lost, despite the fact that *CR-C* is used to induce PD-1 (Bally et al., 2015). In this case, NF-κB was the primary transcription factor binding to *CR-C* and NFATc1 does not play a role. In the LPS system in macrophages, PD-1 expression was short lived. Together, with previous work (Youngblood et al., 2011) these data suggest that prolonged and full expression of PD-1 may require demethylation of the locus.

CR-C's in vivo role in regulating PD-1 expression appears to be most critical at early time points following infection. In an acute infection, PD-1 expression by both mRNA and surface protein was abrogated by over 50% in CRC^- animals compared to WT. Despite this, CRC^- mice and WT mice demonstrated comparable viral clearance in blood by day 8, as well as peak viral titers at day 4. A number of mechanisms may explain why lower PD-1 fails to correlate with improved anti-viral function. First, the decreased level of PD-1 expression during acute infections may be insufficient to inhibit T cell effector functions. Alternatively, in agreement with previous reports (Odorizzi et al.,

2015) and recapitulated here, a loss of PD-1 expression resulted in higher up regulation of other inhibitory receptors, particularly Tigit. This may compensate for the lower PD-1 expression, ultimately yielding a balance in overall cellular activation. However, as CRC^- mice had fewer T_{SLEC} compared to WT, it is possible that early, optimal PD-1 expression may be required to coordinate an effective immune response, in agreement with some previous reports (Talay et al., 2009), rather than acting as a cellular inhibitor as occurs during chronic stimulation.

One of the more striking findings here was the ability of CRC^- mice to generate a much stronger antigen-specific T cell memory response. This corroborates previous findings that the absence or antibody blockade of PD-1 signaling skews CD8 T cell populations towards a memory phenotype (Allie et al., 2011; Ribas et al., 2016; Rutishauser et al., 2009). Here, the loss of early PD-1 expression mediated by *CR-C* deletion resulted in greater number and quality of memory CD8 T cells. Together, these results indicate that the level of PD-1 expression may regulate the nature of the initial immune response; with a decrease approximating 50% PD-1 expression having profound phenotype on T cell memory formation. From a clinical standpoint, this may indicate that a limited blockade in PD-1 signaling during an immune challenge, such as vaccination, may improve memory formation and be a viable protocol for improving vaccination regimens. Furthermore, antigen-specific CRC^- memory CD8 T cells, generated here by a primary viral infection, showed a greater ability to combat existing early melanoma tumors upon adoptive transfer into tumor-bearing hosts. This may suggest future cancer therapies in which PD-1 expression is altered, possibly through CRISPR/Cas9 deletion of *CR-C*. As CRC^- mice showed no increased propensity to autoimmunity and still developed signs of exhaustion during chronic antigen encounter, such an approach may prevent any potential immune-related adverse events (Topalian et al., 2014) associated with current PD-1/PD-L1 checkpoint blockade therapies.

Figure 1

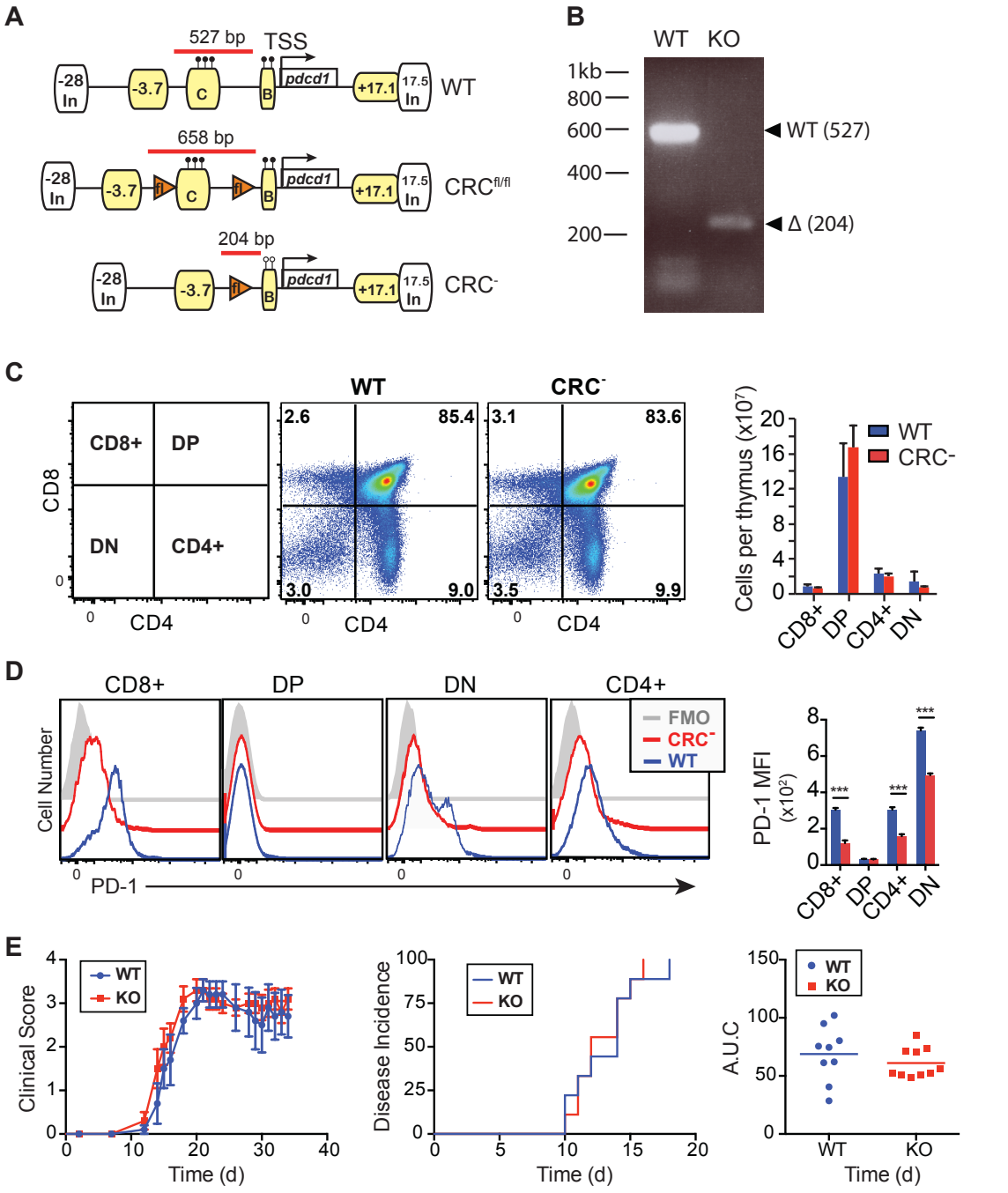

Figure 3- 1: Deletion of CR-C does not affect immune development

A) Schematic showing the *Pdcd1* region in CRC$^{fl/fl}$ and CRC^{-} mice compared to wild-type B6. Known regulatory elements are labeled in yellow(Austin et al., 2014; Oestreich et al., 2008). Chromatin insulator sites are labeled with white boxes. B) Representative genotyping gel for WT or CRC^{-} mice. PCR amplicons and relative sizes for genotyping

are shown using red bars in (a). C) Representative flow plots and characterization of frequencies of different T cell populations collected from the thymi of naïve, 6-week old WT or CRC^- mice. N=6. D) Representative histograms and quantification of PD-1 expression on each population of immature thymocytes from (C). E) Average clinical score of EAE in WT or CRC^- mice (left), time of onset to disease symptoms per mouse (middle), and total disease severity as measured by area under the curve (right). Graphs indicate mean plus standard deviation. Two groups of 5 mice per genotype were analyzed. Panels C and D were analyzed for significance by Student's T test. Statistical significance for Panel E was determined using a Mann-Whitney test. *** $P<.001$.

Figure 3- 2: CRC is necessary for PD-1 expression during ex vivo stimulation

Figure 2

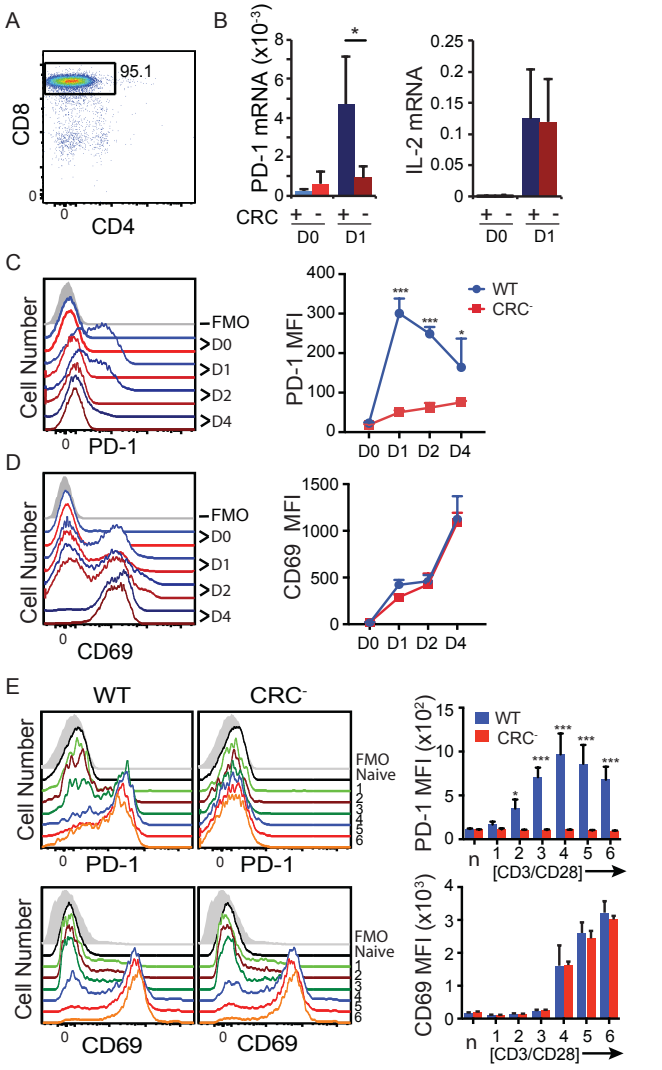

A) Representative enrichment by MACS of CD8 T cells from total splenocytes used for ex vivo experiments. B-D) Enriched CD8 T cells were stimulated with CD3/CD28 antibodies. B) mRNA was harvested at 0 and 24 hours, and analyzed by real-time PCR. Values for *Pdcd1* and *IL2* mRNA are graphed as a percentage of 18s rRNA. C and D) Cells were harvested at 0, 24, 48, and 96 hours after stimulation as above and stained for flow cytometry. Representative plots (left) and MFI (right) at each time point are shown for PD-1 (C) and CD69 (D). Data are graphed as mean plus standard deviation, and represent six independent experiments. Panel B used a Student's T test and Panels C and D used a two-way ANOVA to determine statistical significance. * P< .05; *** P<.001

Figure 3

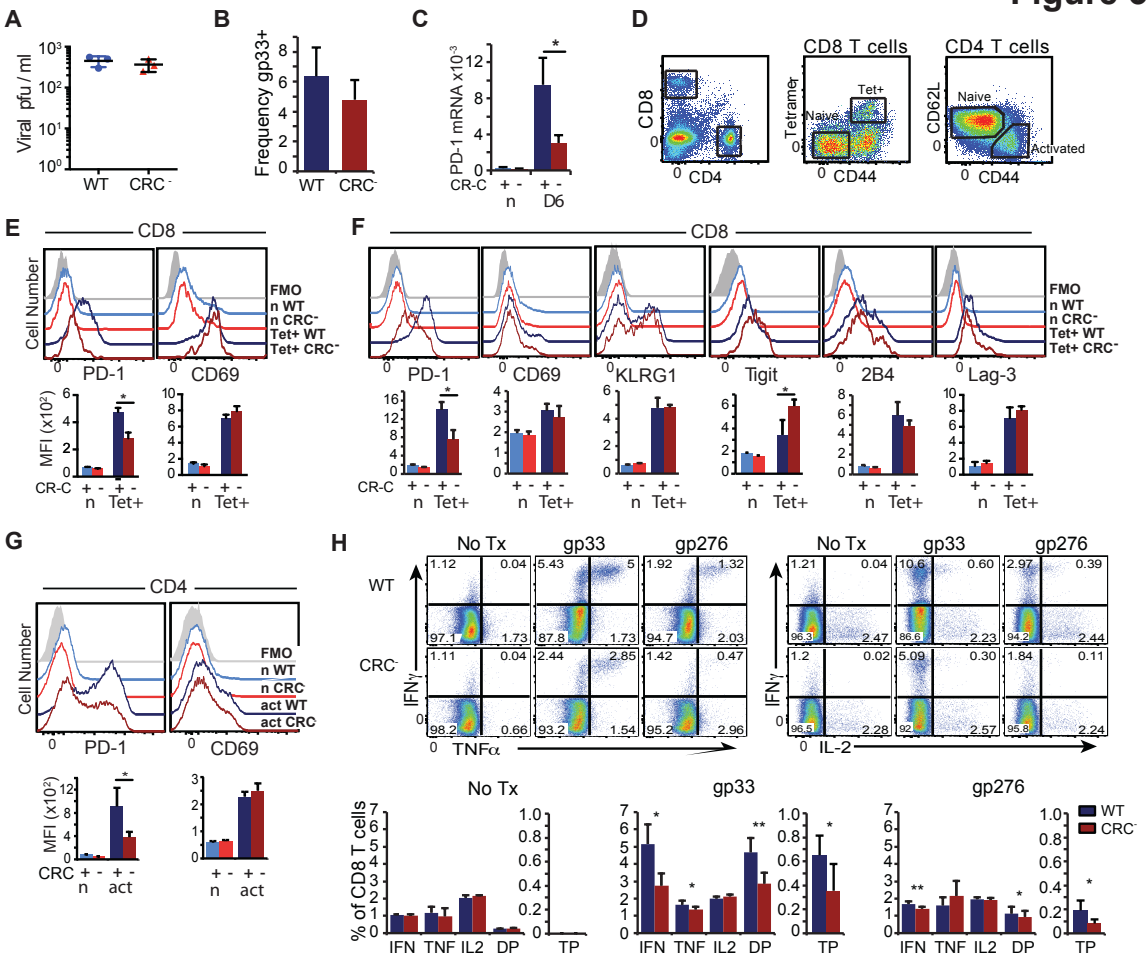

Figure 3- 3: Acute viral infection induces PD-1 through CR-C

A) Frequency of LCMV gp33-specific CD8 T cells as a percentage of total CD8 T cells from WT (Blue) or CRC$^-$ (Red) mice day 6 PI with LCMV Armstrong. B) Viral titers in the serum of LCMV Armstrong infected animals at day 4. C) PD-1 mRNA as a % or18s rRNA from virus-specific CD8 T cells collected from naïve mice (grey), or WT (blue) and *CR-C* (red) mice infected with LCMV Armstrong for 6 days. D) Gating strategy showing naïve (n) and tetramer+ (Tet+) populations of CD8 T cells, or naïve (n) and activated (act) populations of CD4 T cells. Representative flow cytometry histograms and quantification of MFIs from CD8 T cells collected from WT or CRC$^-$ mice at day 4 (E) or

day 6 (F). Flow analysis of CD4 T cells at Day 6 PI is shown in (G). H) CD8 T cells from day 6 LCMV Armstrong infected mice were stimulated with no peptide, gp33, or gp276 ex vivo in the presence of brefeldin A for 5 hours. Frequency of IFNγ, TNFα, and IL-2 single positive cells, cells expressing any two cytokines (DP), and triple positive (TP) cells as a proportion of all CD8 T cells were graphed below. For panels A, B, C, D, F, and G, four groups of 3 or more mice/genotype were used. For panels E and H, two groups of 3 mice per genotype were used. Graphs represent mean plus standard deviation for individual representative experiments. Student's T test was used to determine significance with * P< .05; ** P<.01.

Figure 3- 4: Changes to PD-1 expression in CR-C mice are cell intrinsic

Figure 4

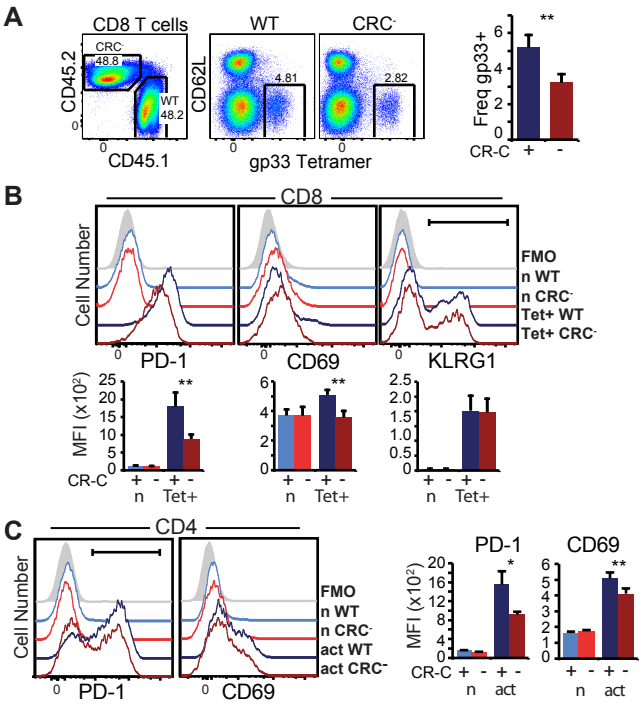

Bone marrow chimeras were established in RAG-/- mice irradiated with 500 rads. 10^7 WT (CD45.1+) or CRC$^-$ (CF45.2+) bone marrow cells from the femurs of healthy mice were adoptively transferred into irradiated hosts. 6 weeks after transfer, mice were bled to ensure chimerism and then infected with LCMV Armstrong. Splenocytes from infected animals were analyzed at day 6 post infection. A) Flow cytometry plots showing WT (CD45.2+) and CRC$^-$ (CD45.1+) CD8 T cells in chimeric animals at day 6, and gp33 tetramer-specific cells within each population. The frequency of virus-specific cells in WT (CRC+) and CRC- populations within each chimera are shown to the right. B) Flow cytometry histograms (top) and average MFI (bottom) in naïve (CD44+ CD62L-) or virus-specific CD8 T cells within WT (CD45.1+) or CRC$^-$ (CD45.2+) populations. C) Flow cytometry histograms for CD4 cells from the above animals. Two groups of 3-4 host mice with independent donors of each genotype were used for these experiments. Mean and standard deviation of a representative experiment is graphed. Paired Student's T test was used to calculate significance. * P< .05; ** P<.01

Figure 5

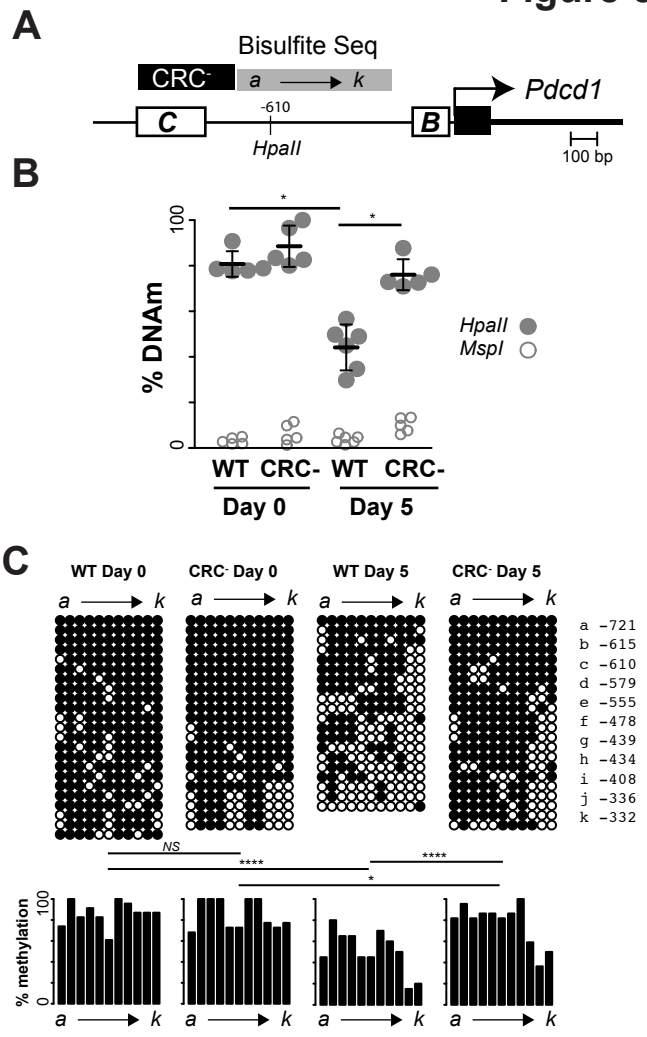

Figure 3- 5: CR-C coordinates epigenetic changes at the PD-1 locus

A) Schematic of bisulfite sequencing primers relative to the *CR-C* and PD-1 promoter. The region deleted in the CRC$^-$ mice is also indicated. B) % of DNA methylation at a CpG site (-610 from the promoter) within the bisulfite sequencing region, as identified by its inability to be cleaved by the methylation sensitive restriction enzyme *Hpa*II at days 0 and 5 after LCMV Armstrong infection. C) Clonal bisulfite sequencing from virus-specific CD8 T cells at days 0 and 5 after LCMV Armstrong in WT or CRC$^-$ mice. Each lettered column represents a specific CpG locus as designated in the side bar. Each row represents an allele. Black circles indicate methylated CpGs, whereas white circles are unmethylated. Frequency of methylation and statistical differences between groups are shown below. Panel B used two groups of 2-3 mice for each experiment and Panel C used two mice from independent experiments. Error bars in (B) represent standard deviation. The Fishers-Exact test was used to determine significance. * P< .05; *** P<.001

Figure 6

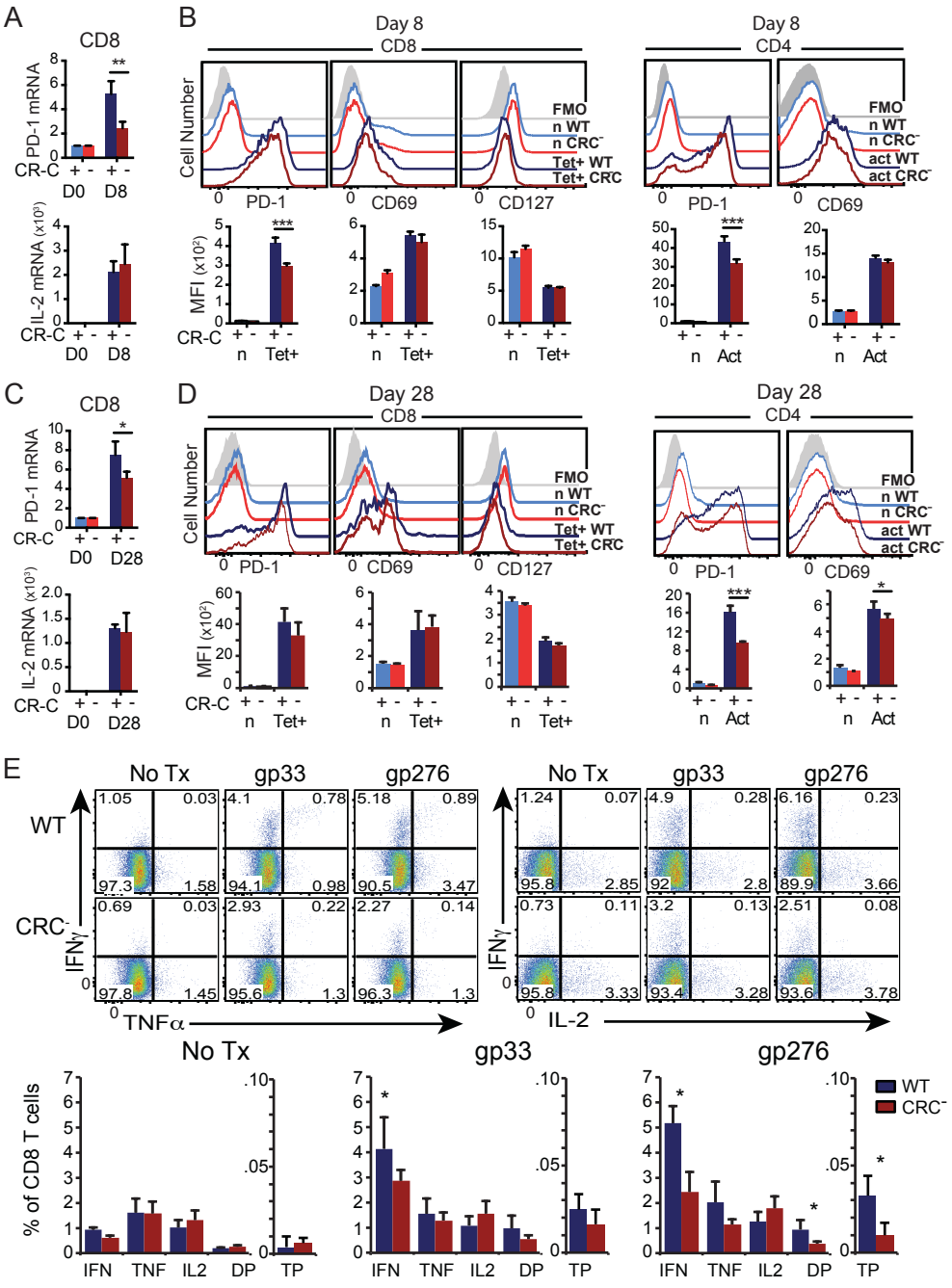

Figure 3- 6: CR-C is not necessary for PD-1 expression in chronic viral infection

WT or CRC⁻ mice were infected with LCMV Cl-13 for 8 (A-B) or 28 (C-E) days, and spleens were harvested for analysis. A and C) mRNA from MACS-purified CD8 T cells, graphed as a percentage of 18s rRNA. B and D) Representative flow cytometry

histograms (top) and MFI quantifications (below) for naïve (n) or tetramer-specific (Tet+) CD8 T cells (left), or naïve and activated (act) CD4 T cells (right). E) Total splenic cells were stimulated with no peptide, gp33, or gp276 ex vivo in the presence of brefeldin A for 5 hours, and then stained by ICCS for flow cytometry. Frequency and estimated total number of cells per spleen of IFNγ, TNFα, and IL-2 single positive cells, cells expressing any two cytokines (DP), and triple positive (TP) cells out of all CD8 T cells are graphed below. Two groups of 4 mice per genotype were used for these experiments. Graphs show mean of a single group plus standard deviation for each genotype. Student's T tests were used to assess statistical significance. * P< .05; ** P<.01; *** P<.001

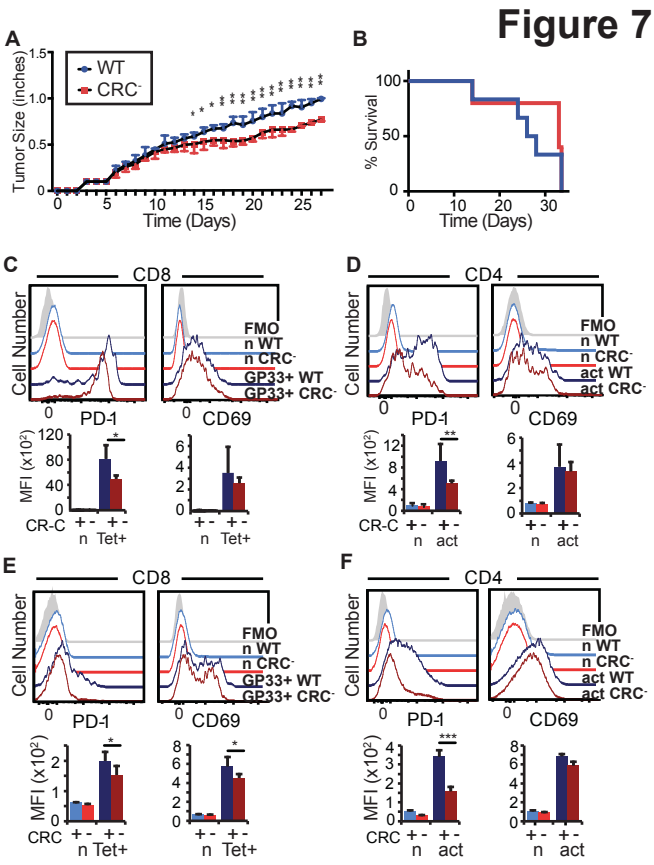

Figure 3- 7: Anti-melanoma immune response is improved by CRC deletion

A) WT or CRC$^-$ mice were injected subcutaneously with 10^6 B16.F10-gp33 melanoma cells, and tumor growth was measured every day by calipers along the largest diameter. N=2 groups of 5 mice for each genotype. B) Survival of mice injected with melanoma as in (a). Mice were allowed to continue growing tumors until tumor size, tumor infection, tumor ulceration/bleeding, or hindered mobility mandated sacrifice. C-D) Mice from (a) were sacrificed at Day 28 after tumor injection. Tumors were collected, and TILs isolated by ficoll gradient centrifugation. Cells were then stained for flow cytometry. E-F) Tumor-draining lymph nodes (inguinal and mesenteric) were harvested from mice in (A) at 28 days after injection, and stained for flow cytometry. Two groups of 5 or 6 mice per genotype were used for these experiments. Error bars represent mean plus standard deviation. Two-way ANOVA was used to calculate statistical significance in (A). Wilcoxon rank-sum was used to calculate significance in (B). Panels C-F used Student's T tests to calculate statistical significance. * P< .05; ** P<.01; *** P<.001

Figure 8

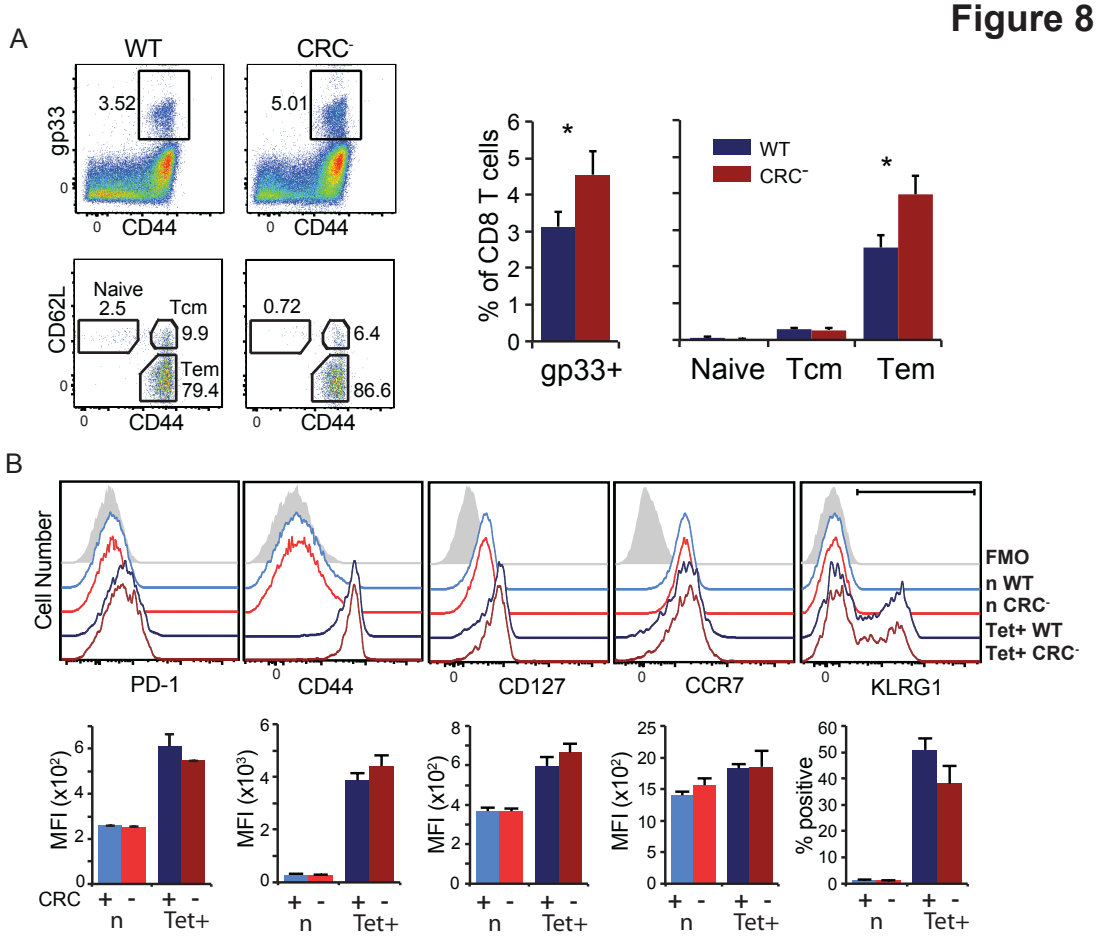

Figure 3- 8: Memory cell generation in CRC$^-$ mice is skewed towards Tem

WT or CRC$^-$ mice were infected with LCMV Armstrong and sac'd on day 35 after infection. Totally splenocytes were stained for flow. A) Frequency of gp33-specific cells out of total CD8 T cell population. B) Analysis of gp33-specific cells characterizing them as naïve T cells (CD62L^{hi} CD44^{lo}), Tcm (CD62L^{hi} CD44^{hi}), or Tem (CD62L^{lo} CD44^{hi}), with overall frequencies plotted to the right. C) Flow cytometry histograms of gp33-specific T cells identifying naïve, T_{SLEC} or memory cell markers. Two groups of 5 mice for each genotype were used for these experiments. Each graph represents a single group of 5, shown as mean plus standard deviation. Statistical significance was calculated using Student's T tests. * P< .05; ** P<.01; *** P<.001

Figure 3- 9: Immune memory is more functional in CRC⁻ mice

Figure 9

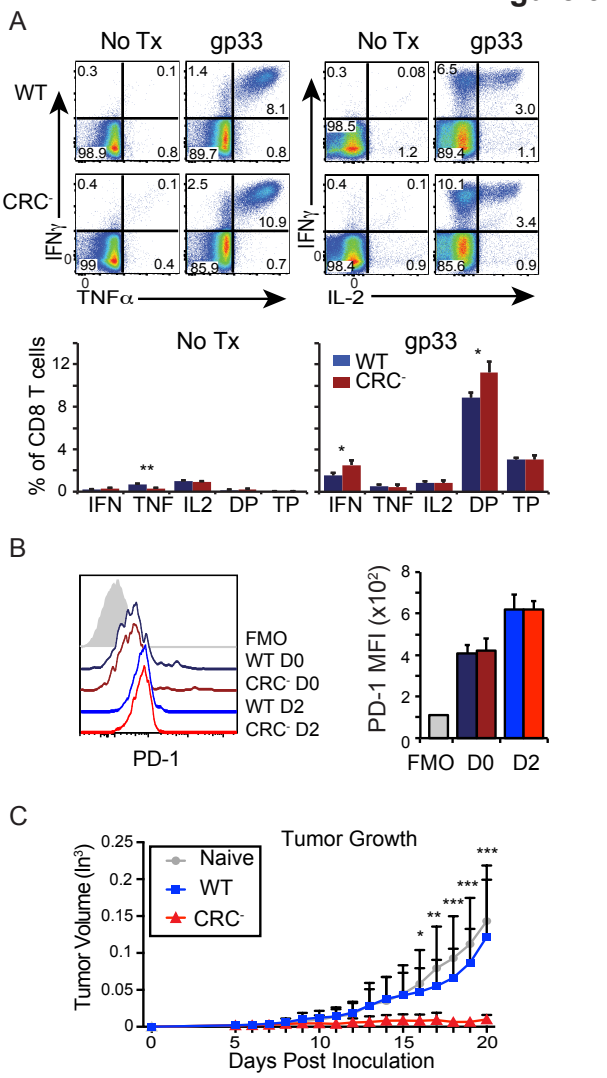

A) WT or CRC⁻ mice 35 days after LCMV Armstrong infection were sac'd and total splenocytes stimulated with no treatment or gp33 peptide in the presence of brefeldin A for 5 hours. IFNγ, TNFα, and IL-2 expressing populations were characterized by ICCS. B) 4000 WT or CRC⁻ gp33-specific memory T cells from day 35 Armstrong-immune mice, or 4000 naïve T cells, were adoptively transferred into WT hosts bearing day 5 B16.F10-gp33 tumors. Subsequent tumor growth was measured daily by calipers along the major and minor diameters of the tumor, and tumor volume was calculated as ½ LxW^2. Two groups of 5 mice per genotype were used for these experiments. Each bar represents a mean of a single group of mice. Error bars indicate standard deviation. Student's T tests were used to calculate significance in (A). Two-way ANOVA was used to calculate significance in (B). * P< .05; ** P<.01; *** P<.001

Chapter 4: LSD1 and its effects on PD-1 through epigenetic programming

Alexander P. R. Bally[1], Peiyuan Lu[1], Benjamin G. Barwick[1], and Jeremy M. Boss[1]

[1]Department of Microbiology & Immunology and Emory Vaccine Center; Emory University School of Medicine; Atlanta, GA 30322

APRB performed flow cytometry for figure 2, and isolated material for figures 3, 4, and 5.

APRB and BGB performed bisulfite sequencing for figure 6.

PL generated cells and mRNA for figure 1, and performed ChIPs in figures 3, 4, and 5.

JMB provided scientific insight and guidance

This chapter was written by APRB and JMB

Introduction

During prolonged adaptive immune activation, such as in chronic viral infection or anti-cancer responses, sustained T cell receptor (TCR) stimulation by cognate peptide:MHC complexes results in T cell exhaustion and an inability to appropriately respond to pathogenic antigens (Wherry et al., 2003). This is in part mediated by upregulation of PD-1 on a responding T cell (Barber et al., 2006) and subsequent engagement with its ligands PD-L1 or PD-L2 (Blank et al., 2004; Chemnitz et al., 2004; Freeman et al., 2000). Although antibody blockade of PD-1/PD-L interactions can temporarily reinvigorate immune function for the duration of treatment (Barber et al., 2006), PD-1 remains stably expressed on T cells during a chronic infection even during reinvigoration (Youngblood et al., 2013), and continues to be expressed even upon removal of the cell from a chronic stimulatory environment (Utzschneider et al., 2013). Although most PD-1^{hi} exhausted CD8 T cells die upon loss of TCR stimulation, these cells and subsequent daughter cells remain less functional compared to PD-1^{lo} cells after transfer into an acute inflammatory environment (Utzschneider et al., 2013). The stability of PD-1 expression and inhibition of effector functions across generations of cell division even after changing from chronic to acute TCR signals suggests that an epigenetic program stably enforces transcription at the *Pdcd1* locus.

Epigenetics provide the primary mechanism for enforcing a unique transcriptional program across cellular generations, with dynamic modifications to genomic DNA including DNA methylation and histone modifications to alter chromatin accessibility and control gene transcription (Araki et al., 2009; Lee et al., 2001; Li, 2002; Scharer et al., 2013; Shih et al., 2014). CpG methylation within gene promoters or enhancers is often associated with transcriptional silencing (Xu et al., 2007). Two such CpG regions regulate expression of *Pdcd1* and exhibit dynamic methylation in T cells in correlation

with gene expression during an infection (Youngblood et al., 2013; Youngblood et al., 2011). Similarly, histone protein modifications within gene regulatory chromatin regions can affect transcriptional activity. Histone H3 can contain pro-transcriptional monomethylation on the lysine 4 residue (H3K4^{me1}) and lysine acetylation (H3K27^{ac} and H3K9^{ac}) (Creyghton et al., 2010). Both H3K27^{ac} and H3K9^{ac} marks at proximal regulatory elements have been correlated with *Pdcd1* expression driven by TCR stimulation (Lu et al., 2014; McPherson et al., 2015), and H3K4^{me1} is added in response to cytokine stimulation which further drives gene expression (Austin et al., 2014). Furthermore, the repressive modifications H3K9^{me3}, H3K27^{me3}, and H4K20^{me3} appear at the locus corresponding with *Pdcd1* gene silencing following acute stimulation (Lu et al., 2014).

During acute activation of T cells, exogenous expression of the transcriptional repressor Blimp-1 induced the repressive modifications H3K9^{me3}, H3K27^{me3}, and H4K20^{me3}, and subsequently silenced PD-1 expression (Lu et al., 2014). Surprisingly, during a chronic infection where PD-1 levels are at their highest, Blimp-1 is also expressed in exhausted CD8 T cells yet fails to repress PD-1 (Shin et al., 2009). In exhausted CD8 T cells of Blimp-1 KO mice, the high levels of PD-1 expression were in fact slightly reduced (Shin et al., 2009), suggesting a role for Blimp-1 in activating rather than suppressing *Pdcd1* during a chronic infection. The molecular mechanism for how Blimp-1 could function differentially as a repressor or activator of gene expression is unclear.

As a repressor, Blimp-1 is known to recruit additional transcriptional repressors that result in silencing the local chromatin environment (Shin et al., 2013; Su et al., 2009; Yu et al., 2000). Along with histone deacetylases HDAC1 and HDAC2 and the histone methyltransferase G9a, Blimp-1 is known to recruit the lysine-specific demethylase LSD1 (Gyory et al., 2004; Su et al., 2009; Yu et al., 2000). This histone modifying enzyme removes the marks H3K4$^{me1/me2}$ associated with transcriptional activation

(Jenuwein and Allis, 2001; Shi et al., 2004), thereby facilitating gene silencing. Furthermore, LSD1 has been shown to specifically act on immune genes to mediate repression (Janzer et al., 2012; Su et al., 2009). Given the ability of Blimp-1 to repress genes through recruitment of histone modifiers such as LSD1, these cofactors are likely mediators of the PD-1 phenotypes seen in Blimp-1 knockout mice following an acute stimulation, and differential recruitment by Blimp-1 of factors such as LSD1 during chronic infection could account for the failure to down-regulate PD-1 in the continued presence of high Blimp-1. In this study, we show that Blimp-1 is necessary to recruit LSD1 to the PD-1 gene, and that when bound LSD1 actively down-regulates PD-1 transcription and expression. Furthermore, although Blimp-1 is bound to the *Pdcd1* locus in both acute (PD-1^{low}) and chronic (PD-1^{hi}) settings, LSD1 is only recruited following an acute stimulation, correlating with removal of proximal H3K4me1/me2 modifications and appearance of a repressive epigenetic profile concurrent with *Pdcd1* silencing.

Methods

Mouse lines and cell isolation

C57BL/6J mice were obtained from Jackson laboratories. $LSD1^{fl/fl}$ mice (Wang et al., 2007) were kindly provided by D. Katz (Emory University), crossed to mice containing a Granzyme B promoter-driven Cre provided by J. Jacob (Emory University) (B6;FVB-Tg(GMB-cre)1Jcb), and subsequently back-crossed to the C57BL/6 mouse line. Blimp-$1^{fl/fl}$ mice were provided by K. Calame (Columbia University) and similarly crossed to Granzyme B-cre mice. Blimp-$1^{fl/fl}$;$LSD1^{fl/fl}$;Granzyme B-cre conditional double knockout mice were generated by crossing these two strains.

For cell analysis or ex vivo cell culture, CD8 T cells were isolated from splenocytes using a MACS mouse CD8 T cell isolation kit (Miltenyi). Where indicated,

cells were further purified by FACS on a BD FACSAria II (Emory SOM flow cytometry core). Cells were cultured ex vivo in RPMI supplemented with 5% FBS, 5% BCS, L-glutamine, and Penicillin/streptomycin, and stimulated with CD3/CD28 beads (life technologies).

Virus Infection

Viral stocks of LCMV strains Armstrong and Clone 13 were generated as previously described (Matloubian et al., 1990) and kindly provided by Rafi Ahmed. Mice were infected with $2x10^5$ pfu Armstrong i.p or with $2x10^6$ pfu LCMV Clone 13 i.v. Viral titers were determined by plaque assay using vero cells (ATCC CCL-81) as previously described (Ahmed et al., 1984).

Flow cytometry

Cells were stained for flow cytometry in FACS buffer (PBS, 1% BSA, 1 mM EDTA) for 30 minutes, and subsequently fixed using 1% paraformaldehyde for 30 minutes. Events were collected on a BD LSR II and analyzed using FlowJo 9 software. Antibodies used to stain cells included: CD4 PerCP-Cy5.5 (clone RM4.5); CD8 FITC (clone 53-6.7); CD44 APC-Cy7 (clone IM7); CD62L Alexa Fluor 700 (clone MEL-14); CD69 PE-Cy7 (Clone H1.2F3); CD127 BV510 (Clone SB/199); PD-1 PE (clone RMP1-30). gp33 var C41M (KAVYNFATM), gp276 (SGVENPGGYCL), and np396 (FQPQNGQFI) biotinylated peptide:MHC-I monomers on H-$2D^b$ were obtained from the NIH Tetramer Core facility at Emory University and subsequently tetramerized to streptavidin-APC (Prozyme).

Quantitative Real-time PCR

RNA was isolated from at least 3 independent preparations of cells using the RNeasy kit (Qiagen), and cDNA was prepared from RNA libraries using SuperScript II reverse

transcriptase (Life Technologies Co). RT-PCR was used to quantitate mRNA levels in technical duplicates, and values were normalized using 18s ribosomal RNA as previously described (Yoon et al., 2012)

Chromatin Immunoprecipitation.

Chromatin immunoprecipitation (ChIP) assays were performed as previously described (Beresford and Boss, 2001; Lu et al., 2014). Purified cell populations were cross-linked for 10 minutes in 1% formaldehyde, and subsequently lysed in cell lysis buffer (5mM PIPES pH 8.0, 85 mM KCl, 0.5% NP-40). Chromatin was extracted using nuclei lysis buffer (50 mM TRIS pH 8.1, 10 mM EDTA, 1% SDS) and sonicated to an average length of 400-600bp. 5 µg of chromatin was used for immunoprecipitation reactions on Protein A beads with 0.5µg of polyclonal antibodies for H3K4me1 (rabbit polyclonal antibody, EMD Millipore), H3K4me3 (rabbit polyclonal antibody), or H3K27ac (rabbit polyclonal antibody). Precipitates were quantitated by qRT-PCR and calculated as a percent of input.

Bisulfite Sequencing

Bisulfite sequencing was performed as previously described (Youngblood et al., 2011). Genomic DNA was isolated from CD8 T cells and bisulfite converted using the EpiTect Bisulfite Kit (Qiagen). Converted DNA was amplified by PCR and cloned with the TOPO TA cloning kit (Life Technologies), and subsuently sequenced using primers in Table 4-1. Data were aligned *in silico* using the R / Bioconductor Biostrings package and custom scripts as previously described (Scharer et al., 2013).

Results

LSD1 represses PD-1 following acute stimulation

The histone demethylase LSD1 represses multiple immune related genes (Hill et al., 2014; Su et al., 2009) and can be recruited to loci by Blimp-1 (Su et al., 2009), a known repressor of PD-1 (Lu et al., 2014). To determine if LSD1 represses PD-1 expression, $LSD1^{fl/fl}$ mice were crossed to a granzyme B cre background, which causes conditional of the gene in activated T cells (Jacob and Baltimore, 1999). When stimulated in culture using anti-CD3/CD28 beads, CD8 T cells from $LSD1^{fl/fl}$ cre+ (KO) animals displayed nearly two-fold higher levels of PD-1 mRNA compared to cre- littermate controls at 24 hours, the peak of PD-1 expression by this method of stimulation (Figure 4-1). Furthermore, PD-1 mRNA levels remained higher in the KO for four days after initial stimulation, while levels returned to baseline in the WT mice (Figure 4-1). This suggests that LSD1 represses *Pdcd1* transcription.

To test if PD-1 expression is modulated by LSD1 during an acute viral infection, mice were infected with LCMV Armstrong. At day 8 after infection, when viral loads have been cleared and WT mice have down-regulated PD-1 expression on virus-specific CD8 T cells (Figure 4-2A, blue line), T cells from LSD1 conditional knockout mice retained high PD-1 expression (Figure 4-2A). This was comparable to the higher expression of PD-1 seen at day 8 in Blimp-1 knockout mice (Figure 4-2A middle, and (Lu et al., 2014)). The comparable increase in PD-1 expression on CD8 T cells from both Blimp-1 and LSD1 knockout mice suggests that these factors may operate along the same pathway. At the same time point during an acute infection, Blimp-1 LSD1 double knockout virus-specific CD8 T cells showed a similar phenotype, which was similar to either individual knockout (Figure 4-2A right). This suggests that these factors operate along the same pathway, and that Blimp-1 recruits LSD1 in order to mediate gene repression. However, 28 days after infection, LSD1 knockout CD8 T cells no longer showed an increase in PD-1 expression, unlike cells from Blimp-1 knockout mice (Figure 4-2B). This suggests that while LSD1 is a part of the pathway responsible for

decreasing PD-1 expression and is required for early rapid loss of transcription after infection, it is not necessary for long-term repression of PD-1 expression in a Blimp-1-mediated manner. Instead, other factors known to be recruited by Blimp-1, such as G9A, HDAC1, and HDAC 2 (Gyory et al., 2004; Su et al., 2009; Yu et al., 2000), may be sufficient to mediate long-term gene repression.

At early time-points during a chronic infection mediated by LCMV clone-13, when PD-1 is close to its peak expression, deletion of LSD1 had no effect on PD-1 expression (Figure 4-2C). However, at day 28 post infection with LCMV, when PD-1 has decreased slightly from peak levels but remained highly expressed overall, LSD1 knockout virus-specific CD8 T cells showed an increase in PD-1 expression, (Figure 4-2D) indicating a conserved role for LSD1 in suppressing PD-1 in both acute and chronic inflammatory settings. This is in contrast to the role of Blimp-1, which overall serves as an activator rather than a suppressor of PD-1 during chronic infection: the Blimp-1 knockout mouse shows decreased PD-1 expression at this late stage in chronic infection (Figure 4-2D), consistent with previous reports (Shin et al., 2009). Intriguingly, at day 8 during a chronic infection, before CD8 T cells are truly exhausted, Blimp-1 continues to act as a repressor, much like it does during an acute infection (Figure 4-2C). The differential roles performed by Blimp-1 and LSD1 at day 28 of a chronic infection may indicate that while Blimp-1 still recruits LSD1 to suppress gene expression, Blimp-1 performs additional functions that ultimately serve as an activator.

Blimp-1 recruits LSD1 to Pdcd1 *after TCR stimulation*

In order to determine if LSD1 interacts directly with the *Pdcd1* locus concurrent with PD-1 silencing, and whether it is recruited there by Blimp-1, chromatin IPs were performed using CD8 T cells stimulated in vitro. At day 4, when PD-1 expression has nearly returned to baseline levels, both LSD1 and Blimp-1 were bound at the *Pdcd1* locus in

WT mice (Figure 4-3A and 4-3B, WT). This indicates LSD1 directly affects the *Pdcd1* locus. However, LSD1 binding at the *Pdcd1* locus was also not observed in Blimp-1 knockout mice (Figure 4-3A, cre+), indicating that Blimp-1 is necessary to recruit LSD1 to the region. Importantly, LSD1 binding was not observed at the locus in LSD1 knockout mice (Figure 4-3B). However, Blimp-1 was still bound in LSD1 knockout mice (Figure 4-3B), indicating that Blimp-1 is capable of independently interacting with *Pdcd1*. Overall, these data indicate the LSD1 directly interacts with *Pdcd1* to suppress expression, and is recruited to the region by Blimp-1.

LSD1 is not recruited during chronic infection

Blimp-1 binds directly to *Pdcd1* following an acute infection, and acts as a transcriptional repressor (Lu et al., 2014). However, during a chronic infection, Blimp-1 is expressed at even higher levels, and is necessary for maximal PD-1 expression (Shin et al., 2009). To determine if Blimp-1 interacted directly with *Pdcd1* during chronic inflammation, a chromatin IP was performed on virus-specific CD8 T cells from naïve, acutely-infected, or chronically-infected mice. As previously reported, Blimp-1 was found bound to *Pdcd1* at a late time point following acute infection, correlating with loss of PD-1 expression. However, despite continued high levels of PD-1, Blimp-1 was also bound during a chronic infection (Figure 4-4). LSD1 was also bound to *Pdcd1* after an acute infection, correlating with its repressive role (Figure 4-4). However, unlike Blimp-1, LSD1 was not recruited to the region during a chronic infection. This suggests that although Blimp-1 interacts with *Pdcd1* during a chronic infection, it fails to down-regulate the gene because it does not recruit LSD1 to the site.

To further characterize this interaction, specific histone modifications associated with gene activation were examined across the *Pdcd1* regulatory region by ChIP. The histone modifications H3K4me1 and H3K4me2, which are targeted by LSD1 for removal,

were present during chronic infection, but absent in naïve mice and during an acute infection (Figure 4-5). This correlates with silencing of the PD-1 locus in CD8 T cells from both naïve mice and at day 8 after an acute infection. This also suggests that the binding of LSD1 to the *Pdcd1* region functions to remove these activating marks and suppress gene expression.

Epigenetic silencing of the locus following acute infection is enforced by LSD1

During viral infection, loss of CpG methylation at the *Pdcd1* locus is correlated with gene expression, and reappearance of methylation is concurrent with gene silencing (Youngblood et al., 2011). As the loss of H3K4me1/me2, potentially mediated by LSD1, is necessary for acquisition of DNA methylation (Wang et al., 2009), changes in methylation were analyzed by bisulfite sequencing in LSD1^{-} animals during acute infection. At day 8 after LCMV Armstrong, LSD1$^{fl/fl}$ cre^{-} mice show a relative abundance of CpG methylation across the *CR-B* region of *Pdcd1* (Figure 4-6), in accordance with the remethylation observed in WT animals at this time (Youngblood et al., 2011). In contrast, LSD1$^{fl/fl}$ Cre^{Gzmb} mice (lacking functional LSD1) showed minimal remethylation across the region (Figure 4-6). This suggests that the inability to remove H3K4 methylation due to the knockout of LSD1 inhibits the acquisition of DNA methylation, thereby providing a further mechanism for retaining prolonged gene expression.

Discussion

Multiple recent studies have highlighted the important effects of dynamic epigenetic regulation in driving immune responses (Pauken et al., 2016; Scharer et al., 2017; Scharer et al., 2016; Sen et al., 2016). Here, LSD1 is identified as a novel epigenetic regulator of PD-1. Using knockout mice, Blimp-1 was identified as necessary to recruit LSD1 to the *Pdcd1* promoter. Although the repressor Blimp-1 itself associates with

Pdcd1 in both acute (PD-1 silencing) and chronic (PD-1 permissive) inflammatory environments, LSD-1 is only recruited to the locus in acute situations, providing a mechanistic switch for the differential expression of PD-1 in the two infectious modalities. Furthermore, the association of LSD1 with *Pdcd1* during resolution of an acute infection correlates with disappearance of the active histone modifications targeted by LSD1: H3K4me1 and me2.

Blimp-1, a protein associated with B cell maturation into antibody-secreting plasma cells, is a critical inhibitor of *Pdcd1* transcription following acute CD8 T cell stimulation (Lu et al., 2014). Increases in Blimp-1 mRNA and protein following antigen clearance are associated with reciprocal decreases in PD-1. Paradoxically, if antigen persists and stimulation through the TCR continues, Blimp-1 levels nonetheless increase (Shin et al., 2009). Whereas in an acute infection the Blimp-1 knockout mouse showed higher PD-1 on T cells, suggesting an inhibitory function, the same deletion resulted in modestly lower levels of PD-1 in a chronic infection, suggesting Blimp-1 acted as an activator. In this study, Blimp-1 was identified as bound at *Pdcd1* in both patterns of infection, thereby precluding the possibility that the changing function of Blimp-1 was mediated indirectly through Blimp-1 binding to other target genes. Instead, recruitment of LSD1, which was dependent on the presence of Blimp-1, was found to be unique to acute infections.

Splice variants of Blimp-1 have been shown both to be involved in different timing of expression (Morgan et al., 2009) and to have alternative functions (Morgan et al., 2012). In particular, artificial isoforms generated by a genetic deletion of the C-terminal zinc-finger domain and proline-rich domain in exon 7 fail to bind DNA or recruit the histone modifiers HDAC1/2 and G9a. This same proline-rich domain has also been shown to be necessary for Blimp-1 to associate with and recruit LSD1 to DNA (Shin et al., 2009). An alternative study analyzing artificial constructs with Blimp-1 zinc-finger

domains showed that only the first 2 zinc-finger domains of Blimp-1 are necessary for DNA binding (Keller and Maniatis, 1992), suggesting that the native isoform lacking exon 7 may still bind DNA, but be unable to recruit histone modifiers. Although in a chronic infection Blimp-1 does successfully bind DNA, expression as an alternative isoform could account for its inability to recruit LSD1 and subsequent failure to inhibit *Pdcd1* expression. Thus, TCR stimulation drives transcription at the Blimp-1 promoter in both acute and chronic settings, but variant splicing may produce a protein with radically different functionality in regards to PD-1. Although Blimp-1 was bound to *pdcd1* during a chronic infection, it is unknown which isoform is present at the locus.

While this study focuses on the effects of epigenetics on determining the expression of a single immune-related gene during infection, it emphasizes the ramifications epigenetic systems have on immune outcomes. Most immune events involve the stable differentiation from a naïve precursor into a cell with discrete and sustainable functions. It is likely that genome-wide epigenetic patterns are necessary to maintain a quiescent, naïve state in many cell types, and stimulus-driven alterations to these patterns drive differentiation into a novel yet stable cell type. Understanding the epigenetic landscapes that define functional profiles and the cellular machinery that is capable of altering them may ultimately enable an unprecedented control over inflammatory environments.

Figure 1

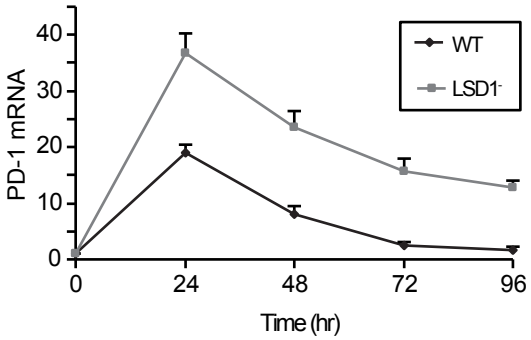

Figure 4- 1: LSD1 inhibits PD-1 expression ex vivo

CD8 T cells were isolated by MACS from Cre- (WT) or granzyme B Cre+ (LSD1-) $LSD^{fl/fl}$ mice and stimulated with anti-CD3/CD28 beads for the times indicated. At each timepoint, mRNA was analyzed by qRT-PCR. Data represent three independently isolated biological replicates.

Figure 2

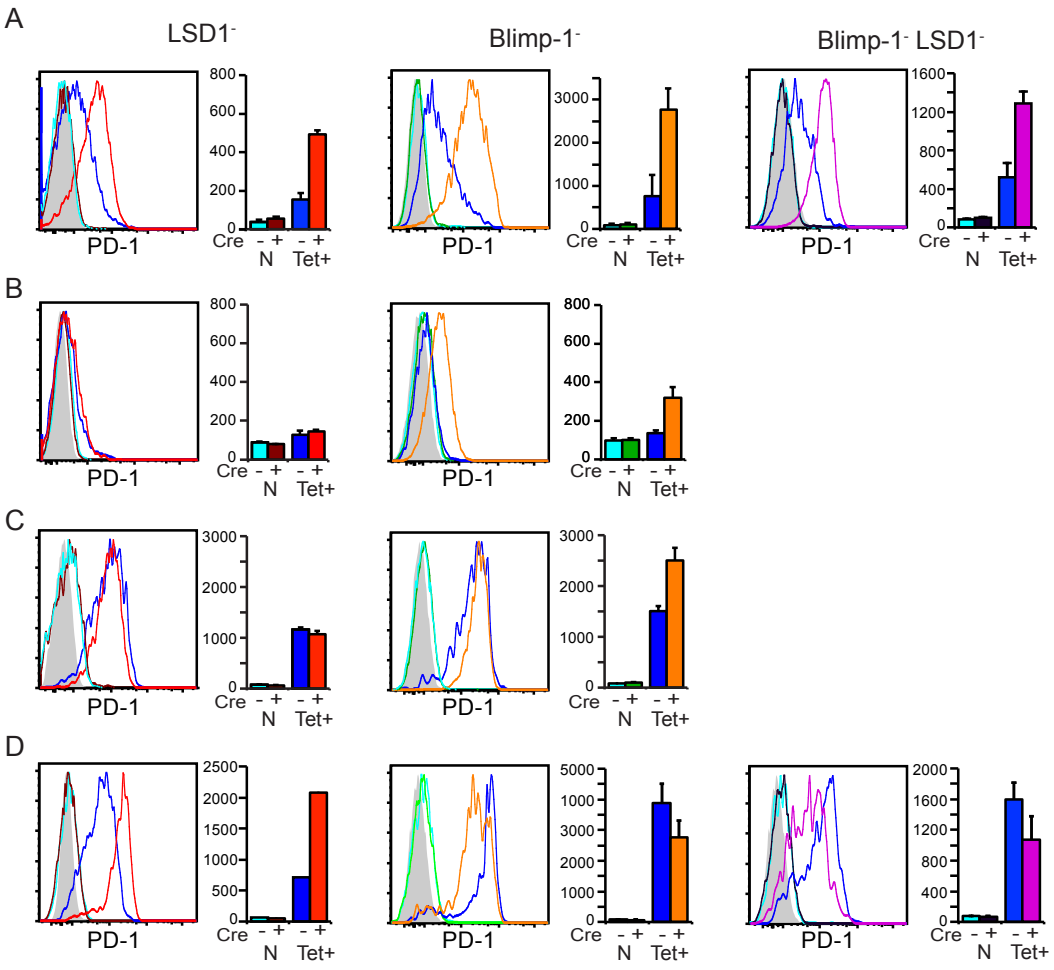

Figure 4- 2: PD-1 down-regulation after acute infection requires LSD1

LSD1$^{fl/fl}$ (left), Blimp-1$^{fl/fl}$ (middle), or LSD1$^{fl/fl}$:Blimp-1$^{fl/fl}$ (right) mice were infected with LCMV Armstrong for 8 days (A), Armstrong for 28 days (B), Clone-13 for 8 days (C) or Clone-13 for 28 days (D). At day 8 (A and C) or day 28 (B and D) mice were sacrificed, and splenocytes were stained and analyzed by flow cytometry. Naïve cells (CD8+ tetramer- CD44- CD62L+) and virus-specific cells (CD8+ gp33 tetramer+ CD44+ CD62L-) were analyzed from each mouse.

Figure 3

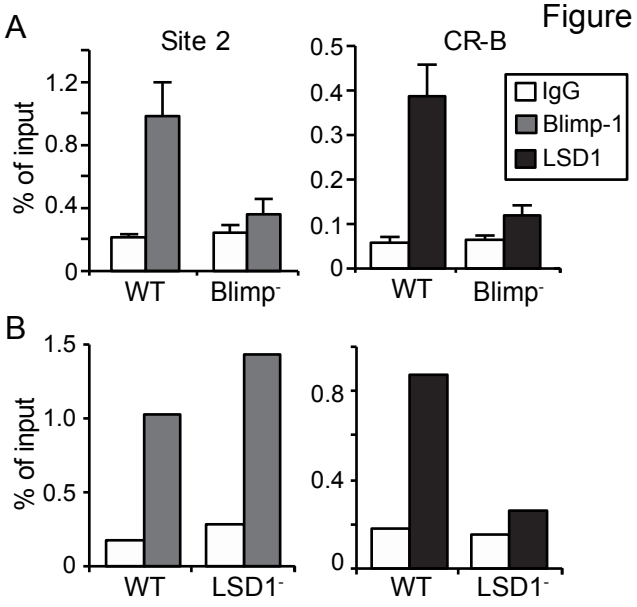

Figure 4- 3: Blimp-1 recruits LSD1 to the *Pdcd1* locus

A) CD8 T cells from Blimp-1$^{fl/fl}$ Granzyme B cre mice were isolated by MACS and simulated with CD3/CD28 beads. 96 hours after stimulation, chromatin was prepared and IPs against Blimp-1, LSD1, or control IgG were performed. B) Chromatin IPs were performed from cells prepared as in (A) from LSD1$^{fl/fl}$ Granzyme B cre mice.

Figure 4- 4: LSD1 is recruited only after an acute infection

Figure 4

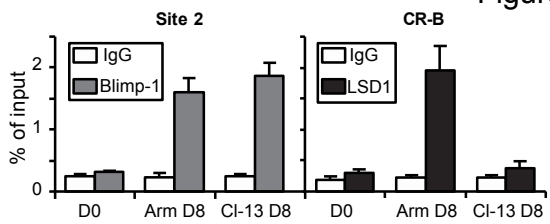

CD8 T cells were isolated by MACS from WT naïve mice, or mice infected with LCMV Armstrong or Clone-13 for 8 days. Chromatin was prepared from these cells, and chromatin IPs were performed using antibodies specific to Blimp-1, LSD1, or a control IgG. These data represent three independent biological replicates.

Figure 4- 5: Histone targets of LSD1 are removed after an acute infection

Figure 5

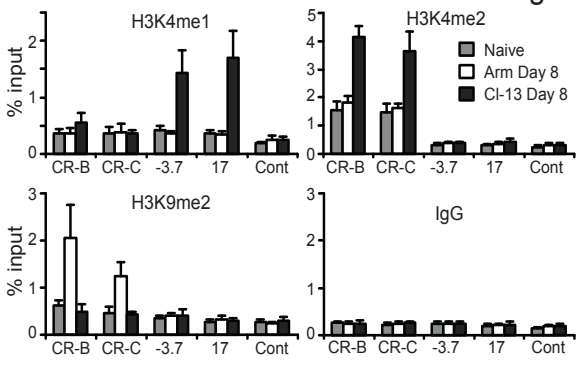

WT mice were infected with LCMV Armstrong or Clone-13 for 8 days. CD8 T cells were isolated by MACS from these mice, or from uninfected naïve mice, and used to generate chromatin. Chromatin IPs were performed with antibodies to detect H3K4 monomethylation and demethylation, H3K9 dimethylation, or using a control IgG across the *Pdcd1* regulatory region, using primers for the indicated sites. Three independent biological replicates were used to generate these data.

Figure 4- 6: LSD1 is required for remethylation of the PD-1 locus after infection

Figure 6

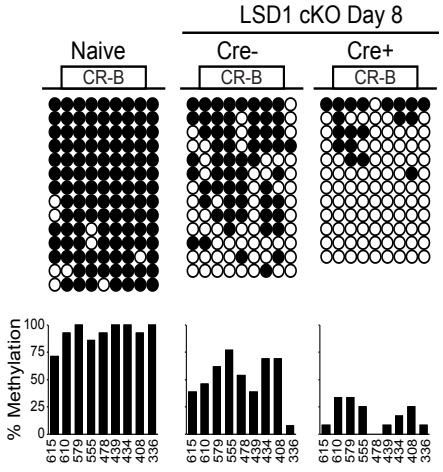

$LSD1^{fl/fl}$ cre- or cre+ mice were infected with LCMV Armstrong for 8 days. CD8 T cells from these mice or naïve, uninfected Cre- mice were isolated by MACS, and tetramer-specific cells were sorted by FACS. DNA from each population was bisulfite converted and PCR amplified. 8 clones from each mouse was sequenced, and incomplete sequences were discarded. At each CpG site across the CR-B region, presence of DNA methylation within each clone is indicated by a closed circle and unmethylated CpG sites are indicated by an open circle. Frequency of methylation at each site across all clones is indicated below. Data are combined from two biological replicates.

Chapter 5: Genome-wide chromatin accessibility during viral infection

*Data originally published in the *Journal of Immunology*. Scharer CD, Bally AP, Gandham B, and Boss JM. Cutting Edge: Chromatin accessibility programs CD8 T cell memory. J Immunol. 2017 Mar 15;198(6):2238-2243. Copyright © 2017

Viral infections and cell isolation was performed by APRB

Flow cytometry in figure 1 was performed by APRB

Memory cell stimulation and RT-PCR in figure 5 was performed by APRB

Sequencing libraries were generated by CDS

Bioinformatic analyses (including generating read tracks, K-means clustering analyses, Gene ontology analyses, and transcription factor footprinting) were performed by CDS and BG

This chapter was written by APRB and JMB

Introduction

After stimulation through the TCR, CD8 T cells proliferate and differentiate into antigen-specific short lived effector cells (T_{SLEC}). Following antigen clearance and subsequent loss of TCR signaling, this T_{SLEC} population contracts, leaving a proportionally smaller population of long-lived memory cells with distinct activation requirements and functional properties compared to both naïve and acute-phase effector cells, including lower activation requirements, enhanced proliferative capacity, and more rapid induction of effector genes (Kersh et al., 2006; Pihlgren et al., 1999; Veiga-Fernandes et al., 2000; Zimmermann et al., 1999). Similarly, during a chronic antigenic infection, following the initial burst of inflammatory cell division, the effector population also contracts, but leaves behind a small population of non-responsive, "exhausted" T cells with limited capacity to effectively combat pathogens, despite the presence of an ongoing infection (Gallimore et al., 1998). Although the altered inflammatory capabilities of both memory and exhausted T cells have been extensively described, the mechanisms that program and maintain these profiles are still poorly understood.

Some transcriptional and epigenetic changes that occur during T cell responses to infection have been examined through systems biology. Unique epigenetic states, including changes to DNA methylation and histone modifications, program aspects of CD8 T cell differentiation during acute and chronic viral infections (Scharer et al., 2013; Youngblood et al., 2011; Zediak et al., 2011), however these epigenetic profiles have not been integrated with transcriptional paradigms established within each state. (Doering et al., 2012; Kaech et al., 2002a; Russ et al., 2014). The ability of some transcription factors, such as NFATc1, to influence genome wide transcriptional changes during T cell responses have been probed by ChIP-seq and manipulation of binding partner choices.

(Martinez et al., 2015). These data indicate that the functional fate of T cells involves the integration of multiple external signals at distinct *cis*-regulatory sites.

In this study, genome-wide epigenetic profiles of CD8 T cells during acute and chronic viral infections are queried using the assay for transposase accessible chromatin sequencing (ATAC-seq) (Buenrostro et al., 2013). When integrated with published RNA-seq datasets, these profiles revealed unique epigenetic states dependent on the time and type of infection. This study revealed a novel set of "primed" loci enriched at accessible but low-expressed genes in resting memory CD8 T cells, which may provide a mechanism for enhanced and more rapid function upon secondary antigen encounter.

Methods

Mice and LCMV Infection

Wild-type C57BL/6J mice were obtained from Jackson laboratories and bred on site. Thy1.1+ P14 mice and viral stocks of LCMV strains Armstrong and Clone 13 were kindly provided by Dr. Rafi Ahmed (Emory University). Infections were performed on 6-8 week old mice as previously described (Wherry et al., 2007) and viral titers confirmed by plaque assay (Ahmed et al., 1984). All animal protocols were approved by the Emory University Institutional Animal Care and Use Committee.

Cell Isolation and analysis

CD8 T cells were enriched from splenocytes by MACS (Miltenyi Biotec) in accordance with manufacturer's instructions, stained in FACS buffer (PBS, 1% BSA, 1mM EDTA), and sorted on a BD FACSAria II. Antibodies used for sorting were from Tonbo Biosciences: CD8:FITC, CD4:PerCP-Cy5.5, CD44:APC-Cy7; or BioLegend: CD62L:Alex Fluor 700, Thy1.1:Pacific Blue, and PD-1:PE. Mouse MHC-I ($H\text{-}2D^b$) tetramers corresponding to LCMV peptides gp33 var C41M (KAVYNFATM), gp276

(SGVENPGGYCL) and np396 (FQPQNGQFI) obtained from the NIH Tetramer Core facility at Emory University.

For *ex vivo* experiments, 10^4 P14 CD8 T cells were adoptively transferred into WT hosts. After 1 day, mice were infected with LCMV Armstrong. At day 28, splenocytes from immune mice or naïve P14 mice were stimulated with 4 μM LCMV gp33 var C41M peptide for the times indicated. Cells were fixed in 1% paraformaldehyde and virus-specific P14 cells were sorted by FACS using markers described above. RNA was prepared using the Pinpoint Slide RNA Isolation System (Zymo Research).

ATAC-seq and data analyses

ATAC-seq libraries were generated from 10^4 cells for each sample, sequenced, and data processed as detailed previously (Scharer et al., 2016). Loci with accessibility changes > 2-fold and FDR < 0.05 were called significant. Gene Ontology (GO) term enrichment was determined using DAVID (Huang da et al., 2009) and motifs identified with HOMER (Heinz et al., 2010) using all significant acute time point peaks as background. All other data display and analysis was performed using custom R/Bioconductor scripts. ATAC-seq data are available under accession GSE83081 in the GEO database (www.ncbi.nlm.nih.gov/geo/). Raw microarray data was downloaded from accession GSE30341 (Doering et al., 2012). Data processing was performed using the Affy R/Bioconductor package (Gautier et al., 2004). Mapping of ATAC-seq peaks to genes was performed by annotating each peak to the nearest gene transcription start site and microarray data annotated using the ENTREZ ID.

qRT-PCR

cDNA was prepared from total RNA using SuperScript II Reverse Transcriptase (Invitrogen). Relative cDNA quantities for each gene listed were quantitated using real-

time PCR, and calculated as a percentage of *Actb* expression within each sample. All primer sequences are available on request.

Results

Chromatin accessibility is remodeled during acute LCMV infection

In order to study the epigenetic changes that occur during an immune response, mice were infected with either LCMV Armstrong or Clone 13 to induce an acute or chronic infection, respectively (Wherry et al., 2003). At distinct stages of the immune response, virus-specific CD8 T cells were isolated and ATAC-seq was performed to identify genome wide chromatin accessibility (Buenrostro et al., 2013; Scharer et al., 2016). The time points chose represent naïve cells (n) early effector (aD4), late effector (aD8), memory (aD30), early chronically infected cells (clD8), and exhausted CD8 T cells (clD28) (Figure 5-1A). A principle component (PC) analysis of all 89,746 accessible regions from the ATAC-seq data revealed a linear shift from naïve to late timepoints along PC1 correlating with antigen experience, while PC2 differentiates memory populations and PC3 differentiates exhausted populations (Figure 5-1B).

After antigen encounter, cells predominantly gained chromatin accessibility through day 8, with the greatest changes in accessibility gains and losses seen at day 8 after an acute infection compared to naive, and subsequently showed an overall loss in accessible regions from day 8 to day 30 during an acute infection (Figure 5-1C). The *Pdcd1* gene exemplified this, with a gain in accessibility after differentiation from naïve cells in correlation with gene activation, and showed a unique region accessible during chronic infections (Figure 5-1D), correlating with previously published data (Sen et al., 2016). Similarly, the locus encoding L-Selectin (Sell) contained regions that transiently lose accessibility at day 4 and day 8 after acute infection, and regained accessibility by day 30, again correlating with gene expression (Figure 5-1D). Global averages of all

differentially accessible regions (DARs) showed an average gain during both acute and chronic infections over time (Figure 5-1E), although gene expression data (Doering et al., 2012; Youngblood et al., 2011) showed a peak at day 8 in both infectious modalities.

A K-means clustering was used to identify discrete patterns of dynamic genomic accessibility changes in both acute and chronic infections (Figure 5-1F). In acute infections, 2 K-means modules (1 and 2) showed loci that gained accessibility at aD8 and lost it by memory cell formation (aD30). Modules 3 and 4 identified genes that lost accessibility over time from naïve cells, while module 5 identified loci with initially high accessibility that gained moderately more accessibility over time. Similar patterns can be seen during chronic infection with modules representing loci that gained and subsequently lost accessibility (Module 3), lost accessibility over time (1 and 2), or showed overall high accessibility (module 4). However, the relative size of these modules shifted between acute and chronic infections (Figure 5-1F). For example, loci that started with low accessibility and transiently gained accessibility (acute module 1, chronic module 3) represented a much greater proportion of total DARs in chronic than acute settings. To further corroborate the link between accessibility changes and gene expression, DARs were identified at 4 genes that exhibited dynamic mRNA expression (Doering et al., 2012; Youngblood et al., 2011). Various regions near the *Irf8*, *Ctsc*, *Kntc1*, and *Kif23* genes each showed increases in accessibility at time points and infectious types associated with high mRNA expression (Figure 5-2A).

Chromatin accessibility and gene expression patterns are linked to T cell function

Chromatin accessibility data from naïve, D8 and D30 cells from acutely infected mice were correlated with respective gene expression data from similar cells (Doering et al., 2012). 8,239 DARs were associated with local differentially expressed genes (DEG). A Euclidean-distance metric characterizing normalized two-dimensional changes in both

accessibility and expression over progressive cell types was ascribed to each DAR/DEG, followed by a K-means clustering that defined unique patterns of expression and accessibility changes (Barwick et al., 2016). This analysis identified seven distinct K-means modules (Figure 5-3A). Some modules demonstrated coordinate, progressive changes in both accessibility and expression from naïve, to day 8, to day 30. These included modules 1 and 7 (increasing) and modules 2 and 6 (decreasing). Module 4 demonstrated both accessibility and gene expression increases at aD8, followed by a subsequent decrease at aD30. The progressive changes in modules 1, 2, 6 and 7 indicate that the majority of memory-related DARs were programmed early and shared with effector cells, while a relatively small subset of loci (module 4) showed a reversal of effector programming during further differentiation from effector to memory. Intriguingly, two modules (3 and 5) showed inverse correlations between gene expression and proximal chromatin accessibility. These loci likely represent *cis*-regions that function as negative regulators of gene expression that are active repressors in undifferentiated (module 3) or differentiated (module 5) cells.

Hierarchal clustering of gene ontology data of the modules defined two distinct groups: modules 1, 3, 4, and 7 define T cell functions such as cell division, immune effector processes, and cell surface receptors (Figure 5-3B); modules 2, 5, and 6 contained genes with roles in transcriptional regulation, chromatin organization, and negative regulators of metabolism. This clustering correlated with genes in 1, 3, 4, and 7 that change from relative quiescence in naïve cells to higher expression at D8/D30, compared to 2, 5, and 6 which represented genes that become progressively more silenced. For example, ontologies associated with in modules 3, 4 and 7 contained genes associated with immune activation (*Prdm1* and MHC-II genes *H2-Ea*, *H2-Eb*, *H2-Oa* and *H2-Ob*) and cell cycling (*Brca1*, *E2F3*), as would be expected during the development of an immune response. In contrast, GO terms in module 2 included

negative regulators of metabolism (such as *Eif2ak3* and *Id3*) and DNA binding proteins (*Tcf7* and *Ikzf1*), possibly representing transcriptional regulators that maintain a naïve CD8 T cell profile prior to antigen experience.

Transcription factor networks coordinate accessibility changes

Individual transcription factor motifs enriched within the above DAR modules were classified into eight categories (I-VIII) based on those shared between multiple modules (I and II) or unique to a specific module (III – VIII) (Figure 5-3C). DARs associated with genes that were repressed upon T cell activation (at aD8) were proximal to binding sites for developmental transcription factors, such as Tcf3 (category VI; module 2) and GATA (category V; module 6).

Transcription factors associated with T cell activation, including AP-1 and NFAT family members, were identified within category I motifs and were shared across modules 1, 5, and 7, each of which was associated with increased accessibility upon T cell activation. Interestingly, GO analysis of module 1, which revealed a strong enrichment for cell surface receptors such as *Ctla4* and *Fasl*, contained monomeric NFAT motifs and displayed maximal changes in chromatin accessibility and gene expression at D8. By contrast, module 7 genes, which were associated with lymphocyte activation and immune effector processes (*Tbx21* and *Zbtb32*), were enriched for NFAT:AP-1 composite motifs, and showed progressive increases in both accessibility and expression through aD30. These data correlate with the distinct regulatory functions of the different NFAT DNA binding modes (Martinez et al., 2015), with NFAT:AP-1 heterodimers regulating later cell response events and monomeric NFAT monomeric sites signaling during earlier TCR stimulation.

The negative correlation between accessibility and gene expression displayed by modules 3 and 5 suggest these loci may represent negative regulatory elements. In

correlation with this, binding motifs for repressive transcriptional regulators were identified as associated with these modules. Module 3 gained expression but lost accessibility with activation, indicating sites that repress activation associated genes. These loci were enriched for motifs from the SOX family of transcription factors (category IV), which are essential for T cell development and memory formation (Hu and Chen, 2013). Similarly, module 5 denoted genes that lost expression and showed enrichment for AP-1 and NFAT consensus motifs (category I) and the transcriptional repressor Tbet (Kao et al., 2011a) (category II). AP-1 transcription factors can function as activators or repressors depending on the dimerization partner (Shaulian and Karin, 2002). Together, the presence of positive and negative regulatory elements provides a mechanism to promote a new cell fate while actively repressing the previous state.

By aligning predicted transcription factor motifs from all genome-wide sites, high-resolution transcription factor footprints can be identified, showing overall changes in chromatin accessibility. Such footprints were concatenated for AP-1, Tbet, and NFATc1 motifs. Although AP-1 and Tbet motifs showed large gains in accessibility within the binding sites, NFATc1 motifs demonstrated little to no change in accessibility within the footprint across all differentiation stages analyzed (Figure 5-4A). This indicates that AP-1 and T-bet binding sites may initially exhibit prohibitively closed chromatin in naïve cells, and events associated with activation open these regions to permit transcription factor binding. Conversely, NFATc1 binding sites may already be open in naïve cells, and are capable of being bound upon activation-induced NFATc1 transcription. For all three factors, the regions immediately proximal to the binding site motifs gained accessibility (Figures 5-4A, B). These data suggest that NFATc1 may bind to already open regions and subsequently initiate the opening of proximal chromatin, thereby facilitating the binding of other factors such as AP-1, which favor nucleosome depleted sites (Buenrostro et al., 2013). In contrast, Tcf3 binding site accessibility decreased

following the initial activation (Figure 5-4B). CTCF motifs, which were not enriched in any module, demonstrated no changes in accessibility genome wide. This suggests that the above changes are specific.

Two loci, *Fasl* and *Tcf7*, demonstrate the complex interplay directed changes to chromatin accessibility and gene expression during cell activation. The Fas ligand (*Fasl*) gene locus, which is induced following CD8 T cell activation (Figure 5-4C), contains enhancer and repressor regions representing k-means clustering modules 1 and 3 (Figure 5-3A) with NFAT and SOX family motifs, respectively. The NFAT motif gained accessibility while the SOX family motifs lost accessibility concurrent with *Fasl* gaining expression in activated cells. This suggests that these elements function to suppress (SOX-family motifs) gene expression in naïve cells or drive (NFAT) gene expression upon activation. By contrast, the expression of the T cell developmental factor *Tcf7* (Mercer et al., 2011) is down regulated in effector cells and subsequently up regulated following antigen clearance (Figure 5-4C). Accessibility was lost at motifs for Tcf3 (module 2) and GATA (module 6) binding motifs concurrent with loss of gene expression. A gain in accessibility at an AP-1 motif (module 5) was shown in both day 8 effectors and day 30 memory cells, indicating this locus may initially have a repressive function, but nonetheless remains open in memory cells (Figure 5-4C), highlighting multiple roles for consensus elements. Thus, dynamically accessible transcription factor binding sites from multiple modules consisting of both positive and negative regulatory control signals can mediate changes in expression of genes associated with distinct phases of CD8 T cell responses.

Memory CD8 T cells contain a unique subset of activation-primed genes

PCA analysis (Figure 5-1A) showed that genome wide chromatin accessibility was distinct in memory CD8 T compared to naïve or effector cells. Furthermore, none of the

K-means modules identifying changes in accessibility (Figure 5-1F) showed showed memory cells reverting to the levels of chromatin accessibility in naïve cells. In order to identify the memory specific program in relation to both the earlier effector cells as well as naïve cells, accessibility changes in the promoters of DEGs were identified during the transitions from naïve to effector (aD8) to memory (aD30). Both effector and memory cells showed a positive correlation with up regulated genes gaining and down regulated genes losing promoter accessibility compared to naïve precursors (Figure 5-5A). During the transition from effector to memory, up regulated active genes were associated with increased promoter accessibility (Figure 5-5A). However, the majority of the down-regulated genes from effector to memory cells showed no reduction in accessibility, or an overall increase in accessibility at promoters (Figure 5-5A). We suggests that these genes are therefore "primed" for re-expression in memory cells in order to facilitate rapid effector function upon secondary challenge. These primed genes were enriched for effector functions such as replication, cell activation, and response to stress (Figure 5-5B). Furthermore, these primed genes showed large differences in accessibility in memory cells compared to cells from late chronic infection (clD28) (Figure 5-5C). This further exemplifies the unique programming in memory cells, and the differential programming of T cells during acute and chronic infections.

Increased transcription and rapid induction of effector functions in memory CD8 T cells

Retaining accessibility in memory cells at promoters of genes associated with the immune response suggests that the chromatin state in memory cells allows these genes to be expressed at higher levels or more rapidly during a recall response. The expression levels of representative primed genes from memory P14 CD8 T cells were compared to naïve precursors by quantitative real-time PCR. With the exception of the transcriptional repressor *Zbtb32*, all of the genes chosen, including key effector

molecules (Gzma, Gzmb, IFN-γ), the transcription factor Eomes, and the T cell adhesion molecule CD49a (*Itga1*), demonstrated significantly higher levels of expression in resting memory cells compared to naïve (Figure 5-5D). To quantify the reactivation kinetics of these primed genes, memory or naïve P14 CD8 T cells were stimulated *ex vivo* with gp33 peptide over a time course and gene expression levels were measured. Each gene studied exhibited increased transcription but with distinct kinetic profiles. *Gzma* and *Gzmb* demonstrated increased mRNA in memory cells during early times, but matched with expression levels seen in naïve cells at late times after stimulation. In contrast, *Ifng*, *Zbtb32, Itgal*, and *Eomes*, were induced to final expression levels that were significantly higher than naïve. In particular, Zbtb32 showed increasing mRNA levels much earlier in memory compared to naïve cells, while the initial rate of induction of IFNγ was greater in memory. These data suggest that maintaining an open chromatin state at effector function associated genes in memory CD8 T cells is one mechanism to enhance the magnitude and kinetics of memory CD8 T cell responses.

Discussion

In this study, the chromatin profiles of naïve, early effector, late effector, memory, early exhausted, and late exhausted CD8 T cells were characterized using ATAC-seq. By using MHC:peptide tetramers to identify and purify virus-specific T cells, the molecular profiles of these cell types and how they change over the course of an infection was identified. Overall, chromatin accessibility increased from naïve cells to effector cells, and decreased in late exhausted cells. Overall, this correlated with gene expression, with the majority of genes gaining accessibility coordinately with increased mRNA transcription. Accessibility at a subset of loci anti-correlated with gene transcription, likely identifying regions of transcriptional reppressors. Specific transcription factors

were associated with certain patterns of changes to both accessibility and expression during the course of an acute infection. In particular, NFAT was associated with gains in gene expression and chromatin accessibility, while Tbet was associated with losses in gene expression/accessibility. Furthermore, a set of genes that remained highly accessible but not expressed in memory cells were capable of greater responses to secondary challenge, identifying a molecular, chromatin-associated mechanism to define the improved response to antigen seen in memory cells.

Recently, other analyses of chromatin accessibility changes in CD8 T cells were reported (Pauken et al., 2016; Scott-Browne et al., 2016; Sen et al., 2016). These studies primarily focused on the unique features of the exhausted CD8 T cell program compared to acutely activated T cells. Our data corroborates those studies and adds a unique integrative analysis of gene expression, accessibility, and transcription factor binding. Furthermore, this study specifically identifies a set of primed gene promoters associated with the memory differentiation state.

Compared to naïve cells, memory CD8 T cells are pre-programmed with effector gene-associated open loci to respond to environmental cues and stimuli, thereby reducing the epigenetic changes necessary to induce effector function. The function of the primed loci in memory CD8 T cells may serve as an epigenetic history of functional effector programs, even though those programs are not actively expressed by mRNA in resting memory cells. Even though primed genes maintain an “open” state in both effector and memory cells, they are not expressed in memory and thus yield the phenotypic quiescent memory cell type. The failure to express these genes may be due to lack of availability of active transcription factors, which are either activated or transcribed (or both) upon secondary T cell activation.

Figure 5-1

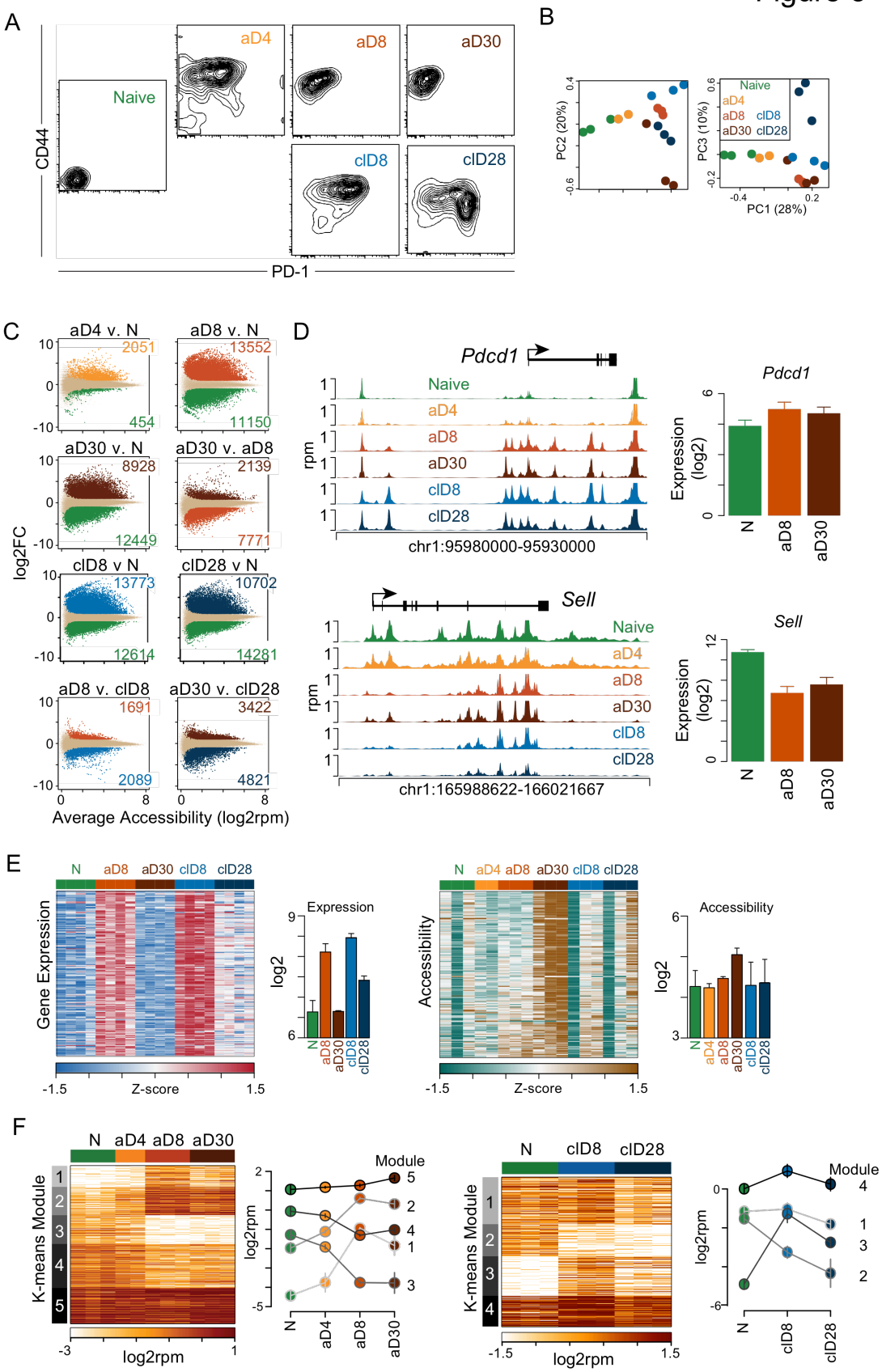
A
Naive
aD4
aD8
aD30
cID8
cID28
CD44
PD-1
B
PC2 (20%)
PC3 (10%)
PC1 (28%)
Naive
aD4
aD8
cID8
aD30
cID28
C
aD4 v. N
2051
454
aD8 v. N
13552
11150
aD30 v. N
8928
12449
aD30 v. aD8
2139
7771
cID8 v N
13773
12614
cID28 v N
10702
14281
aD8 v. cID8
1691
2089
aD30 v. cID28
3422
4821
log2FC
Average Accessibility (log2rpm)
D
Pdcd1
Naive
aD4
aD8
aD30
cID8
cID28
rpm
chr1:95980000-95930000
Expression (log2)
N
aD8
aD30
Sell
chr1:165988622-166021667
E
N
aD8
aD30
cID8
cID28
Gene Expression
Z-score
Expression
log2
aD4
Accessibility
F
K-means Module
log2rpm
Module
cID8
cID28

Figure 5- 1: Genome wide chromatin accessibility dynamically changes during inflammation

WT mice were infected with LCMV Armstrong (a) or Clone-13 (cl). At day 4, 8, or 28, virus specific cells were isolated from spleens of hosts by FACS based on staining for LCMV gp33, gp276, or np396 tetramers. Representative flow plots of isolates are shown in (A). ATAC-seq was performed on all samples. B) Principle component analysis of chromatin accessibility at 89,746 accessible regions. C) Scatter plots of changes in accessibility between each pair of cell types. Increases (top) indicate enrichment in first cell type, while loci below 0 indicate enrichment in the second cell type. D) *Pdcd1* and *Sell* loci showing changes in accessibility and corresponding changes in gene expression. E) Bichromatic plot showing global changes in gene expression (left) (Doering et al., 2012) or accessibility (right). F) K means clustering identifying regions with similar dynamic accessibility during acute (left) or chronic (right) infections. ATAC-seq data are representative of 2 (aD4) or 3 (all other time points) independent mice. RPM: reads per million

Figure 5-2

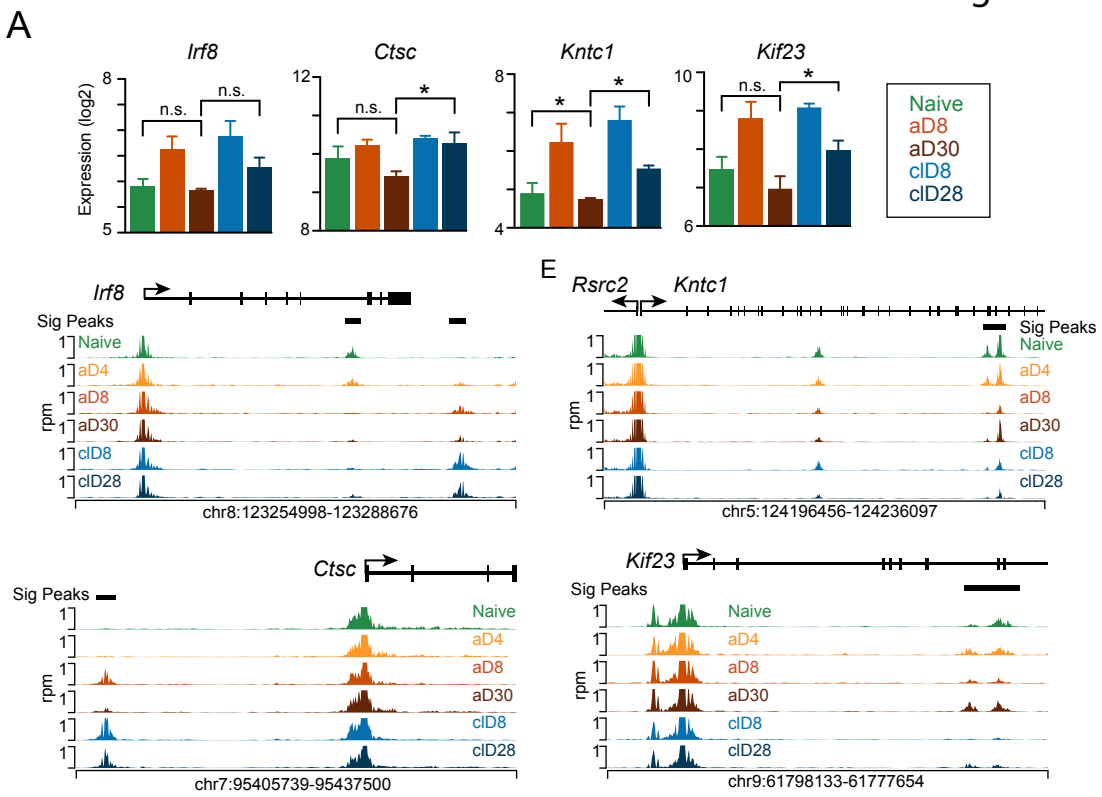

Figure 5- 2: Chromatin accessability correlates with gene expression

A) Relative gene expression (top) and chromatin accessibility (bottom) at timepoints during acute and chronic infection are shown for 4 dynamically changing genes: Irf8,Ctsc, Kntc1, and Kif23.

Figure 5-3

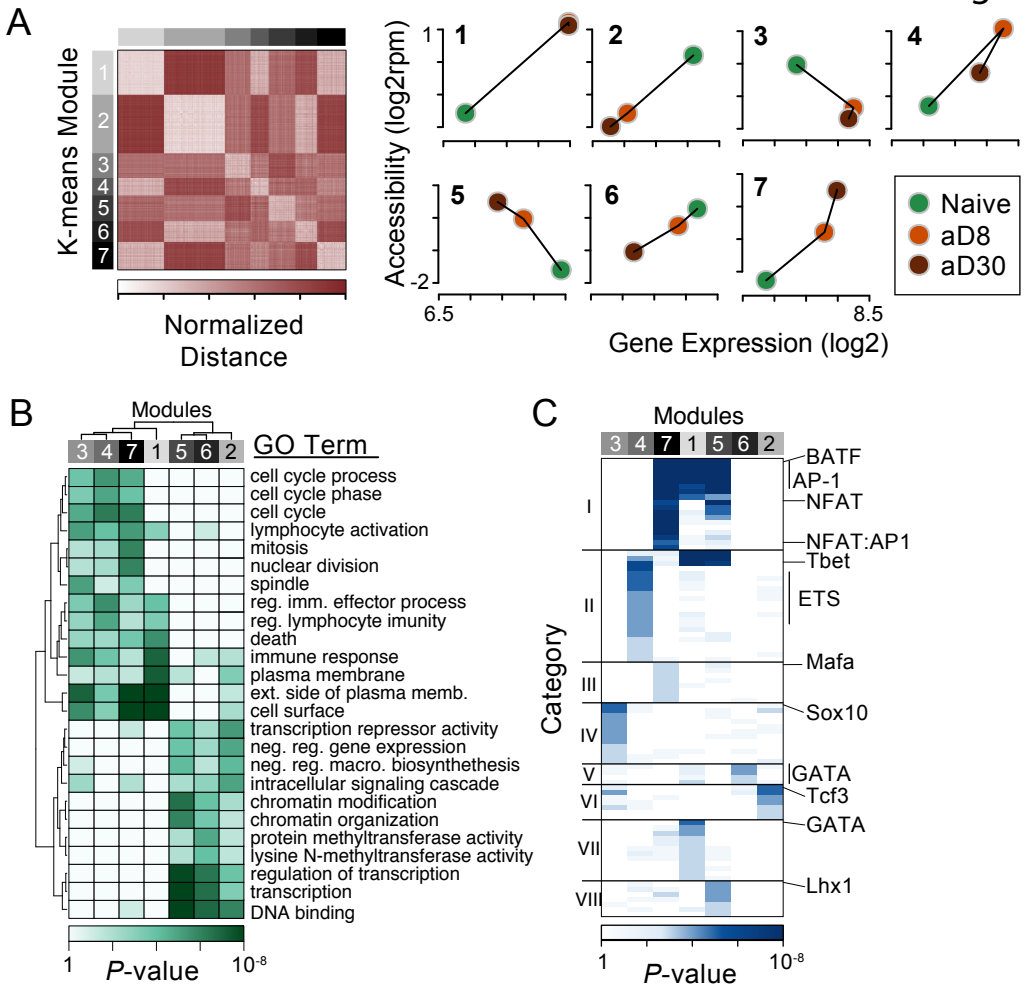

Figure 5- 3: Accessible regions correlate with transcriptional changes

A) The relative changes in accessibility and gene expression were assigned a normalized Euclidean distance metric, and *k*-means clustering was performed, generating 7 distinct modules. B) Heat map displaying the top 5 enriched gene ontology terms identified within each module. Map is organized by hierarchical clustering. C) Transcription factor motifs enriched within each module from (B) were identified and organized into 8 distinct categories based on motifs shared between multiple *k*-means modules (categories I-II) or those distinct to a specific module (categories III-VIII).

Figure 5-4

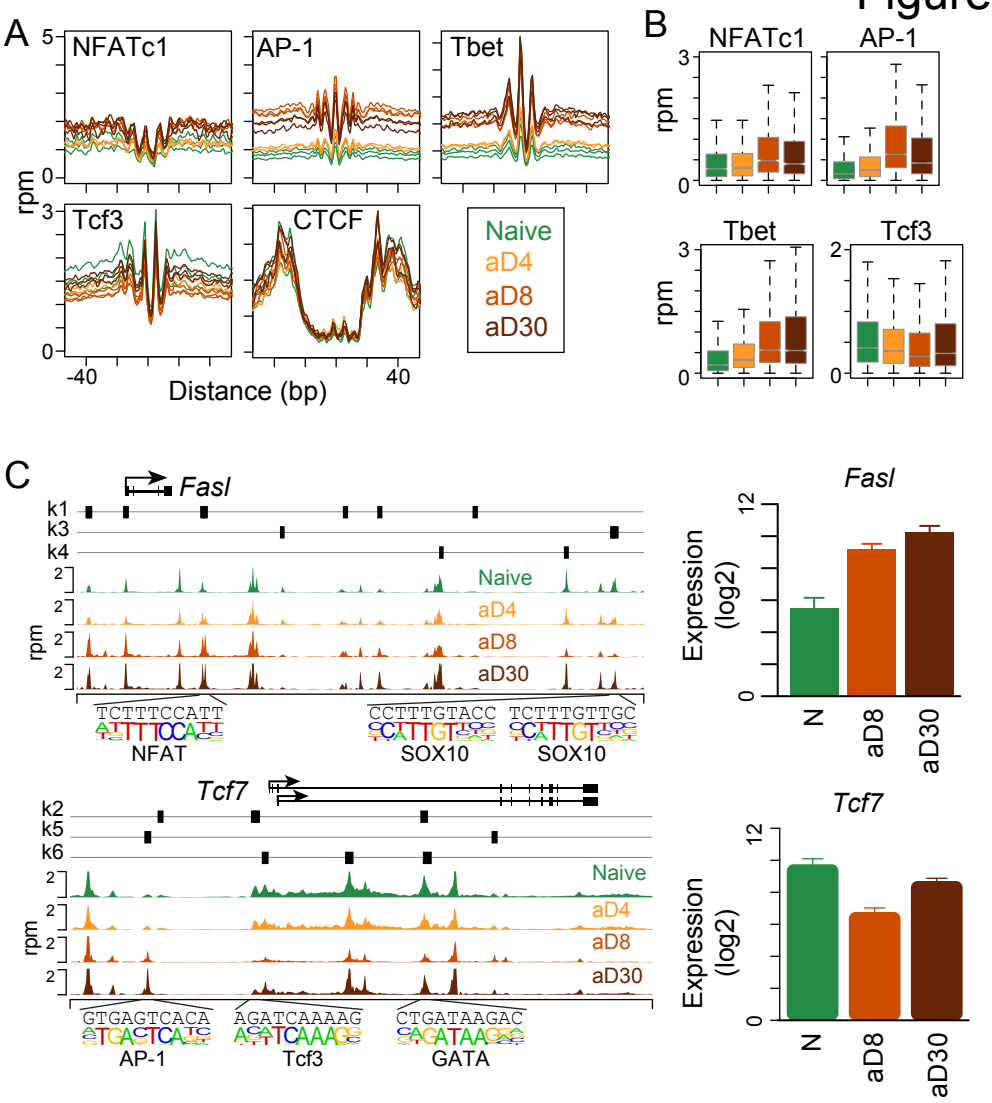

Figure 5- 4: Transcription factor motifs are dynamically accessible during infection

A) Genome wide loci containing the indicated transcription factor motifs were aligned to show chromatin accessibility at base-pair resolution. B) The sum of all reads as a metric of average accessibility within 200bp of the motifs used in (A) is graphed. C) Plots of chromatin accessibility and gene expression of two genes (*Fasl* and *Tcf7*) which each illustrate loci from multiple modules defined in Figure 5-3.

Figure 5-5

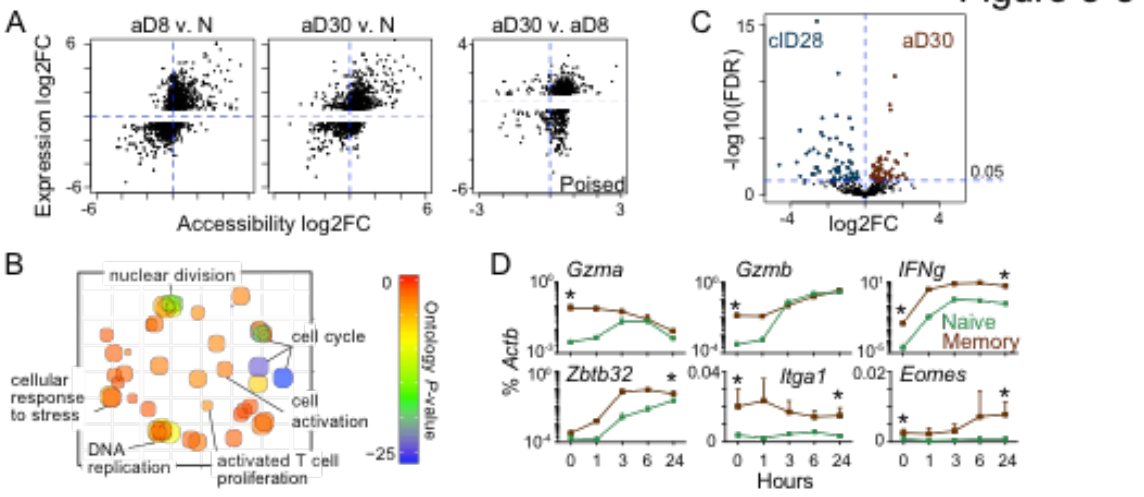

Figure 5- 5: Primed accessible memory loci enable more rapid response to secondary antigen challenge

A) Changes in locus accessibility and gene expression between naïve (N), effector (aD8) or memory (aD30) cells are graphed. B) Summary gene ontology data of the primed genes identified in (A) which do not show a decrease in chromatin accessibility between effector and memory cells. C) Non-promoter peaks within the primed loci set are graphed on a volcano plot to identify significantly increased or decreased accessible regions. D) 10,000 P14 CD8 T cells were adoptively transferred into naïve WT mice which were infected with LCMV Armstrong 1 day later. Spleens were isolated from host mice 28 days after infection to generate memory cells. Whole splenocytes from naïve or memory mice were stimulated in culture with 4μM gp33-41 peptide for the indicated times. At each time point, cells were fixed in 1% paraformaldehyde for 5 minutes, and subsequently stained and FACS-sorted to obtain P14 cells (CD8+ Thy1.1+ gp33+). mRNA was generated from each sample and quantitated by RT-PCR. Data represent cells isolated from three independent memory or naïve mice. Statistical significance was

determined by two-way ANOVA with a Bonferroni post-test. All genes shown were significant across the entire time-course. * indicates $p<.05$ at specific time points.

Chapter 6: Discussion

Written by Alexander P.R. Bally and Jeremy M. Boss

Summary

In this dissertation, systems that drive and regulate PD-1 expression are studied. A novel driver of PD-1 expression (NF-κB) was identified as the primary driver of PD-1 expression in macrophages. This transcription factor, similarly to the previously identified NFATc1 and STAT3 activators as well as the repressors Blimp-1 and FoxO1, binds to the CR-C region upstream of the *Pdcd1* locus. Here, we identified that the function of this cis-element is primarily involved in driving early changes to PD-1 expression, and is not necessary for the prolonged high expression of PD-1 seen during chronic inflammation. Furthermore, abrogating early PD-1 expression through deletion of CR-C, without altering later modalities of expression, results in a shift away from effector cell formation towards a stronger memory cell formation.

In addition, the histone modifier LSD1 was shown to regulate PD-1 on an epigenetic level, enforcing a silenced profile following the transient expression seen in the late stages of an acute infection.

PD-1 expression on multiple immune cell types

Although targeted therapeutically for its function in mediating exhaustion of CD8 T cells, PD-1 expression on a variety of both adaptive and innate immune cells evinces the broad immune function of this protein and has implications for autoimmunity, vaccinations, and even modulation of acute immune responses. Early effector CD8 T cells, CD4 T cells, and B cells each express PD-1 upon encounter with cognate antigen. Furthermore, macrophages, dendritic cells, and NK cells also express PD-1 when stimulated through pattern recognition receptors such as TLRs (Agata et al., 1996; Costa et al., 2015; Haynes et al., 2007; Honda et al., 2014; Okazaki et al., 2001; Yao et al., 2009; Zhang et al., 2011). In each of these cases, it is likely that in a proximate sense PD-1 is acting to inhibit immune function within an individual cell. However, PD-1

expression in many of these cells during an acute infection is necessary for an optimal response; thus the act of transiently inhibiting early immune function appears to effectively coordinate durable immune function and ultimately helps drive the immune response.

The regulation of PD-1 has been primarily studied in T cells. Its most pathological role (that of inducing immune exhaustion) is epitomized in this context, and thus knowledge of the PD-1 regulome in T cells is most critical to developing and understanding PD-1 centric therapies. The LCMV model in particular has been used extensively, as this virus provides a method to directly compare both acute and chronic modalities using alternative strains that share epitopes recognize by T cells and antibodies, and consequently activate the same population of immune cells within a host (Ahmed et al., 1984). This has made it possible to compare differences between transient and prolonged presentation of the same antigen to the same cells, and observe how repeated stimulation over time (chronic infection) drives differential gene expression, and the exact mechanisms that alter the epigenome and transcriptome without having to account for any other alterations to the nature of TCR binding (such as peptide affinity).

In this work, the PD-1 regulome in macrophages was further characterized. The primary factor that drives PD-1 expression in adaptive immune cells, NFATc1, was inoperative in macrophages. This is perhaps unsurprising, as in B cells and T cells, NFATc1 operates downstream of B- or T- cell receptors to activate *Pdcd1*, and macrophages have no analogous pathway. The elucidation of NF-κB as an activator of PD-1 following TLR ligation in these cells opens up the potential for new therapy targets. Although T cells do not induce PD-1 in response to LPS stimulation, the function of NF-κB was not cross examined in T cells in response to other stimuli, and it is unknown if a

PRR-mediated signal can induce PD-1 expression in T cells, and whether or not this can lead to or enhance T cell exhaustion.

PD-1 outside of T cell exhaustion

Although this work focused primarily on the systems that alter expression of PD-1 in non-exhausted cells (i.e. macrophages, B cells, and T cells during acute inflammatory responses), the function of PD-1 expression is nonetheless intriguing. PD-1 expression outside the context of T cell exhaustion could be categorized into groups: constitutive expression on inhibitory cell types, and transient expression upon cell activation. In macrophages, PD-1 expression is associated primarily with a more repressive M2 macrophage phenotype (Chen et al., 2016; Said et al., 2010). Similarly, PD-1 is a functional marker of repressive T_{REG} cells, on which it is constitutively expressed (Park et al., 2015). Intriguingly, T_{FH} cells represent another mode of constitutive PD-1 expression, yet unlike M2 macrophages and T_{REG}s, T_{FH} cells are not a repressive cell (Crotty, 2011). In this context, PD-1 is necessary for T_{FH} cell formation and ultimately germinal center formation necessary for a B cell mediated immune response (Jogdand et al., 2016). One hypothesis to reconcile this posits that PD-1 stabilizes the T_{FH} cell population within the germinal center, preventing emigration and division and thereby providing a stable scaffold on which B cell affinity maturation can occur.

As aforementioned, PD-1 expression also occurs in a transient manner during B and T cell activation, as well as on M1 macrophages. In this context, PD-1 expression is not directly associated with an anti-inflammatory function, much as is the case with expression on T_{FH} cells. One hypothesis for this suggests that PD-1 expression is necessary to align early immune events and coordinate a strong and effective immune response, providing time for effector cells to divide and differentiate upon encountering antigen prior to commencing effector functions. This is fueled by the observation that

PD-1 expression peaks prior to the peak in numbers of effector cells and systemic cytokines. In an acute LCMV infection, this correlates to a peak of PD-1 expression at days 5-6, compared to a peak of effector cell numbers around day 8 (see Figure 3-3 and (Wherry et al., 2003). An alternative hypothesis suggests this temporary PD-1 expression instead acts as a brake *after* anti-viral responses in vivo. This hypothesis takes into account the observation that, although antigen-specific cell numbers peak at day 8, the number of T cells actively recognizing virus and secreting cytokines *in vivo* peaks prior to day 4, when viral titers are at their highest (Hosking et al., 2013; Liu and Whitton, 2005). After this timepoint, cells continue to proliferate but encounter virus in lower quantities and thus do not actively secrete cytokines unless stimulated further with additional viral antigen, as is the case in most ex vivo ICCS experiments at day 8. This agrees with data that after an initial pulse with antigen effector T cells will continue to divide in the absence of antigen (Kaech et al., 2003; van Stipdonk et al., 2001).

A key factor in answering which of these two hypotheses is accurate is deciphering the timing of events. While it is known that PD-1 expression peaks shortly after viral titers but before cell numbers, it is not known precisely how this integrates over time with other activation events, including expression of cytokines and effector molecules such as Granzymes A and B, as well as large genome-wide reprogramming into a terminally differentiated memory or effector cell. Identifying when PD-1 expression occurs in relation to each of these other events could help identify if PD-1 is acting to align the immune system prior to effector differentiation, or acting as a brake to prevent effector cells from continuing to function after viral clearance.

PD-1 and memory formation

Alterations to PD-1 expression both during primary and secondary responses have been shown in previous work and here to have an effect on memory formation. This could

hypothetically be due to two temporal events: changes in PD-1 expression during primary antigen encounter resulting in an altered programming of long-lived cells, thereby affecting the down-stream effector function upon secondary challenge; alternatively, changed PD-1 expression on memory cells during the secondary encounter could directly alter their ability to respond. This study provides evidence that the first of these hypotheses is true (PD-1 during primary infection affects down-stream memory), although it doesn't exclude the possibility of a synergistic/antagonistic effect of altered PD-1 expression at both primary and secondary infections. Prior to the secondary infection, mice with altered PD-1 expression during the primary response (via the CR-C^- mutant allele) show a greater quantity of resting memory cells. Furthermore, these memory cells appear qualitatively more functional in responding to a secondary challenge. Although PD-1 was upregulated to a comparable degree in both WT and mutant memory cells at day 2 during a secondary challenge, it is nonetheless possible that altered kinetics of PD-1 expression may occur in the mutant mouse, and thus drive a more functional cell phenotype via proximal PD-1 expression, rather than by encoding a more functional cell upon initial primary antigen encounter.

Ultimately, the best way to discern if the effects on memory cells are due to altered PD-1 during the primary or secondary immune response would be an experiment in which a PD-1 or PD-L blockade was employed either during the primary response alone (followed by sufficient time to clear the antibody prior to re-challenge), blockade during the secondary response alone, or blockade during both challenges compared to non-blockaded mice. This would determine if PD-1 signaling during primary challenge affects cell function during secondary challenge, independently of any changes to PD-1 during the secondary challenge. Similarly, it would determine if altered signaling during the secondary challenge affects cell function at the time of expression, and perhaps help to elucidate the role of PD-1 expression on memory cells.

Many changes define the differences between a naïve and memory cell. In some ways, the *Pdcd1* locus exemplifies this. In a naïve cell, few epigenetic programs have been identified around *Pdcd1*. CpG methylation is present, but neither activation-associated marks such as H3K4me1/2/3 and H3k27ac, nor repressive H3K27me3 and H3K9me2 have been identified in naïve cells, although each of these change dynamically in early and late stages of PD-1 expression. In contrast, after antigen experience, *Pdcd1* in a T cell display additional repressive modifications (H3K27me3 and H3K9me2) that were not present at the locus in naïve cells. This may result in the observed lower induced expression of PD-1 upon subsequent secondary antigen encounter by a memory cell. This suggests that in regards to PD-1, the memory cell is primed to not express the inhibitory receptor, thereby providing a mechanism for a more robust recall response.

Epigenetics of the antiviral immune response

In embryonic development, pluripotent or omnipotent precursor cells differentiate into multiple novel, stable cell types with wildly different functions. Epigenetics have primarily been studied in this context as the mechanism of enforcing heritable change on differentiated daughter cells. However, a comparable effect occurs during within the immune system, both in immune maturation occurring in post-fetal stages, as well as during immune responses occurring throughout life.

Most immune-related events in response to antigen exposure involve the stable differentiation from a naïve precursor into a discrete cell type with novel functions. Genome-wide epigenetic patterns define and maintain a quiescent state in mature naïve B and T cells. Stimulus-driven alterations to these patterns irreversibly drive differentiation into a novel yet stable cell type, enabling the formation of both terminally differentiated effector cells and memory cells primed to respond faster and more strongly

than their naïve precursors. Understanding the epigenetic landscapes that define discrete functional profiles and the cellular machinery that is capable of altering those profiles not only provides insight into workings of a complex pathogen defense system, but also may ultimately enable an unprecedented control over inflammatory environments. Future studies into the specific mechanisms that can alter expressions on individual genes, as well as genome-wide modifications that occur sequentially in response to multiple antigenic stimuli lay the foundations for novel toolkits to remodel and control dysfunctional inflammatory situations.

The future of immune checkpoint therapies

Recently, a novel therapeutic method, called immune checkpoint blockade, has become a popular and effective treatment for multiple cancer types (Brahmer et al., 2012; Topalian et al., 2012; Topalian et al., 2014). These therapies target the functional immune cell inhibitor/ligand dyads such as PD-1/PD-L1 and CTLA-4/CD28 (Duraiswamy et al., 2013a; Parry et al., 2005). Often such immunotherapies prevent ligand binding by using antibodies that bind the ligand itself and obscure recognition by the receptor, but may also use antibodies against the receptor that sterically hinder ligand binding without stimulating the receptors themselves. These therapies have shown enormous capability in re-invigorating anti-cancer immune cells (Topalian et al., 2014). In some cases, this leads to full cancer clearance. However, often therapy leads to only tumor stability or moderate regression. As PD-1 and CTLA-4 remain expressed on target anti-tumor cells, discontinuation of therapy results in target cells reverting to an underlying exhausted phenotype, and tumor burden again increases. Improved quality of life may be transiently obtained in these patients, but without full tumor clearance these antibody therapies must be maintained indefinitely. This can be problematic given the both the high cost of therapy, and in particular in the occurrence of therapy-related side-effects

(particularly the development of autoimmune-like symptoms caused by bystander cells which PD-1/CTLA-4 may had been previously blocking) (Brahmer et al., 2012) (Topalian et al., 2012). Ultimately, this necessitates a poly-directional approach combining blockade therapy with other existing anti-cancer treatments to facilitate rapid clearance, or the development and tailoring of new blockade therapies to specifically and potently target only the anti-cancer immune cells.

Works Cited

Agata, Y., A. Kawasaki, H. Nishimura, Y. Ishida, T. Tsubata, H. Yagita, and T. Honjo. 1996. Expression of the PD-1 antigen on the surface of stimulated mouse T and B lymphocytes. *Int Immunol* 8:765-772.

Agnellini, P., P. Wolint, M. Rehr, J. Cahenzli, U. Karrer, and A. Oxenius. 2007. Impaired NFAT nuclear translocation results in split exhaustion of virus-specific CD8+ T cell functions during chronic viral infection. *Proceedings of the National Academy of Sciences of the United States of America* 104:4565-4570.

Ahmed, R., A. Salmi, L.D. Butler, J.M. Chiller, and M.B. Oldstone. 1984. Selection of genetic variants of lymphocytic choriomeningitis virus in spleens of persistently infected mice. Role in suppression of cytotoxic T lymphocyte response and viral persistence. *The Journal of experimental medicine* 160:521-540.

Allie, S.R., W. Zhang, S. Fuse, and E.J. Usherwood. 2011. Programmed death 1 regulates development of central memory CD8 T cells after acute viral infection. *Journal of immunology* 186:6280-6286.

Araki, Y., Z. Wang, C. Zang, W.H. Wood, 3rd, D. Schones, K. Cui, T.Y. Roh, B. Lhotsky, R.P. Wersto, W. Peng, K.G. Becker, K. Zhao, and N.P. Weng. 2009. Genome-wide analysis of histone methylation reveals chromatin state-based regulation of gene transcription and function of memory CD8+ T cells. *Immunity* 30:912-925.

Austin, J.W., P. Lu, P. Majumder, R. Ahmed, and J.M. Boss. 2014. STAT3, STAT4, NFATc1, and CTCF regulate PD-1 through multiple novel regulatory regions in murine T cells. *Journal of immunology* 192:4876-4886.

Bally, A.P., J.W. Austin, and J.M. Boss. 2016. Genetic and Epigenetic Regulation of PD-1 Expression. *Journal of immunology* 196:2431-2437.

Bally, A.P., P. Lu, Y. Tang, J.W. Austin, C.D. Scharer, R. Ahmed, and J.M. Boss. 2015. NF-kappaB regulates PD-1 expression in macrophages. *Journal of immunology* 194:4545-4554.

Barber, D.L., E.J. Wherry, D. Masopust, B. Zhu, J.P. Allison, A.H. Sharpe, G.J. Freeman, and R. Ahmed. 2006. Restoring function in exhausted CD8 T cells during chronic viral infection. *Nature* 439:682-687.

Barwick, B.G., C.D. Scharer, A.P. Bally, and J.M. Boss. 2016. Plasma cell differentiation is coupled to division-dependent DNA hypomethylation and gene regulation. *Nature immunology*

Beresford, G.W., and J.M. Boss. 2001. CIITA coordinates multiple histone acetylation modifications at the HLA-DRA promoter. *Nature immunology* 2:652-657.

Bernardi, P., P. Veronese, and V. Petronilli. 1993. Modulation of the mitochondrial cyclosporin A-sensitive permeability transition pore. I. Evidence for two separate Me2+ binding sites with opposing effects on the pore open probability. *J Biol Chem* 268:1005-1010.

Blackburn, S.D., H. Shin, W.N. Haining, T. Zou, C.J. Workman, A. Polley, M.R. Betts, G.J. Freeman, D.A. Vignali, and E.J. Wherry. 2009. Coregulation of CD8+ T cell exhaustion by multiple inhibitory receptors during chronic viral infection. *Nature immunology* 10:29-37.

Blank, C., I. Brown, R. Marks, H. Nishimura, T. Honjo, and T.F. Gajewski. 2003. Absence of programmed death receptor 1 alters thymic development and enhances generation of CD4/CD8 double-negative TCR-transgenic T cells. *Journal of immunology* 171:4574-4581.

Blank, C., I. Brown, A.C. Peterson, M. Spiotto, Y. Iwai, T. Honjo, and T.F. Gajewski. 2004. PD-L1/B7H-1 inhibits the effector phase of tumor rejection by T cell receptor (TCR) transgenic CD8+ T cells. *Cancer research* 64:1140-1145.

Boussiotis, V.A., P. Chatterjee, and L. Li. 2014. Biochemical signaling of PD-1 on T cells and its functional implications. *Cancer J* 20:265-271.

Brahmer, J.R., S.S. Tykodi, L.Q. Chow, W.J. Hwu, S.L. Topalian, P. Hwu, C.G. Drake, L.H. Camacho, J. Kauh, K. Odunsi, H.C. Pitot, O. Hamid, S. Bhatia, R. Martins, K. Eaton, S. Chen, T.M. Salay, S. Alaparthy, J.F. Grosso, A.J. Korman, S.M. Parker, S. Agrawal, S.M. Goldberg, D.M. Pardoll, A. Gupta, and J.M. Wigginton. 2012. Safety and activity of anti-PD-L1 antibody in patients with advanced cancer. *The New England journal of medicine* 366:2455-2465.

Breton, G., N. Chomont, H. Takata, R. Fromentin, J. Ahlers, A. Filali-Mouhim, C. Riou, M.R. Boulassel, J.P. Routy, B. Yassine-Diab, and R.P. Sekaly. 2013. Programmed death-1 is a marker for abnormal distribution of naive/memory T cell subsets in HIV-1 infection. *Journal of immunology* 191:2194-2204.

Buchele, B., W. Zugmaier, O. Lunov, T. Syrovets, I. Merfort, and T. Simmet. 2010. Surface plasmon resonance analysis of nuclear factor-kappaB protein interactions with the sesquiterpene lactone helenalin. *Anal Biochem* 401:30-37.

Buenrostro, J.D., P.G. Giresi, L.C. Zaba, H.Y. Chang, and W.J. Greenleaf. 2013. Transposition of native chromatin for fast and sensitive epigenomic profiling of open chromatin, DNA-binding proteins and nucleosome position. *Nat Methods* 10:1213-1218.

Burke, J.R., M.A. Pattoli, K.R. Gregor, P.J. Brassil, J.F. MacMaster, K.W. McIntyre, X. Yang, V.S. Iotzova, W. Clarke, J. Strnad, Y. Qiu, and F.C. Zusi. 2003. BMS-345541 is a highly selective inhibitor of I kappa B kinase that binds at an allosteric site of the enzyme and blocks NF-kappa B-dependent transcription in mice. *J Biol Chem* 278:1450-1456.

Busch, D.H., and E.G. Pamer. 1999. T cell affinity maturation by selective expansion during infection. *The Journal of experimental medicine* 189:701-710.

Butler, N.S., J. Moebius, L.L. Pewe, B. Traore, O.K. Doumbo, L.T. Tygrett, T.J. Waldschmidt, P.D. Crompton, and J.T. Harty. 2012. Therapeutic blockade of PD-L1 and LAG-3 rapidly clears established blood-stage Plasmodium infection. *Nature immunology* 13:188-195.

Carter, L., L.A. Fouser, J. Jussif, L. Fitz, B. Deng, C.R. Wood, M. Collins, T. Honjo, G.J. Freeman, and B.M. Carreno. 2002. PD-1:PD-L inhibitory pathway affects both CD4(+) and CD8(+) T cells and is overcome by IL-2. *European journal of immunology* 32:634-643.

Chauvin, J.M., O. Pagliano, J. Fourcade, Z. Sun, H. Wang, C. Sander, J.M. Kirkwood, T.H. Chen, M. Maurer, A.J. Korman, and H.M. Zarour. 2015. TIGIT and PD-1 impair tumor antigen-specific CD8+ T cells in melanoma patients. *The Journal of clinical investigation* 125:2046-2058.

Chemnitz, J.M., R.V. Parry, K.E. Nichols, C.H. June, and J.L. Riley. 2004. SHP-1 and SHP-2 associate with immunoreceptor tyrosine-based switch motif of programmed death 1 upon primary human T cell stimulation, but only receptor ligation prevents T cell activation. *Journal of immunology* 173:945-954.

Chen, L. 2004. Co-inhibitory molecules of the B7-CD28 family in the control of T-cell immunity. *Nature reviews. Immunology* 4:336-347.

Chen, W., J. Wang, L. Jia, J. Liu, and Y. Tian. 2016. Attenuation of the programmed cell death-1 pathway increases the M1 polarization of macrophages induced by zymosan. *Cell Death Dis* 7:e2115.

Cho, H.Y., E.K. Choi, S.W. Lee, K.O. Jung, S.K. Seo, I.W. Choi, S.G. Park, and I. Choi. 2009a. Programmed death-1 receptor negatively regulates LPS-mediated IL-12 production and differentiation of murine macrophage RAW264.7 cells. *Immunol Lett* 127:39-47.

Cho, H.Y., S.W. Lee, S.K. Seo, I.W. Choi, and I. Choi. 2008. Interferon-sensitive response element (ISRE) is mainly responsible for IFN-alpha-induced upregulation of programmed death-1 (PD-1) in macrophages. *Biochimica et biophysica acta* 1779:811-819.

Cho, O.H., H.M. Shin, L. Miele, T.E. Golde, A. Fauq, L.M. Minter, and B.A. Osborne. 2009b. Notch regulates cytolytic effector function in CD8+ T cells. *Journal of immunology* 182:3380-3389.

Cohen, H.B., and D.M. Mosser. 2013. Extrinsic and intrinsic control of macrophage inflammatory responses. *J Leukoc Biol* 94:913-919.

Costa, P.A., F.M. Leoratti, M.M. Figueiredo, M.S. Tada, D.B. Pereira, C. Junqueira, I.S. Soares, D.L. Barber, R.T. Gazzinelli, and L.R. Antonelli. 2015. Induction of Inhibitory Receptors on T Cells During Plasmodium vivax Malaria Impairs Cytokine Production. *J Infect Dis*

Creyghton, M.P., A.W. Cheng, G.G. Welstead, T. Kooistra, B.W. Carey, E.J. Steine, J. Hanna, M.A. Lodato, G.M. Frampton, P.A. Sharp, L.A. Boyer, R.A. Young, and R. Jaenisch. 2010. Histone H3K27ac separates active from poised enhancers and predicts developmental state. *Proceedings of the National Academy of Sciences of the United States of America* 107:21931-21936.

Crotty, S. 2011. Follicular helper CD4 T cells (TFH). *Annu Rev Immunol* 29:621-663.

Curiel, T.J., S. Wei, H. Dong, X. Alvarez, P. Cheng, P. Mottram, R. Krzysiek, K.L. Knutson, B. Daniel, M.C. Zimmermann, O. David, M. Burow, A. Gordon, N. Dhurandhar, L. Myers, R. Berggren, A. Hemminki, R.D. Alvarez, D. Emilie, D.T. Curiel, L. Chen, and W. Zou. 2003. Blockade of B7-H1 improves myeloid dendritic cell-mediated antitumor immunity. *Nat Med* 9:562-567.

Davis, L., and P.E. Lipsky. 1986. Signals involved in T cell activation. II. Distinct roles of intact accessory cells, phorbol esters, and interleukin 1 in activation and cell cycle progression of resting T lymphocytes. *Journal of immunology* 136:3588-3596.

Day, C.L., D.E. Kaufmann, P. Kiepiela, J.A. Brown, E.S. Moodley, S. Reddy, E.W. Mackey, J.D. Miller, A.J. Leslie, C. DePierres, Z. Mncube, J. Duraiswamy, B. Zhu, Q. Eichbaum, M. Altfeld, E.J. Wherry, H.M. Coovadia, P.J. Goulder, P. Klenerman, R. Ahmed, G.J. Freeman, and B.D. Walker. 2006. PD-1 expression on HIV-specific T cells is associated with T-cell exhaustion and disease progression. *Nature* 443:350-354.

Dirks, J., A. Egli, U. Sester, M. Sester, and H.H. Hirsch. 2013. Blockade of programmed death receptor-1 signaling restores expression of mostly proinflammatory cytokines in anergic cytomegalovirus-specific T cells. *Transpl Infect Dis* 15:79-89.

Doering, T.A., A. Crawford, J.M. Angelosanto, M.A. Paley, C.G. Ziegler, and E.J. Wherry. 2012. Network analysis reveals centrally connected genes and pathways involved in CD8+ T cell exhaustion versus memory. *Immunity* 37:1130-1144.

Duraiswamy, J., G. Freeman, and G. Coukos. 2013a. Replenish the source within: Rescuing tumor-infiltrating lymphocytes by double checkpoint blockade. *Oncoimmunology* 2:e25912.

Duraiswamy, J., K.M. Kaluza, G.J. Freeman, and G. Coukos. 2013b. Dual blockade of PD-1 and CTLA-4 combined with tumor vaccine effectively restores T-cell rejection function in tumors. *Cancer research* 73:3591-3603.

Francisco, L.M., P.T. Sage, and A.H. Sharpe. 2010. The PD-1 pathway in tolerance and autoimmunity. *Immunol Rev* 236:219-242.

Frebel, H., V. Nindl, R.A. Schuepbach, T. Braunschweiler, K. Richter, J. Vogel, C.A. Wagner, D. Loffing-Cueni, M. Kurrer, B. Ludewig, and A. Oxenius. 2012. Programmed death 1 protects from fatal circulatory failure during systemic virus infection of mice. *The Journal of experimental medicine* 209:2485-2499.

Freeman, G.J., A.J. Long, Y. Iwai, K. Bourque, T. Chernova, H. Nishimura, L.J. Fitz, N. Malenkovich, T. Okazaki, M.C. Byrne, H.F. Horton, L. Fouser, L. Carter, V. Ling, M.R. Bowman, B.M. Carreno, M. Collins, C.R. Wood, and T. Honjo. 2000. Engagement of the PD-1 immunoinhibitory receptor by a novel B7 family member leads to negative regulation of lymphocyte activation. *The Journal of experimental medicine* 192:1027-1034.

Fuller, M.J., B. Callendret, B. Zhu, G.J. Freeman, D.L. Hasselschwert, W. Satterfield, A.H. Sharpe, L.B. Dustin, C.M. Rice, A. Grakoui, R. Ahmed, and C.M. Walker. 2013. Immunotherapy of chronic hepatitis C virus infection with antibodies against programmed cell death-1 (PD-1). *Proceedings of the National Academy of Sciences of the United States of America* 110:15001-15006.

Gallimore, A., A. Glithero, A. Godkin, A.C. Tissot, A. Pluckthun, T. Elliott, H. Hengartner, and R. Zinkernagel. 1998. Induction and exhaustion of lymphocytic choriomeningitis virus-specific cytotoxic T lymphocytes visualized using soluble tetrameric major histocompatibility complex class I-peptide complexes. *The Journal of experimental medicine* 187:1383-1393.

Gautier, L., L. Cope, B.M. Bolstad, and R.A. Irizarry. 2004. affy--analysis of Affymetrix GeneChip data at the probe level. *Bioinformatics* 20:307-315.

Goding, S.R., K.A. Wilson, Y. Xie, K.M. Harris, A. Baxi, A. Akpinarli, A. Fulton, K. Tamada, S.E. Strome, and P.A. Antony. 2013. Restoring immune function of tumor-specific CD4+ T cells during recurrence of melanoma. *Journal of immunology* 190:4899-4909.

Golden-Mason, L., B. Palmer, J. Klarquist, J.A. Mengshol, N. Castelblanco, and H.R. Rosen. 2007. Upregulation of PD-1 expression on circulating and intrahepatic hepatitis C virus-specific CD8+ T cells associated with reversible immune dysfunction. *Journal of virology* 81:9249-9258.

Goldrath, A.W., P.V. Sivakumar, M. Glaccum, M.K. Kennedy, M.J. Bevan, C. Benoist, D. Mathis, and E.A. Butz. 2002. Cytokine requirements for acute and Basal homeostatic proliferation of naive and memory CD8+ T cells. *The Journal of experimental medicine* 195:1515-1522.

Grakoui, A., E. John Wherry, H.L. Hanson, C. Walker, and R. Ahmed. 2006. Turning on the off switch: regulation of anti-viral T cell responses in the liver by the PD-1/PD-L1 pathway. *Journal of hepatology* 45:468-472.

Guo, Z., G.H. Boekhoudt, and J.M. Boss. 2003. Role of the intronic enhancer in tumor necrosis factor-mediated induction of manganous superoxide dismutase. *J Biol Chem* 278:23570-23578.

Gyory, I., J. Wu, G. Fejer, E. Seto, and K.L. Wright. 2004. PRDI-BF1 recruits the histone H3 methyltransferase G9a in transcriptional silencing. *Nature immunology* 5:299-308.

Hagar, J.A., D.A. Powell, Y. Aachoui, R.K. Ernst, and E.A. Miao. 2013. Cytoplasmic LPS activates caspase-11: implications in TLR4-independent endotoxic shock. *Science* 341:1250-1253.

Hamid, O., C. Robert, A. Daud, F.S. Hodi, W.J. Hwu, R. Kefford, J.D. Wolchok, P. Hersey, R.W. Joseph, J.S. Weber, R. Dronca, T.C. Gangadhar, A. Patnaik, H. Zarour, A.M. Joshua, K. Gergich, J. Elassaiss-Schaap, A. Algazi, C. Mateus, P.

Boasberg, P.C. Tumeh, B. Chmielowski, S.W. Ebbinghaus, X.N. Li, S.P. Kang, and A. Ribas. 2013. Safety and tumor responses with lambrolizumab (anti-PD-1) in melanoma. *The New England journal of medicine* 369:134-144.

Hashimoto, H., Y. Liu, A.K. Upadhyay, Y. Chang, S.B. Howerton, P.M. Vertino, X. Zhang, and X. Cheng. 2012. Recognition and potential mechanisms for replication and erasure of cytosine hydroxymethylation. *Nucleic Acids Res* 40:4841-4849.

Haynes, N.M., C.D. Allen, R. Lesley, K.M. Ansel, N. Killeen, and J.G. Cyster. 2007. Role of CXCR5 and CCR7 in follicular Th cell positioning and appearance of a programmed cell death gene-1high germinal center-associated subpopulation. *Journal of immunology* 179:5099-5108.

Heinz, S., C. Benner, N. Spann, E. Bertolino, Y.C. Lin, P. Laslo, J.X. Cheng, C. Murre, H. Singh, and C.K. Glass. 2010. Simple Combinations of Lineage-Determining Transcription Factors Prime cis-Regulatory Elements Required for Macrophage and B Cell Identities. *Mol Cell* 38:576-589.

Hill, J.M., D.C. Quenelle, R.D. Cardin, J.L. Vogel, C. Clement, F.J. Bravo, T.P. Foster, M. Bosch-Marce, P. Raja, J.S. Lee, D.I. Bernstein, P.R. Krause, D.M. Knipe, and T.M. Kristie. 2014. Inhibition of LSD1 reduces herpesvirus infection, shedding, and recurrence by promoting epigenetic suppression of viral genomes. *Sci Transl Med* 6:265ra169.

Hiroyuki Nishimura, Y.A., Akemi Kawasaki, Masaki Sato, Sadao Imamura, Nagahiro Minato, Hideo Yagita, Toru Nakano and Tasuku Honjo. 1996. Developmentally regulated expression of the PD-1 protein on the surface of double- negative (CD4~CD8~) thymocytes. *International Immunology* 8:773-780.

Honda, T., J.G. Egen, T. Lammermann, W. Kastenmuller, P. Torabi-Parizi, and R.N. Germain. 2014. Tuning of antigen sensitivity by T cell receptor-dependent negative feedback controls T cell effector function in inflamed tissues. *Immunity* 40:235-247.

Horvath, C.M., G.R. Stark, I.M. Kerr, and J.E. Darnell, Jr. 1996. Interactions between STAT and non-STAT proteins in the interferon-stimulated gene factor 3 transcription complex. *Mol Cell Biol* 16:6957-6964.

Hosking, M.P., C.T. Flynn, J. Botten, and J.L. Whitton. 2013. CD8+ memory T cells appear exhausted within hours of acute virus infection. *Journal of immunology* 191:4211-4222.

Hou, C., H. Zhao, K. Tanimoto, and A. Dean. 2008. CTCF-dependent enhancer-blocking by alternative chromatin loop formation. *Proceedings of the National Academy of Sciences of the United States of America* 105:20398-20403.

Hu, G., and J. Chen. 2013. A genome-wide regulatory network identifies key transcription factors for memory CD8(+) T-cell development. *Nat Commun* 4:2830.

Huang da, W., B.T. Sherman, and R.A. Lempicki. 2009. Systematic and integrative analysis of large gene lists using DAVID bioinformatics resources. *Nature protocols* 4:44-57.

Ishida, Y., Y. Agata, K. Shibahara, and T. Honjo. 1992. Induced expression of PD-1, a novel member of the immunoglobulin gene superfamily, upon programmed cell death. *EMBO J* 11:3887-3895.

Jacob, J., and D. Baltimore. 1999. Modelling T-cell memory by genetic marking of memory T cells in vivo. *Nature* 399:593-597.

Jaikumar Duraiswamy, J.D.M., David Masopust, Chris C Ibegbu, Hong Wu, Gordon J Freeman and Rafi Ahmed. 2007. PD-1 expression on memory CD8 and CD4 T-cell subsets in healthy humans. *The Journal of Immunology* 178:

Jameson, S.C., and D. Masopust. 2009. Diversity in T cell memory: an embarrassment of riches. *Immunity* 31:859-871.

Janzer, A., S. Lim, F. Fronhoffs, N. Niazy, R. Buettner, and J. Kirfel. 2012. Lysine-specific demethylase 1 (LSD1) and histone deacetylase 1 (HDAC1) synergistically repress proinflammatory cytokines and classical complement pathway components. *Biochemical and biophysical research communications* 421:665-670.

Jenuwein, T., and C.D. Allis. 2001. Translating the histone code. *Science* 293:1074-1080.

Jin, H.T., A.C. Anderson, W.G. Tan, E.E. West, S.J. Ha, K. Araki, G.J. Freeman, V.K. Kuchroo, and R. Ahmed. 2010. Cooperation of Tim-3 and PD-1 in CD8 T-cell exhaustion during chronic viral infection. *Proceedings of the National Academy of Sciences of the United States of America* 107:14733-14738.

Jogdand, G.M., S. Mohanty, and S. Devadas. 2016. Regulators of Tfh Cell Differentiation. *Front Immunol* 7:520.

Johnston, R.J., A.C. Poholek, D. DiToro, I. Yusuf, D. Eto, B. Barnett, A.L. Dent, J. Craft, and S. Crotty. 2009. Bcl6 and Blimp-1 are reciprocal and antagonistic regulators of T follicular helper cell differentiation. *Science* 325:1006-1010.

Jones, P.L., D. Ping, and J.M. Boss. 1997. Tumor necrosis factor alpha and interleukin-1beta regulate the murine manganese superoxide dismutase gene through a complex intronic enhancer involving C/EBP-beta and NF-kappaB. *Molecular and cellular biology* 17:6970-6981.

Joshi, N.S., W. Cui, A. Chandele, H.K. Lee, D.R. Urso, J. Hagman, L. Gapin, and S.M. Kaech. 2007. Inflammation directs memory precursor and short-lived effector CD8(+) T cell fates via the graded expression of T-bet transcription factor. *Immunity* 27:281-295.

Kaech, S.M., S. Hemby, E. Kersh, and R. Ahmed. 2002a. Molecular and functional profiling of memory CD8 T cell differentiation. *Cell* 111:837-851.

Kaech, S.M., J.T. Tan, E.J. Wherry, B.T. Konieczny, C.D. Surh, and R. Ahmed. 2003. Selective expression of the interleukin 7 receptor identifies effector CD8 T cells that give rise to long-lived memory cells. *Nature immunology* 4:1191-1198.

Kaech, S.M., and E.J. Wherry. 2007. Heterogeneity and cell-fate decisions in effector and memory CD8+ T cell differentiation during viral infection. *Immunity* 27:393-405.

Kaech, S.M., E.J. Wherry, and R. Ahmed. 2002b. Effector and memory T-cell differentiation: implications for vaccine development. *Nature reviews. Immunology* 2:251-262.

Kaikkonen, M.U., N.J. Spann, S. Heinz, C.E. Romanoski, K.A. Allison, J.D. Stender, H.B. Chun, D.F. Tough, R.K. Prinjha, C. Benner, and C.K. Glass. 2013. Remodeling of the enhancer landscape during macrophage activation is coupled to enhancer transcription. *Mol Cell* 51:310-325.

Kakaradov, B., J. Arsenio, C.E. Widjaja, Z. He, S. Aigner, P.J. Metz, B. Yu, E.J. Wehrens, J. Lopez, S.H. Kim, E.I. Zuniga, A.W. Goldrath, J.T. Chang, and G.W. Yeo. 2017. Early transcriptional and epigenetic regulation of CD8+ T cell differentiation revealed by single-cell RNA sequencing. *Nature immunology*

Kallies, A., A. Xin, G.T. Belz, and S.L. Nutt. 2009. Blimp-1 transcription factor is required for the differentiation of effector CD8(+) T cells and memory responses. *Immunity* 31:283-295.

Kanki, H., H. Suzuki, and S. Itohara. 2006. High-efficiency CAG-FLPe deleter mice in C57BL/6J background. *Exp Anim* 55:137-141.

Kao, C., K.J. Oestreich, M.A. Paley, A. Crawford, J.M. Angelosanto, M.A. Ali, A.M. Intlekofer, J.M. Boss, S.L. Reiner, A.S. Weinmann, and E.J. Wherry. 2011a. Transcription factor T-bet represses expression of the inhibitory receptor PD-1 and sustains virus-specific CD8+ T cell responses during chronic infection. *Nature immunology* 12:663-671.

Kao, C., K.J. Oestreich, M.A. Paley, A. Crawford, J.M. Angelosanto, M.A. Ali, A.M. Intlekofer, J.M. Boss, S.L. Reiner, A.S. Weinmann, and E.J. Wherry. 2011b. Transcription factor T-bet represses expression of the inhibitory receptor PD-1 and sustains virus-specific CD8+ T cell responses during chronic infection. *Nature immunology* 12:663-671.

Kawai, T., O. Adachi, T. Ogawa, K. Takeda, and S. Akira. 1999. Unresponsiveness of MyD88-deficient mice to endotoxin. *Immunity* 11:115-122.

Kayagaki, N., M.T. Wong, I.B. Stowe, S.R. Ramani, L.C. Gonzalez, S. Akashi-Takamura, K. Miyake, J. Zhang, W.P. Lee, A. Muszynski, L.S. Forsberg, R.W. Carlson, and V.M. Dixit. 2013. Noncanonical inflammasome activation by intracellular LPS independent of TLR4. *Science* 341:1246-1249.

Keller, A.D., and T. Maniatis. 1992. Only two of the five zinc fingers of the eukaryotic transcriptional repressor PRDI-BF1 are required for sequence-specific DNA binding. *Mol Cell Biol* 12:1940-1949.

Kerdiles, Y.M., D.R. Beisner, R. Tinoco, A.S. Dejean, D.H. Castrillon, R.A. DePinho, and S.M. Hedrick. 2009. Foxo1 links homing and survival of naive T cells by regulating L-selectin, CCR7 and interleukin 7 receptor. *Nature immunology* 10:176-184.

Kersh, A.E., L.J. Edwards, and B.D. Evavold. 2014. Progression of relapsing-remitting demyelinating disease does not require increased TCR affinity or epitope spread. *Journal of immunology* 193:4429-4438.

Kersh, E.N., D.R. Fitzpatrick, K. Murali-Krishna, J. Shires, S.H. Speck, J.M. Boss, and R. Ahmed. 2006. Rapid demethylation of the IFN-gamma gene occurs in memory but not naive CD8 T cells. *Journal of immunology* 176:4083-4093.

Kim, S.K., K.S. Schluns, and L. Lefrancois. 1999. Induction and visualization of mucosal memory CD8 T cells following systemic virus infection. *Journal of immunology* 163:4125-4132.

Kloverpris, H.N., R. McGregor, J.E. McLaren, K. Ladell, A. Stryhn, C. Koofhethile, J. Brener, F. Chen, L. Riddell, L. Graziano, P. Klenerman, A. Leslie, S. Buus, D.A. Price, and P. Goulder. 2014. Programmed death-1 expression on HIV-1-specific CD8+ T cells is shaped by epitope specificity, T-cell receptor clonotype usage and antigen load. *Aids* 28:2007-2021.

Kroner, A., M. Mehling, B. Hemmer, P. Rieckmann, K.V. Toyka, M. Maurer, and H. Wiendl. 2005. A PD-1 polymorphism is associated with disease progression in multiple sclerosis. *Ann Neurol* 58:50-57.

Laura L. Carter, L.A.F., Jason Jussif, Lori Fitz, Bija Deng, Clive R. Wood, Mary Collins, Tasuku Honjo, Gordon J. Freeman and Beatriz M. Carreno. 2002. PD-1:PD-L inhibitory pathway affects both CD4+

and CD8+ T cells and is overcome by IL-2. *Eur. J. Immunol* 32:634-643.

Lee, P.P., D.R. Fitzpatrick, C. Beard, H.K. Jessup, S. Lehar, K.W. Makar, M. Perez-Melgosa, M.T. Sweetser, M.S. Schlissel, S. Nguyen, S.R. Cherry, J.H. Tsai, S.M. Tucker, W.M. Weaver, A. Kelso, R. Jaenisch, and C.B. Wilson. 2001. A critical role for Dnmt1 and DNA methylation in T cell development, function, and survival. *Immunity* 15:763-774.

Li, E. 2002. Chromatin modification and epigenetic reprogramming in mammalian development. *Nat Rev Genet* 3:662-673.

Liu, F., and J.L. Whitton. 2005. Cutting edge: re-evaluating the in vivo cytokine responses of CD8+ T cells during primary and secondary viral infections. *Journal of immunology* 174:5936-5940.

Liu, J. 1993. FK506 and ciclosporin: molecular probes for studying intracellular signal transduction. *Trends in pharmacological sciences* 14:182-188.

Lu, P., B.A. Youngblood, J.W. Austin, A.U. Rasheed Mohammed, R. Butler, R. Ahmed, and J.M. Boss. 2014. Blimp-1 represses CD8 T cell expression of PD-1 using a feed-forward transcriptional circuit during acute viral infection. *The Journal of experimental medicine* 211:515-527.

Lyss, G., A. Knorre, T.J. Schmidt, H.L. Pahl, and I. Merfort. 1998. The anti-inflammatory sesquiterpene lactone helenalin inhibits the transcription factor NF-kappaB by directly targeting p65. *J Biol Chem* 273:33508-33516.

Macian, F., C. Lopez-Rodriguez, and A. Rao. 2001. Partners in transcription: NFAT and AP-1. *Oncogene* 20:2476-2489.

Maekawa, Y., Y. Minato, C. Ishifune, T. Kurihara, A. Kitamura, H. Kojima, H. Yagita, M. Sakata-Yanagimoto, T. Saito, I. Taniuchi, S. Chiba, S. Sone, and K. Yasutomo. 2008. Notch2 integrates signaling by the transcription factors RBP-J and CREB1 to promote T cell cytotoxicity. *Nature immunology* 9:1140-1147.

Martinez, G.J., R.M. Pereira, T. Aijo, E.Y. Kim, F. Marangoni, M.E. Pipkin, S. Togher, V. Heissmeyer, Y.C. Zhang, S. Crotty, E.D. Lamperti, K.M. Ansel, T.R. Mempel, H. Lahdesmaki, P.G. Hogan, and A. Rao. 2015. The transcription factor NFAT promotes exhaustion of activated CD8(+) T cells. *Immunity* 42:265-278.

Mathieu, M., N. Cotta-Grand, J.F. Daudelin, P. Thebault, and N. Labrecque. 2013. Notch signaling regulates PD-1 expression during CD8(+) T-cell activation. *Immunol Cell Biol* 91:82-88.

Matloubian, M., T. Somasundaram, S.R. Kolhekar, R. Selvakumar, and R. Ahmed. 1990. Genetic basis of viral persistence: single amino acid change in the viral glycoprotein affects ability of lymphocytic choriomeningitis virus to persist in adult mice. *The Journal of experimental medicine* 172:1043-1048.

McPherson, R.C., J.E. Konkel, C.T. Prendergast, J.P. Thomson, R. Ottaviano, M.D. Leech, O. Kay, S.E. Zandee, C.H. Sweenie, D.C. Wraith, R.R. Meehan, A.J. Drake, and S.M. Anderton. 2015. Epigenetic modification of the PD-1 (Pdcd1) promoter in effector CD4(+) T cells tolerized by peptide immunotherapy. *eLife* 4:

Mercer, E.M., Y.C. Lin, and C. Murre. 2011. Factors and networks that underpin early hematopoiesis. *Semin Immunol* 23:317-325.

Meyers, E.N., M. Lewandoski, and G.R. Martin. 1998. An Fgf8 mutant allelic series generated by Cre- and Flp-mediated recombination. *Nat Genet* 18:136-141.

Moll, M., C. Kuylenstierna, V.D. Gonzalez, S.K. Andersson, L. Bosnjak, A. Sonnerborg, M.F. Quigley, and J.K. Sandberg. 2009. Severe functional impairment and elevated PD-1 expression in CD1d-restricted NKT cells retained during chronic HIV-1 infection. *European journal of immunology* 39:902-911.

Morgan, M.A., E. Magnusdottir, T.C. Kuo, C. Tunyaplin, J. Harper, S.J. Arnold, K. Calame, E.J. Robertson, and E.K. Bikoff. 2009. Blimp-1/Prdm1 alternative promoter usage during mouse development and plasma cell differentiation. *Mol Cell Biol* 29:5813-5827.

Morgan, M.A., A.W. Mould, L. Li, E.J. Robertson, and E.K. Bikoff. 2012. Alternative splicing regulates Prdm1/Blimp-1 DNA binding activities and corepressor interactions. *Mol Cell Biol* 32:3403-3413.

Mueller, S.N., W.A. Langley, G. Li, A. Garcia-Sastre, R.J. Webby, and R. Ahmed. 2010. Qualitatively different memory CD8+ T cells are generated after lymphocytic

choriomeningitis virus and influenza virus infections. *Journal of immunology* 185:2182-2190.

Nielsen, C., D. Hansen, S. Husby, B.B. Jacobsen, and S.T. Lillevang. 2003. Association of a putative regulatory polymorphism in the PD-1 gene with susceptibility to type 1 diabetes. *Tissue Antigens* 62:492-497.

Nishimura, H., Y. Agata, A. Kawasaki, M. Sato, S. Imamura, N. Minato, H. Yagita, T. Nakano, and T. Honjo. 1996. Developmentally regulated expression of the PD-1 protein on the surface of double-negative (CD4-CD8-) thymocytes. *Int Immunol* 8:773-780.

Nishimura, H., T. Honjo, and N. Minato. 2000. Facilitation of beta selection and modification of positive selection in the thymus of PD-1-deficient mice. *The Journal of experimental medicine* 191:891-898.

Nishimura, H., M. Nose, H. Hiai, N. Minato, and T. Honjo. 1999. Development of lupus-like autoimmune diseases by disruption of the PD-1 gene encoding an ITIM motif-carrying immunoreceptor. *Immunity* 11:141-151.

Nishimura, H., T. Okazaki, Y. Tanaka, K. Nakatani, M. Hara, A. Matsumori, S. Sasayama, A. Mizoguchi, H. Hiai, N. Minato, and T. Honjo. 2001. Autoimmune dilated cardiomyopathy in PD-1 receptor-deficient mice. *Science* 291:319-322.

Odorizzi, P.M., K.E. Pauken, M.A. Paley, A. Sharpe, and E.J. Wherry. 2015. Genetic absence of PD-1 promotes accumulation of terminally differentiated exhausted CD8+ T cells. *The Journal of experimental medicine* 212:1125-1137.

Oestreich, K.J., H. Yoon, R. Ahmed, and J.M. Boss. 2008. NFATc1 regulates PD-1 expression upon T cell activation. *Journal of immunology* 181:4832-4839.

Okazaki, T., A. Maeda, H. Nishimura, T. Kurosaki, and T. Honjo. 2001. PD-1 immunoreceptor inhibits B cell receptor-mediated signaling by recruiting src homology 2-domain-containing tyrosine phosphatase 2 to phosphotyrosine. *Proceedings of the National Academy of Sciences of the United States of America* 98:13866-13871.

Overwijk, W.W., and N.P. Restifo. 2001. B16 as a mouse model for human melanoma. *Current protocols in immunology / edited by John E. Coligan ... [et al.]* Chapter 20:Unit 20 21.

Pan, T., Z. Liu, J. Yin, T. Zhou, J. Liu, and H. Qu. 2015. Notch Signaling Pathway Was Involved in Regulating Programmed Cell Death 1 Expression during Sepsis-Induced Immunosuppression. *Mediators Inflamm* 2015:539841.

Park, H.J., J.S. Park, Y.H. Jeong, J. Son, Y.H. Ban, B.H. Lee, L. Chen, J. Chang, D.H. Chung, I. Choi, and S.J. Ha. 2015. PD-1 upregulated on regulatory T cells during chronic virus infection enhances the suppression of CD8+ T cell immune response via the interaction with PD-L1 expressed on CD8+ T cells. *Journal of immunology* 194:5801-5811.

Parry, R.V., J.M. Chemnitz, K.A. Frauwirth, A.R. Lanfranco, I. Braunstein, S.V. Kobayashi, P.S. Linsley, C.B. Thompson, and J.L. Riley. 2005. CTLA-4 and PD-1 receptors inhibit T-cell activation by distinct mechanisms. *Mol Cell Biol* 25:9543-9553.

Pauken, K.E., M.A. Sammons, P.M. Odorizzi, S. Manne, J. Godec, O. Khan, A.M. Drake, Z. Chen, D. Sen, M. Kurachi, R.A. Barnitz, C. Bartman, B. Bengsch, A.C. Huang, J.M. Schenkel, G. Vahedi, W.N. Haining, S.L. Berger, and E.J. Wherry. 2016. Epigenetic stability of exhausted T cells limits durability of reinvigoration by PD-1 blockade. *Science*

Peng, G., S. Li, W. Wu, X. Tan, Y. Chen, and Z. Chen. 2008. PD-1 upregulation is associated with HBV-specific T cell dysfunction in chronic hepatitis B patients. *Mol Immunol* 45:963-970.

Petrovas, C., J.P. Casazza, J.M. Brenchley, D.A. Price, E. Gostick, W.C. Adams, M.L. Precopio, T. Schacker, M. Roederer, D.C. Douek, and R.A. Koup. 2006. PD-1 is a regulator of virus-specific CD8+ T cell survival in HIV infection. *The Journal of experimental medicine* 203:2281-2292.

Pettitt, S.J., Q. Liang, X.Y. Rairdan, J.L. Moran, H.M. Prosser, D.R. Beier, K.C. Lloyd, A. Bradley, and W.C. Skarnes. 2009. Agouti C57BL/6N embryonic stem cells for mouse genetic resources. *Nat Methods* 6:493-495.

Pihlgren, M., C. Arpin, T. Walzer, M. Tomkowiak, A. Thomas, J. Marvel, and P.M. Dubois. 1999. Memory CD44(int) CD8 T cells show increased proliferative responses and IFN-gamma production following antigenic challenge in vitro. *Int Immunol* 11:699-706.

Piras, V., and K. Selvarajoo. 2014. Beyond MyD88 and TRIF Pathways in Toll-Like Receptor Signaling. *Front Immunol* 5:70.

Prevost-Blondel, A., C. Zimmermann, C. Stemmer, P. Kulmburg, F.M. Rosenthal, and H. Pircher. 1998. Tumor-infiltrating lymphocytes exhibiting high ex vivo cytolytic activity fail to prevent murine melanoma tumor growth in vivo. *Journal of immunology* 161:2187-2194.

Prokunina, L., C. Castillejo-Lopez, F. Oberg, I. Gunnarsson, L. Berg, V. Magnusson, A.J. Brookes, D. Tentler, H. Kristjansdottir, G. Grondal, A.I. Bolstad, E. Svenungsson, I. Lundberg, G. Sturfelt, A. Jonssen, L. Truedsson, G. Lima, J. Alcocer-Varela, R. Jonsson, U.B. Gyllensten, J.B. Harley, D. Alarcon-Segovia, K. Steinsson, and M.E. Alarcon-Riquelme. 2002. A regulatory polymorphism in PDCD1 is associated with susceptibility to systemic lupus erythematosus in humans. *Nat Genet* 32:666-669.

Rao, A., C. Luo, and P.G. Hogan. 1997. Transcription factors of the NFAT family: regulation and function. *Annu Rev Immunol* 15:707-747.

Rao, R.R., Q. Li, M.R. Gubbels Bupp, and P.A. Shrikant. 2012. Transcription factor Foxo1 represses T-bet-mediated effector functions and promotes memory CD8(+) T cell differentiation. *Immunity* 36:374-387.

Ribas, A., D.S. Shin, J. Zaretsky, J. Frederiksen, A. Cornish, E. Avramis, E. Seja, C. Kivork, J. Siebert, P. Kaplan-Lefko, X. Wang, B. Chmielowski, J.A. Glaspy, P.C. Tumeh, T. Chodon, D. Pe'er, and B. Comin-Anduix. 2016. PD-1 Blockade Expands Intratumoral Memory T Cells. *Cancer Immunol Res* 4:194-203.

Rogge, L., L. Barberis-Maino, M. Biffi, N. Passini, D.H. Presky, U. Gubler, and F. Sinigaglia. 1997. Selective expression of an interleukin-12 receptor component by human T helper 1 cells. *The Journal of experimental medicine* 185:825-831.

Rui, Y., T. Honjo, and S. Chikuma. 2013. Programmed cell death 1 inhibits inflammatory helper T-cell development through controlling the innate immune response. *Proceedings of the National Academy of Sciences of the United States of America* 110:16073-16078.

Russ, B.E., M. Olshanksy, H.S. Smallwood, J. Li, A.E. Denton, J.E. Prier, A.T. Stock, H.A. Croom, J.G. Cullen, M.L. Nguyen, S. Rowe, M.R. Olson, D.B. Finkelstein, A. Kelso, P.G. Thomas, T.P. Speed, S. Rao, and S.J. Turner. 2014. Distinct epigenetic signatures delineate transcriptional programs during virus-specific CD8(+) T cell differentiation. *Immunity* 41:853-865.

Rutishauser, R.L., G.A. Martins, S. Kalachikov, A. Chandele, I.A. Parish, E. Meffre, J. Jacob, K. Calame, and S.M. Kaech. 2009. Transcriptional repressor Blimp-1 promotes CD8(+) T cell terminal differentiation and represses the acquisition of central memory T cell properties. *Immunity* 31:296-308.

Said, E.A., F.P. Dupuy, L. Trautmann, Y. Zhang, Y. Shi, M. El-Far, B.J. Hill, A. Noto, P. Ancuta, Y. Peretz, S.G. Fonseca, J. Van Grevenynghe, M.R. Boulassel, J.

Bruneau, N.H. Shoukry, J.P. Routy, D.C. Douek, E.K. Haddad, and R.P. Sekaly. 2010. Programmed death-1-induced interleukin-10 production by monocytes impairs CD4+ T cell activation during HIV infection. *Nat Med* 16:452-459.

Scharer, C.D., A.P. Bally, B. Gandham, and J.M. Boss. 2017. Cutting Edge: Chromatin Accessibility Programs CD8 T Cell Memory. *Journal of immunology* 198:2238-2243.

Scharer, C.D., B.G. Barwick, B.A. Youngblood, R. Ahmed, and J.M. Boss. 2013. Global DNA methylation remodeling accompanies CD8 T cell effector function. *Journal of immunology* 191:3419-3429.

Scharer, C.D., E.L. Blalock, B.G. Barwick, R.R. Haines, C. Wei, I. Sanz, and J.M. Boss. 2016. ATAC-seq on biobanked specimens defines a unique chromatin accessibility structure in naive SLE B cells. *Sci Rep* 6:27030.

Schurich, A., L.J. Pallett, M. Lubowiecki, H.D. Singh, U.S. Gill, P.T. Kennedy, E. Nastouli, S. Tanwar, W. Rosenberg, and M.K. Maini. 2013. The third signal cytokine IL-12 rescues the anti-viral function of exhausted HBV-specific CD8 T cells. *PLoS pathogens* 9:e1003208.

Scott-Browne, J.P., I.F. Lopez-Moyado, S. Trifari, V. Wong, L. Chavez, A. Rao, and R.M. Pereira. 2016. Dynamic Changes in Chromatin Accessibility Occur in CD8+ T Cells Responding to Viral Infection. *Immunity*

Sen, D.R., J. Kaminski, R.A. Barnitz, M. Kurachi, U. Gerdemann, K.B. Yates, H.W. Tsao, J. Godec, M.W. LaFleur, F.D. Brown, P. Tonnerre, R.T. Chung, D.C. Tully, T.M. Allen, N. Frahm, G.M. Lauer, E.J. Wherry, N. Yosef, and W.N. Haining. 2016. The epigenetic landscape of T cell exhaustion. *Science*

Severson, J.J., H.S. Serracino, V. Mateescu, C.D. Raeburn, R.C. McIntyre, Jr., S.B. Sams, B.R. Haugen, and J.D. French. 2015. PD-1+Tim-3+ CD8+ T Lymphocytes Display Varied Degrees of Functional Exhaustion in Patients with Regionally Metastatic Differentiated Thyroid Cancer. *Cancer Immunol Res* 3:620-630.

Shaffer, A.L., X. Yu, Y. He, J. Boldrick, E.P. Chan, and L.M. Staudt. 2000. BCL-6 represses genes that function in lymphocyte differentiation, inflammation, and cell cycle control. *Immunity* 13:199-212.

Shaulian, E., and M. Karin. 2002. AP-1 as a regulator of cell life and death. *Nat Cell Biol* 4:E131-136.

Shi, Y., F. Lan, C. Matson, P. Mulligan, J.R. Whetstine, P.A. Cole, R.A. Casero, and Y. Shi. 2004. Histone demethylation mediated by the nuclear amine oxidase homolog LSD1. *Cell* 119:941-953.

Shih, H.Y., G. Sciume, A.C. Poholek, G. Vahedi, K. Hirahara, A.V. Villarino, M. Bonelli, R. Bosselut, Y. Kanno, S.A. Muljo, and J.J. O'Shea. 2014. Transcriptional and epigenetic networks of helper T and innate lymphoid cells. *Immunol Rev* 261:23-49.

Shin, H., S.D. Blackburn, A.M. Intlekofer, C. Kao, J.M. Angelosanto, S.L. Reiner, and E.J. Wherry. 2009. A role for the transcriptional repressor Blimp-1 in CD8(+) T cell exhaustion during chronic viral infection. *Immunity* 31:309-320.

Shin, H.M., V.N. Kapoor, T. Guan, S.M. Kaech, R.M. Welsh, and L.J. Berg. 2013. Epigenetic modifications induced by Blimp-1 Regulate CD8(+) T cell memory progression during acute virus infection. *Immunity* 39:661-675.

Sierro, S.R., A. Donda, R. Perret, P. Guillaume, H. Yagita, F. Levy, and P. Romero. 2011. Combination of lentivector immunization and low-dose chemotherapy or PD-1/PD-L1 blocking primes self-reactive T cells and induces anti-tumor immunity. *European journal of immunology* 41:2217-2228.

Smith, Z.D., and A. Meissner. 2013. DNA methylation: roles in mammalian development. *Nat Rev Genet* 14:204-220.

Staron, M.M., S.M. Gray, H.D. Marshall, I.A. Parish, J.H. Chen, C.J. Perry, G. Cui, M.O. Li, and S.M. Kaech. 2014. The transcription factor FoxO1 sustains expression of the inhibitory receptor PD-1 and survival of antiviral CD8(+) T cells during chronic infection. *Immunity* 41:802-814.

Su, S.T., H.Y. Ying, Y.K. Chiu, F.R. Lin, M.Y. Chen, and K.I. Lin. 2009. Involvement of histone demethylase LSD1 in Blimp-1-mediated gene repression during plasma cell differentiation. *Mol Cell Biol* 29:1421-1431.

Sutherland, B.W., J. Toews, and J. Kast. 2008. Utility of formaldehyde cross-linking and mass spectrometry in the study of protein-protein interactions. *J Mass Spectrom* 43:699-715.

Tahiliani, M., K.P. Koh, Y. Shen, W.A. Pastor, H. Bandukwala, Y. Brudno, S. Agarwal, L.M. Iyer, D.R. Liu, L. Aravind, and A. Rao. 2009. Conversion of 5-methylcytosine to 5-hydroxymethylcytosine in mammalian DNA by MLL partner TET1. *Science* 324:930-935.

Talay, O., C.H. Shen, L. Chen, and J. Chen. 2009. B7-H1 (PD-L1) on T cells is required for T-cell-mediated conditioning of dendritic cell maturation. *Proceedings of the National Academy of Sciences of the United States of America* 106:2741-2746.

Taube, J.M., A.P. Klein, J.R. Brahmer, H. Xu, X. Pan, J.H. Kim, L. Chen, D.M. Pardoll, S.L. Topalian, and R.A. Anders. 2014. Association of PD-1, PD-1 ligands, and other features of the tumor immune microenvironment with response to anti-PD-1 therapy. *Clinical cancer research : an official journal of the American Association for Cancer Research*

Terawaki, S., S. Chikuma, S. Shibayama, T. Hayashi, T. Yoshida, T. Okazaki, and T. Honjo. 2011. IFN-alpha directly promotes programmed cell death-1 transcription and limits the duration of T cell-mediated immunity. *Journal of immunology* 186:2772-2779.

Topalian, S.L., F.S. Hodi, J.R. Brahmer, S.N. Gettinger, D.C. Smith, D.F. McDermott, J.D. Powderly, R.D. Carvajal, J.A. Sosman, M.B. Atkins, P.D. Leming, D.R. Spigel, S.J. Antonia, L. Horn, C.G. Drake, D.M. Pardoll, L. Chen, W.H. Sharfman, R.A. Anders, J.M. Taube, T.L. McMiller, H. Xu, A.J. Korman, M. Jure-Kunkel, S. Agrawal, D. McDonald, G.D. Kollia, A. Gupta, J.M. Wigginton, and M. Sznol. 2012. Safety, activity, and immune correlates of anti-PD-1 antibody in cancer. *The New England journal of medicine* 366:2443-2454.

Topalian, S.L., M. Sznol, D.F. McDermott, H.M. Kluger, R.D. Carvajal, W.H. Sharfman, J.R. Brahmer, D.P. Lawrence, M.B. Atkins, J.D. Powderly, P.D. Leming, E.J. Lipson, I. Puzanov, D.C. Smith, J.M. Taube, J.M. Wigginton, G.D. Kollia, A. Gupta, D.M. Pardoll, J.A. Sosman, and F.S. Hodi. 2014. Survival, durable tumor remission, and long-term safety in patients with advanced melanoma receiving nivolumab. *Journal of clinical oncology : official journal of the American Society of Clinical Oncology* 32:1020-1030.

Trautmann, L., L. Janbazian, N. Chomont, E.A. Said, S. Gimmig, B. Bessette, M.R. Boulassel, E. Delwart, H. Sepulveda, R.S. Balderas, J.P. Routy, E.K. Haddad, and R.P. Sekaly. 2006. Upregulation of PD-1 expression on HIV-specific CD8+ T cells leads to reversible immune dysfunction. *Nat Med* 12:1198-1202.

Urbani, S., B. Amadei, D. Tola, M. Massari, S. Schivazappa, G. Missale, and C. Ferrari. 2006. PD-1 expression in acute hepatitis C virus (HCV) infection is associated with HCV-specific CD8 exhaustion. *Journal of virology* 80:11398-11403.

Utzschneider, D.T., A. Legat, S.A. Fuertes Marraco, L. Carrie, I. Luescher, D.E. Speiser, and D. Zehn. 2013. T cells maintain an exhausted phenotype after antigen withdrawal and population reexpansion. *Nature immunology* 14:603-610.

van Faassen, H., M. Saldanha, D. Gilbertson, R. Dudani, L. Krishnan, and S. Sad. 2005. Reducing the stimulation of CD8+ T cells during infection with intracellular bacteria promotes differentiation primarily into a central (CD62LhighCD44high) subset. *Journal of immunology* 174:5341-5350.

van Stipdonk, M.J., E.E. Lemmens, and S.P. Schoenberger. 2001. Naive CTLs require a single brief period of antigenic stimulation for clonal expansion and differentiation. *Nature immunology* 2:423-429.

Veiga-Fernandes, H., U. Walter, C. Bourgeois, A. McLean, and B. Rocha. 2000. Response of naive and memory CD8+ T cells to antigen stimulation in vivo. *Nature immunology* 1:47-53.

Vibhakar, R., G. Juan, F. Traganos, Z. Darzynkiewicz, and L.R. Finger. 1997. Activation-induced expression of human programmed death-1 gene in T-lymphocytes. *Exp Cell Res* 232:25-28.

Wang, J., S. Hevi, J.K. Kurash, H. Lei, F. Gay, J. Bajko, H. Su, W. Sun, H. Chang, G. Xu, F. Gaudet, E. Li, and T. Chen. 2009. The lysine demethylase LSD1 (KDM1) is required for maintenance of global DNA methylation. *Nat Genet* 41:125-129.

Wang, J., K. Scully, X. Zhu, L. Cai, J. Zhang, G.G. Prefontaine, A. Krones, K.A. Ohgi, P. Zhu, I. Garcia-Bassets, F. Liu, H. Taylor, J. Lozach, F.L. Jayes, K.S. Korach, C.K. Glass, X.D. Fu, and M.G. Rosenfeld. 2007. Opposing LSD1 complexes function in developmental gene activation and repression programmes. *Nature* 446:882-887.

West, E.E., H.T. Jin, A.U. Rasheed, P. Penaloza-Macmaster, S.J. Ha, W.G. Tan, B. Youngblood, G.J. Freeman, K.A. Smith, and R. Ahmed. 2013. PD-L1 blockade synergizes with IL-2 therapy in reinvigorating exhausted T cells. *The Journal of clinical investigation* 123:2604-2615.

Wherry, E.J., J.N. Blattman, K. Murali-Krishna, R. van der Most, and R. Ahmed. 2003. Viral persistence alters CD8 T-cell immunodominance and tissue distribution and results in distinct stages of functional impairment. *Journal of virology* 77:4911-4927.

Wherry, E.J., S.J. Ha, S.M. Kaech, W.N. Haining, S. Sarkar, V. Kalia, S. Subramaniam, J.N. Blattman, D.L. Barber, and R. Ahmed. 2007. Molecular signature of CD8+ T cell exhaustion during chronic viral infection. *Immunity* 27:670-684.

Whitmire, J.K., and R. Ahmed. 2000. Costimulation in antiviral immunity: differential requirements for CD4(+) and CD8(+) T cell responses. *Current opinion in immunology* 12:448-455.

Winograd, R., K.T. Byrne, R.A. Evans, P.M. Odorizzi, A.R. Meyer, D.L. Bajor, C. Clendenin, B.Z. Stanger, E.E. Furth, E.J. Wherry, and R.H. Vonderheide. 2015. Induction of T-cell Immunity Overcomes Complete Resistance to PD-1 and CTLA-4 Blockade and Improves Survival in Pancreatic Carcinoma. *Cancer Immunol Res* 3:399-411.

Xiao, G., A. Deng, H. Liu, G. Ge, and X. Liu. 2012. Activator protein 1 suppresses antitumor T-cell function via the induction of programmed death 1. *Proceedings of the National Academy of Sciences of the United States of America* 109:15419-15424.

Xu, J., S.D. Pope, A.R. Jazirehi, J.L. Attema, P. Papathanasiou, J.A. Watts, K.S. Zaret, I.L. Weissman, and S.T. Smale. 2007. Pioneer factor interactions and unmethylated CpG dinucleotides mark silent tissue-specific enhancers in embryonic stem cells. *Proceedings of the National Academy of Sciences of the United States of America* 104:12377-12382.

Xu, Y., K.K. Kiningham, M.N. Devalaraja, C.C. Yeh, H. Majima, E.J. Kasarskis, and D.K. St Clair. 1999. An intronic NF-kappaB element is essential for induction of the

human manganese superoxide dismutase gene by tumor necrosis factor-alpha and interleukin-1beta. *DNA Cell Biol* 18:709-722.

Yamamoto, M., S. Sato, H. Hemmi, K. Hoshino, T. Kaisho, H. Sanjo, O. Takeuchi, M. Sugiyama, M. Okabe, K. Takeda, and S. Akira. 2003. Role of adaptor TRIF in the MyD88-independent toll-like receptor signaling pathway. *Science* 301:640-643.

Yao, S., S. Wang, Y. Zhu, L. Luo, G. Zhu, S. Flies, H. Xu, W. Ruff, M. Broadwater, I.H. Choi, K. Tamada, and L. Chen. 2009. PD-1 on dendritic cells impedes innate immunity against bacterial infection. *Blood* 113:5811-5818.

Yoon, H.S., C.D. Scharer, P. Majumder, C.W. Davis, R. Butler, W. Zinzow-Kramer, I. Skountzou, D.G. Koutsonanos, R. Ahmed, and J.M. Boss. 2012. ZBTB32 is an early repressor of the CIITA and MHC class II gene expression during B cell differentiation to plasma cells. *Journal of immunology* 189:2393-2403.

Youngblood, B., A. Noto, F. Porichis, R.S. Akondy, Z.M. Ndhlovu, J.W. Austin, R. Bordi, F.A. Procopio, T. Miura, T.M. Allen, J. Sidney, A. Sette, B.D. Walker, R. Ahmed, J.M. Boss, R.P. Sekaly, and D.E. Kaufmann. 2013. Cutting edge: Prolonged exposure to HIV reinforces a poised epigenetic program for PD-1 expression in virus-specific CD8 T cells. *Journal of immunology* 191:540-544.

Youngblood, B., K.J. Oestreich, S.J. Ha, J. Duraiswamy, R.S. Akondy, E.E. West, Z. Wei, P. Lu, J.W. Austin, J.L. Riley, J.M. Boss, and R. Ahmed. 2011. Chronic virus infection enforces demethylation of the locus that encodes PD-1 in antigen-specific CD8(+) T cells. *Immunity* 35:400-412.

Yu, J., C. Angelin-Duclos, J. Greenwood, J. Liao, and K. Calame. 2000. Transcriptional repression by blimp-1 (PRDI-BF1) involves recruitment of histone deacetylase. *Mol Cell Biol* 20:2592-2603.

Zajac, A.J., J.N. Blattman, K. Murali-Krishna, D.J. Sourdive, M. Suresh, J.D. Altman, and R. Ahmed. 1998. Viral immune evasion due to persistence of activated T cells without effector function. *The Journal of experimental medicine* 188:2205-2213.

Zediak, V.P., J.B. Johnnidis, E.J. Wherry, and S.L. Berger. 2011. Cutting edge: persistently open chromatin at effector gene loci in resting memory CD8+ T cells independent of transcriptional status. *Journal of immunology* 186:2705-2709.

Zhang, X., R. Goncalves, and D.M. Mosser. 2008. The isolation and characterization of murine macrophages. *Current protocols in immunology / edited by John E. Coligan ... [et al.]* Chapter 14:Unit 14 11.

Zhang, Y., C.J. Ma, L. Ni, C.L. Zhang, X.Y. Wu, U. Kumaraguru, C.F. Li, J.P. Moorman, and Z.Q. Yao. 2011. Cross-talk between programmed death-1 and suppressor of cytokine signaling-1 in inhibition of IL-12 production by monocytes/macrophages in hepatitis C virus infection. *Journal of immunology* 186:3093-3103.

Zhang, Z.N., M.L. Zhu, Y.H. Chen, Y.J. Fu, T.W. Zhang, Y.J. Jiang, Z.X. Chu, and H. Shang. 2015. Elevation of Tim-3 and PD-1 expression on T cells appears early in HIV infection, and differential Tim-3 and PD-1 expression patterns can be induced by common gamma -chain cytokines. *BioMed research international* 2015:916936.

Zimmermann, C., A. Prevost-Blondel, C. Blaser, and H. Pircher. 1999. Kinetics of the response of naive and memory CD8 T cells to antigen: similarities and differences. *European journal of immunology* 29:284-290.